© September 2025 | IJIRT | Volume 12 Issue 4 | ISSN: 2349-6002

# Effect of Structural Slenderness on Wind Performance of Tall Building

Mr. Mohammed Imtiyaz Qureshi[1], Mr.Syed Farrukh Anwar[2]
[1]*Assistant. Professor & Supervisor Civil Engineering*
[2]*Professor and Head, Department of Civil Engineering*

***Abstract*—Modern architecture, including skyscrapers, can be understood through recognition of the domination of cultural pluralism. In particular, the design of skyscrapers began with the advent of internationalism. Contemporary skyscrapers, however, reflect various building types and design methods. In particular, the modern design trends had created various types nof atypical buildings such as twisted, tapered, tilted, and parametrical. These atypical skyscrapers became the landmark of the city and secured the urban competitiveness via innovative building design. Atypical skyscrapers, however, are a new architectural phenomenon, and research and construction cases are insufficient compared to conventional buildings**

**Tall buildings are seen as iconic landmarks because of their bold effect on the city silhouette. To control this bold effect in an aesthetically desired manner, designers search for intriguing forms such as twisted buildings. There are two main approaches for designing the structural system of a twisted tall building. In the first approach, the twisted form of the building is obtained only by the rotation of the floors, and the structural system is maintained in a conventional, perpendicular way. Alternatively, the structural system and the floors of the building twist together.**

**In this study, structures of G+40, G+30 AND G+20 storeys are selected. A base model is made with an aspect ratio as 1 and other models with aspect ratio of like 1,2.25,4,7and 9. Are made with central core and shear walls. The location of the building is assumed to be in Terrain category 3 according to IS 875-2015, IS 16700:2017. The models were analysed using ETABS 2019 software. The analysis method used for this study is the dynamic wind loadIt is studied using dynamic wind analysis considered Vb= 44 m/s constructed for gravity and wind using IS 875-2015. Moreover, it will be analyzed with Etabs 2021 tools. In the analysis, Story's Displacement, Story's Drift, Base Shear and the time Period of the Structure were analyzed and contrasted with others.**

## 1 INTRODUCTION

### 1.1 GENERAL

It is hard to make an absolute definition of tall buildings. However, there are several criteria to determine what a tall building is and what the features that make us define a building as “tall”. According to CTBUH (Council of Tall Buildings and Urban Habitat), fourteen floors or fifty meters height can be accepted as a threshold for tall buildings, yet it is also noted that such limitations are poor indicators. A building that is shorter than 50 meters can still be classified as a tall building if it is distinctly taller than other buildings in the surrounding. On the other hand, a building higher than 50 meters can be excluded from the definition of tall buildings if its slenderness ratio is not adequate. (CTBUH Height Criteria, 2019) Tall buildings are different from other type of buildings. They introduce new aspects to architecture and structural engineering. A few concerns that are valid specifically for tall buildings can be described as follows;

- Buildings should be in harmony with their surroundings, urban environment. For tall buildings, it is a challenging matter. They are inevitably distinguished from the rest of the built environment and have a bold impact on cities’ silhouette. This impact that tall buildings create on the urban scale should be controlled in an aesthetically desired way by designing the form of the building carefully.
- Because of their slender form, plan dimensions are limited in tall buildings. Therefore, plan area is limited. Since they have large number of occupants, vertical transportation should be sufficient enough to serve a large number of users, so an imported percentage of plan area is occupied by vertical transportation. Relatively large dimensioned structural members also occupy space and divide the plan area

into zones. Therefore, plan area which is already limited is further reduced by vertical transportation system and structural system. Designing the plan layout becomes a challenging task.

- Similarly, because of their slender form, tall buildings are vulnerable to the lateral loads, particularly wind load. Wind load may not be critical for a conventional building, however; it creates a crucial effect on tall buildings. Structural system should be designed in a way to overcome this effect.

The first skyscraper, Home Insurance Building, was built in 1885, which has 55 m. height. (Harbert, 2002). Home Insurance Building is accepted as the first skyscraper because of its "steel skeleton structural system". Masonry load bearing walls were not suitable for high-rise buildings because of their insufficient load bearing capacities and limited adaptations for openings or unconventional forms. With the use of rigid frames made of steel, the structural system became lightweight and more flexible. Therefore, this building with its skeleton system initiated a starting point of possibilities for improvement in the structural design of tall building. New structural systems have been developed for tall buildings since then. With the help of the improvements in the material qualities, the height limit for building has been constantly extended and the developments in the construction techniques followed this process. Also the improvements in the elevator systems play crucial role in tall building design. Early studies on structural systems of tall buildings are done by Bungale Taranath in 1988, who classified tall building structural systems and described their different behaviors. Similar studies are done by Stafford Smith and Alex Coull in 1991, which developed the classification further. In 2014, Mehmet Halis Günel and Emre Ilgın come up with a classification of structural systems for tall buildings which displayed a more refined approach. In 2019, the highest completed building of the world is Burj Khalifa with its 828 meters height (Baker, Korista, & Novak, 2008). According to CTBUH, there are forty vision projects that are proposed to be higher than Burj Khalifa and rise more than a thousand meters. Two of these projects, Nakheel Tower and Sky City have never been completed. Nakheel Tower started to get constructed in 2008 and stopped in 2009, it was supposed to be higher than a thousand meters. Sky City started in 2013 and it was supposed to be 838 meters height; however, like Nakheel Tower, it has never been completed. (https://www.skyscrapercenter.com/). Jeddah Tower (or Kingdom Tower) is still under construction and supposed to be higher than a thousand meters when it will be completed (Weismantle & Stochetti, 2015). At the end of the 19th century, the fundamental causes of designing tall buildings were population growth in cities and increasing land values (Günel & Ilgin, 2014). They were designed with the aim of benefiting from the land as much as possible. However; over time, the rationale behind constructing tall buildings has changed. Since the population growth in the cities is still a valid concern, it can be accepted that buildings must be tall enough to deal with the population density of the cities. Nevertheless; today, tall buildings do not meet this need. Their heights are far more than what is necessarily needed. Also the increasing land values can be seen as a fact in certain cities, but the budgets that are devoted to the tall building projects show that this is not a concern behind shaping tall building design either.

## 1.2EVALUATION OF THE SLENDER TALL BUILDINGS IN TERMS OF ARCHITECTURAL DESIGN

Slender tall buildings—often referred to as super-slender or ultra-slim towers—are characterized by their high aspect ratios, typically exceeding 7:1 (height to width). These buildings present unique challenges and opportunities from an architectural standpoint. Evaluating their architectural design involves multiple parameters such as form, function, structural integration, aesthetics, and performance. In CTBUH's 2016 Awards lineup, 432 Park Avenue was highlighted as a finalist from the Americas region, noted for pushing slenderness limits with its 1:15 ratio. CTBUH defines "super-slender" high-rises generally as those exceeding 10:1 or 12:1 slenderness ratio, aligning with engineering convention

Architectural Form and Aesthetics

- Slender Profile: The narrow footprint demands creative use of vertical space and often results in elegant, minimalistic designs.
- Iconic Shapes: Due to their visibility and prominence on skylines, architects often explore bold and iconic forms (twisting, tapering, and setbacks) to give identity to the building.

- Façade Design: The building envelope is designed to reduce wind loads and improve energy efficiency while enhancing the visual appeal.

Space Planning and Functionality

- Efficient Core Design: A centralized and compact core is essential to maintain usable floor area.
- Zoning: Vertical zoning is implemented, often including luxury residences, sky gardens, amenities, and mechanical floors.
- Maximizing Views: The narrow shape allows for panoramic views and natural lighting, a major selling point in residential towers.

Structural Integration

- Architectural-Structural Coordination: Form must work harmoniously with structural elements such as outrigger systems, shear walls, and braced frames to resist wind and seismic loads.
- Minimal Columns and Open Spaces: Tall slender buildings often require column-free interiors, pushing architects to collaborate closely with structural engineers to maintain structural integrity.

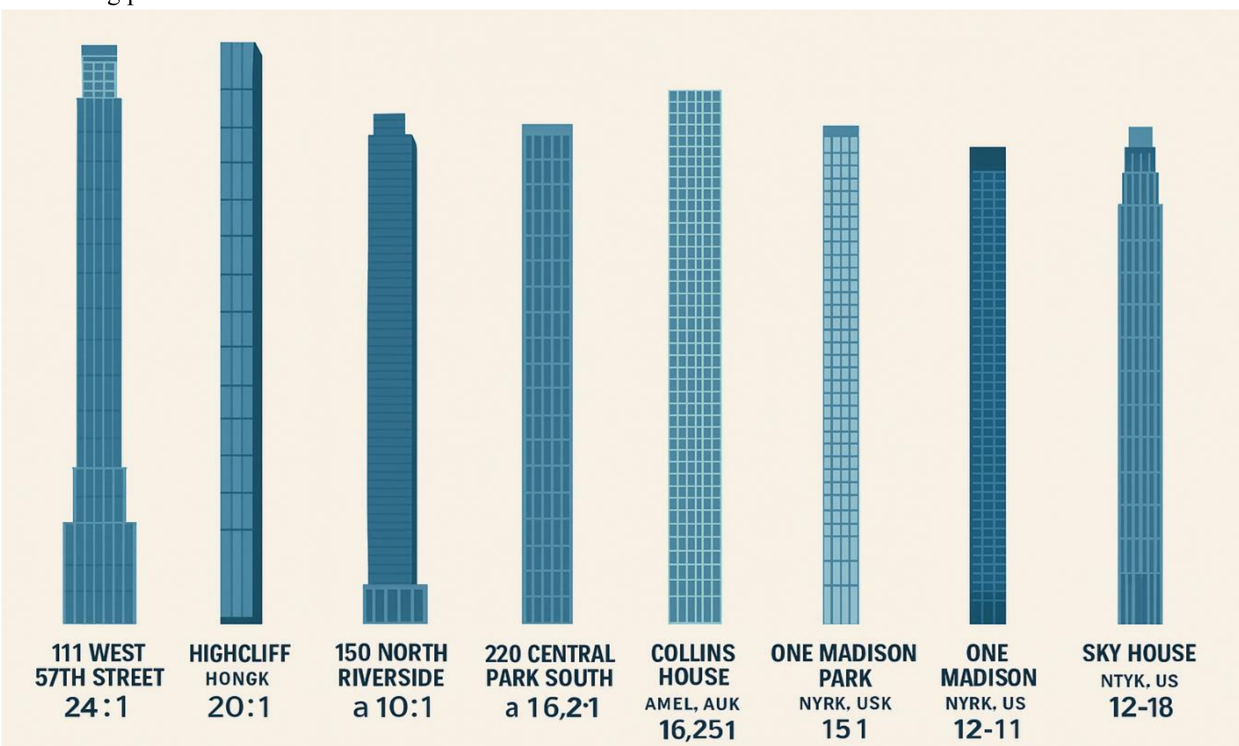


Figure 1.1: The highest eight twisted tall buildings (CTBUH, 2016).

## 1.3 EVALUATION OF THE SLENDER TALL BUILDINGS IN TERMS OF STRUCTURAL DESIGN

Slender tall buildings—typically defined by a slenderness ratio (height-to-width) greater than 10:1—pose unique structural challenges due to their height, narrowness, and flexibility. Effective structural design is crucial to ensure their safety, functionality, and comfort under various loads. Structural design of slender tall buildings requires advanced engineering strategies to deal with lateral loads, dynamic responses, and serviceability. Innovations in materials, structural systems, and damping technologies enable these buildings to perform safely while maintaining architectural elegance.

| Aspect | Structural Evaluation |
|---|---|
| Slenderness Ratio Impact | High slenderness increases lateral displacements, sway, and risk of resonance under wind. |

| Aspect | Structural Evaluation |
|---|---|
| Lateral Load Resistance | Systems like shear walls, outrigger systems, mega-columns, and diagrids are critical to resist wind and seismic forces. |
| Stiffness & Drift Control | Must limit inter-story drift (<0.004h) for comfort and safety. Use of high-modulus materials, tuned mass dampers (TMDs), and stiff core walls helps. |
| Foundation System | Deep foundations like pile groups or piled raft foundations are often required to counteract overturning moments. |
| Dynamic Response | Tall slender buildings must be designed to avoid resonant vibration, especially under wind. Wind tunnel testing is standard. |
| Load Path Continuity | Clear and direct load paths are essential to safely transfer vertical and lateral loads. |
| Material Optimization | Composite systems (steel-concrete), high-strength concrete, and lightweight materials reduce dead load and increase performance. |
| Construction Sequence | Must address differential axial shortening, creep, and construction tolerances due to height. |

1.3.1 111 West 57th Street

111 West 57th Street, also known as Steinway Tower, is an ultra-slender skyscraper located in Midtown Manhattan, New York City. It holds the record as the world's thinnest skyscraper, with an extraordinary slenderness ratio of 24:1 — meaning its height is 24 times greater than its width. Rising to a height of 1,428 feet (435 meters), the tower features 84 stories and combines cutting-edge structural engineering with historic preservation, as it incorporates the original Steinway Hall, a landmarked 1925 concert hall and showroom at its base.

The building's base width is only around 58–59 feet (approximately 18 meters), which contributes to its iconic pencil-like silhouette.

Figure 1.2: 111 West 57th Street (Steinway Tower)

1.3.2 HIGHCLIFF

High cliff is a striking super-slender residential tower perched on the south slope of Happy Valley atop Stubbs Road in Hong Kong Island. Completed in 2003 after construction began in 2000, the building soars to a roof height of 252.4 m (828 ft), with its highest occupied floor at approximately 241.8 m (793 ft). Featuring 73 stories—70 of which are livable—the tower is designed with only two apartments per typical floor up to the 70th level, and single expansive full-floor residences from level 67 upward High cliff achieves an impressive slenderness ratio of approximately 1:20 (height-to-width), making it one of the thinnest residential buildings globally at the time of completion .Due to its pencil-thin profile and the typhoon-prone environment of Hong Kong, a passive water tank damper system was installed at the top—the first of its kind in residential architecture—to mitigate wind-induced sway during strong storms .Architecturally, High cliff is composed of two interlocking oval volumes clad in elegant blue glass and steel curtain walls, designed by Dennis Lau & Ng Chun Man Architects & Engineers (DLN), with structural engineering support by Magnusson Klemencic Associates. The slender form was intentionally selected to minimize the footprint on the hillside while offering 360° panoramic views of Happy Valley, Victoria Harbor, and the South China Sea The lower levels (2/F to 8/F) contain parking and shared amenities, including a clubhouse on levels 7–9 with gym, sauna, function rooms, and outdoor pools, while residential units begin at floor 10 and extend upward In total, the building comprises around 113 units, with sizes ranging from approximately 3,676 sq ft to 7,492 sq ft. Known locally as one half of the pair nicknamed "The Chopsticks" alongside its nearly-identical neighbor The Summit, High cliff has earned acclaim including the Emporia Silver Skyscraper Award (2003) .

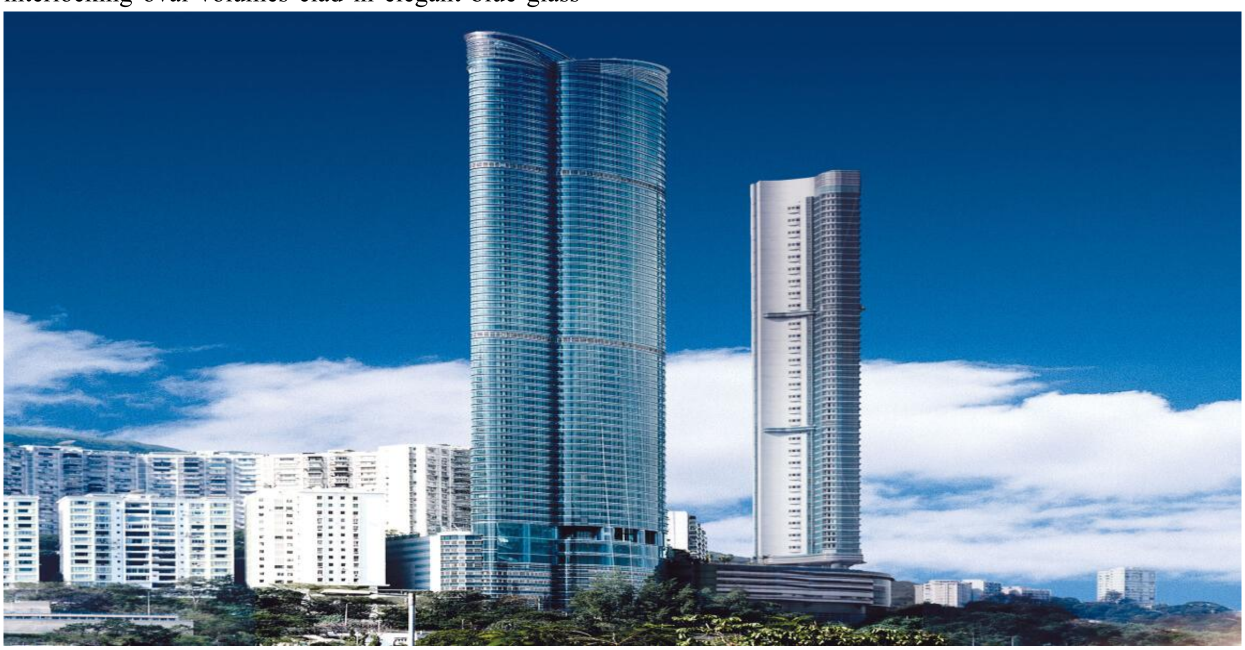

Figure 1.3: High cliff

1.4 PROBLEM DEFINITION

In modern urban environments, the rising demand for vertical expansion due to limited land availability has led to the proliferation of tall slender buildings. These structures, characterized by high height-to-width aspect ratios, pose unique architectural and structural challenges. An aspect ratio is defined as the ratio of the building's total height to the least lateral dimension of its base. While buildings with aspect ratios near 1:1 behave similarly to conventional low- or mid-rise structures, those with ratios of 2.25:1, 4:1, and especially 9:1 enter the category of slender or super-slender buildings. These buildings exhibit significantly different dynamic behavior under lateral loads such as wind and seismic forces.

As the aspect ratio increases, buildings become more prone to excessive lateral displacements, inter-story drifts, and vibrational discomfort. At extreme slenderness (e.g., 9:1), structural stability becomes highly sensitive to wind-induced oscillations, requiring the use of tuned mass dampers, aerodynamic shaping, and stiffening systems such as outrigger trusses, shear walls, and mega-columns. The serviceability criteria particularly acceleration limits for occupant comfort—often govern the design more than strength requirements in such cases. The lack of comprehensive comparative studies addressing how varying aspect ratios (1, 2.25, 4, and 9) affect overall building performance, especially in terms of story drift, base shear, modal response, and structural efficiency, poses a knowledge gap. There is a need to investigate how increasing slenderness influences not only the structural demands but also the architectural feasibility and construction techniques. This study/problem aims to systematically analyze tall buildings with different aspect ratios and assess their behavior under wind and seismic loads. The goal is to identify critical thresholds in slenderness beyond which specialized design interventions become mandatory and to recommend guidelines for optimum performance, occupant comfort, and structural economy.

### 1.5 AIM AND OBJECTIVES

The main aim of this study is to investigate the tradeoff between the potentials and limitations of slender tall buildings concerning structural and architectural design. The objectives of the research can be listed as follows:

- Study of the response of slender tall Buildings using the dynamic wind analysis and understanding the behavior of different aspect ratio of like 1, 2.25,4 and 9.
- Conducting wind performance assessment of the slender tall Buildings considering different aspect ratio and discussing the obtained results.
- To compare the stiffness, displacement, drift, and time period results of the slender tall Buildings.

## 2 LITERATURE REVIEW

### 2.1 GENERAL

In this chapter, literature survey about the slender tall buildings is presented in five sections. Firstly, the definition of a twisted tall building is given from two different sources. Then the subjects are categorized into two as architectural design and the structural design issues. In the second section, the architectural design concerns such as the overall form of the buildings, modelling and construction process and the plan layouts are discussed. In the third section, the structural design concerns such as the wind load response, lateral stiffness of the twisted tall buildings and the inherent torsion effect are discussed. In the fourth section, the existing examples of the twisted tall buildings are investigated and solutions that are specific for these projects are given. Finally, in the critical evaluation section, the given information evaluated with a holistic manner.

### 2.2 LITRATURE REVIEW

Yangjin Yuan a, Bowen Yan (2023):

Supertall buildings are particularly sensitive to wind loads because of their light weight, high slenderness and low damping. The self-excited force induced by the fluid–structure interaction may lead to undesired across-wind vortex-resonance, and affect structural serviceability significantly. Therefore, it is of vital importance to accurately evaluate the characteristics of the oncoming wind flow as well as the aeroelastic responses of supertall buildings. In this study, the influence of TWF on the aeroelastic response of buildings is studied experimentally. The displacement time histories, trajectories and correlation coefficients of wind-induced responses, statistical characteristics, probability density functions and power spectra of across-wind displacement under various levels of reduced wind speeds are examined.

Zuber Ali Shah1, Rahul Satbhaiya (2022):

This research presents the structural behavior of RCC twisted building subjected to dynamic loads. The comparative study between RCC twisted buildings is made. In a twisted tall building various rate of twist for RCC twisted building was analyzed. The different rate of twist as 10, 12.5 & 15 degrees at the center of the RCC twisted building was considered. The modelling and analysis is done using ETABS. Dead loads, live load, seismic load and wind loads are assigned for modelled structures and results obtained are plotted for parameters such as displacement, storey drift, time period and base shear. The analysis for twisted building is done for gravity loads, lateral load using Response spectrum method. The models are considered for Zone V & the analysis is done as per the Indian standard codal provisions. From the comparative study of RCC building under Dynamic loads for various angle of twist for storey it is concluded that RCC twisted building is efficient under seismic and wind load. 10-degree angle of twist is efficient compared to 12.5 & 15 degree of angle of twist.

Kamran Shahab1 , Hassan Irtaza2 , Ashish Agarwal3 (2020)

As the height of the tall buildings is increasing more into the atmospheric boundary layer (ABL) along with complexity in building shape, determination of wind-induced responses became more challenging task. Beside wind loads, across-wind excitation and frequency of vortex shedding are the major concern in designing the tall building. However, wind-induced responses are the function of outer geometry of the building, so by modifying the outer geometry, the aerodynamics of the tall buildings can be controlled and therefore the focus of the researchers is shifted from conventional prismatic geometry along the height towards the twisting buildings to enhance the aerodynamic performance and reduce the wind-induced forces on the tall buildings. In this study, a series of numerical simulations are performed to compare the aerodynamic loads on prismatic tall building square in section with its twisted forms (90º, 180º, 270º and 360º twists) using the unsteady RNG k-ε turbulence model in Computational Fluid Dynamics (CFD). A total of five building models (one prismatic and four twisted) were analyzed and results show that the aerodynamic load on the twisted buildings is on the lower side as compared to the prismatic building.

Yong-Gui Li [a], Jia-Hui Yan(2021):

Wind effects on a square model and a 90° helical model are investigated by both pressure measurement and aero-elastic model tests in a boundary layer wind tunnel. Based on the pressure measurement results, local wind force coefficients, base moment coefficients, vertical correlation coefficients and power spectral densities for the two models were analyzed and discussed in detail. The aerodynamic damping ratios were calculated by the random decrement technique (RDT) based on the wind-induced acceleration obtained from the aero-elastic tests. Comparisons of wind loads and wind-induced accelerations were made for the square and helical models. The results shown that the aerodynamic damping should not be ignored, especially for a cross-wind direction. Moreover, the helical model has been proved to yield a better behavior in aerodynamic performance than square model. This study aims to provide useful information for wind-resistant design of helical building.

K. S. Navya, B. V. Vishal, (2021):

In the present investigation, it is compared between the twisted tower and regular structure. In current investigation considered building height of 20 storied, 40 storied and 60 storied structure, and twisted angles are considered as 1°, 2° and 3° and two plans as symmetric structure and asymmetric for all different heights of building. The symmetric plan consists of number of bays kept 8 along both the direction and bay size kept as 4 m with storey height being 3 m. The asymmetric plan consists of 8 bays along x-direction and 6 bays along y-direction, and bay size kept as 4 m with storey height being 3 m. The building is analyzed by considering zone IV by response spectrum method using Etabs 2016 software. The parameters studied are lateral storey displacement, storey drift, base shear, storey stiffness and modal time period. We can conclude that the conventional structure performs better than the twisted structure under the seismic actions.

Ivan Depina, Vladimir Divić, (2021):

Wind phenomena present significant societal risks in many regions of the world due to, among others, economic losses resulting from damages to the built environment, discomfort to people, and disturbances in marine, air, and road traffic. These risks have motivated the development of performance-based design methodologies to support the decision makers in making rational and optimal measures to mitigate those risks. This paper investigates the application of the Performance-Based Wind Engineering (PBWE) methodology to the risk assessment to the critical telecommunication infrastructure subjected to wind hazard. Motivated by failures of telecommunication infrastructure due to wind load, the focus of the study is on the implementation of the PBWE methodology to estimate the expected annual losses to typical lattice frame steel telecommunication towers subjected to the Bora wind along the Croatian coastline. The statistical description of the wind hazards is based on long-term meteorological measurements available at several locations to capture the local variations characteristic for the Bora wind. The uncertainties in the wind hazard and the structural parameters were propagated to the structural response (e.g., displacements, internal forces) through a set of Monte Carlo analyses. The analyses provided a basis to estimate the probabilities of exceeding the serviceability and ultimate limit states. The resulting probabilities were used as an input to the loss function that evaluates risks from the wind hazard. The risk estimates provide valuable information to the stakeholders and decision makers that enable improved strategies for managing risks from wind hazard.

S. M. J. Spence; W. C. Chuang; P. Tabbuso (2016):

A performance-based design (PBD) approach is replacing the present prescriptive design philosophy, which only focuses on completing standards-mandated requirements, in order to create solutions that logically satisfy society's desire for a truly safe built environment. In earthquake engineering, PBD has been successfully adopted thanks to extensive research; in wind engineering, however, this has not been the case. Thus, it is necessary to start a similar endeavor by developing a framework that incorporates PBD principles completely into the design of building systems that can withstand strong wind events. This paper provides an example of how to construct a PBD framework. Specifically, a technique to reduce structural and non-structural damage and loss is put forth for multi-story wind-excited buildings. Specifically, the theory of dynamic shakedown is applied to simulate the post-yield behavior of the structural system, thereby offering a comprehensive representation of the post-yield behavior without using costly computational non-linear finite element models. A case study that highlights the usefulness of the suggested PBD framework is provided.

Arthriya Subgranon [b], Seymour M.J. Spence (2021):

The creation of an explicit treatment of correlations between component damages and losses in a stochastic simulation-based design optimization approach for dynamic wind-excited structures is presented in this study. To systematically account for the many types of uncertainties involved in system loss prediction, the proposed technique merges a probabilistic performance-based wind engineering methodology with a bi-objective design optimization framework. The bi-objective optimization issue is converted into a sequence of single-objective stochastic optimization problems using the ΔΔ-constraint technique. A pseudo-simulation approach that enables the formulation of an approximate sub-problem that may be solved consecutively to identify solutions that define a set of Pareto optimal designs is proposed to tackle each constraint optimization problem. The suggested plan approximates engineering demand samples using auxiliary variable vectors, which are the result of an augmented simulation run at a specific design point. Based on the idea of fragility, analytical equations are derived connecting the engineering demand samples to the second-order statistics of wind-induced losses. Possible relationships between component losses and capabilities are addressed explicitly. The best designs of moment-resisting frames subject to random wind loads serve as examples of the usefulness of the suggested method and its scalability to high-dimensional situations

Tao Wu [a], Ying Sun [a], Zhenggang Cao (2020):

In contrast to the widely used performance-based design (PBD) approach today, there is not enough study being done by academics on structural performance as a PBD foundation. The wind-resistant performance of a roof system is assessed by looking at the wind uplift failure mechanism, using the failure process of a standing seam roof system as an example. Through numerical simulations, the deformation process of roof-system components is derived. According to the analysis, the relationship between the anti-wind clip and the vertical plate goes through three stages: non-interaction and no contact, anti-wind clips limiting vertical plate deformation, and vertical plates driving anti-wind clip rotation. The alterations in the structural reactions (seam displacement and contact stress) and damage sustained by the roof system during its failure process are acquired through experiments. The structural responses also grow in three phases, according to an analysis of the variation in the load-related structural response curve. It is discovered that the aforementioned three failure stages correlate to three distinct damage stages when combined with the damage sequence. The roof system is at an elastic stage during the first step. Second, curling experiences partial separation when the roof system is in the yield stage, creating an interspace that is detrimental to roof waterproofing. Roof ponding results from permanent plastic deformation in the roof system, which happens in the third stage. The three-stage failure process was found to reflect the various roof system performance levels, and some of the study's findings can be used as a guide for the definition of roof-system performance level in the future.

Seung Yong Jeong and Thomas Kang (2020):

Performance-based wind design (PBWD) research has been conducted recently, however there is still a lack of studies on real-world applications. The PBWD of a residential building with shear walls made of reinforced concrete is done in this study. To add inelastic behavior, the resonant component of the design wind load for the initial elastic design is cut in half. Power spectral density functions are used to calculate time historical wind loads. A nonlinear time history analysis is performed to assess the building's performance in resisting wind. Under historical wind stresses, shear walls maintained their elasticity, while coupling beams displayed some degree of inelastic degradation.

Mingfeng Huang (2016):

An integrated computational design optimization approach for the performance-based design of tall buildings exposed to different wind excitation levels is presented in this chapter. Several performance targets linked to different wind danger levels are defined in order to present a performance-based wind engineering design framework. To forecast the inelastic drift performance of tall buildings exposed to extremely infrequent strong wind events, a nonlinear static pushover approach is utilized. The enhanced optimality criteria technique is used to create and solve the optimal performance-based design issue that takes inelastic deformation into account. A realistic 40-story residential skyscraper serves as an example of the efficiency and usefulness of the best wind-resistant performance-based design technique.

Rodolfo K. Tessari, Henrique M. Kroetz, André T. Beck (2017):

In order to guarantee predictable performance levels for engineered structures, performance-based wind engineering, or PBWE, is a revolutionary design philosophy that attempts to identify and quantify the uncertainties inherent in structural design. Owing to the complexity of the formulation and the recent technique approach, there aren't many studies on PBWE, and the ones that do exist have various drawbacks. In order to estimate wind forces on steel towers, this study suggests using the Performance-based Wind Engineering technique to a probabilistic analysis of the structures. It does this by comparing several computation models. Two methodologies of the Brazilian winds standard NBR6123:88 for the assessment of wind forces on steel towers were studied, and uncertainties involved in the characterization of the wind field and the structural strength were investigated. There was also a case study done on the estimation of a telecommunication tower's reliability. It was discovered that the two calculation models under study produced comparable safety levels and that tower design, which considers the fact that wind always blows from the worst direction, is overly cautious. It is also demonstrated that, in PBWE, multiple mean recurrence intervals for varying performance levels can be assigned with the same target dependability, providing guidance for minimum cost design.

## 3 METHODOLOGIES

### 3.1 GENERAL

This methodology aims to investigate the structural behavior of slender tall buildings with different aspect ratios, focusing on their necessity, advantages, disadvantages, and response to lateral loads such as wind and seismic forces. The research involves parametric modeling, structural analysis, and comparative evaluation to understand how increasing slenderness influences the performance of tall buildings.

### 3.2 NECESSITY OF SLENDER TALL BUILDINGS

In high-density urban environments where land is scarce and expensive, constructing tall and slender buildings has become a practical solution. These vertical structures offer the benefit of maximizing usable floor area without expanding horizontally. They are particularly common in premium locations like New York, Hong Kong, and Dubai, where the skyline becomes an asset and vertical expansion is inevitable. Thus, slender buildings are not only an architectural trend but a functional necessity in urban planning and land-use optimization.

In the context of rapid urbanization, limited land availability, and escalating population density, the necessity of slender tall buildings has become increasingly evident. Urban centers on the world—particularly in cities like New York, Hong Kong, Tokyo, and Dubai—face severe constraints in horizontal land expansion. With premium land parcels shrinking and ground-level infrastructure already saturated, vertical development emerges as the most viable and sustainable approach. Slender tall buildings, defined by their high height-to-width ratios, represent a specialized category of vertical structures designed to maximize usable space within a compact footprint. These buildings make efficient use of restricted plots by rising vertically, accommodating a larger number of residential or commercial units without requiring extensive horizontal sprawl. This not only helps preserve open spaces and green areas in densely developed zones but also aligns with modern urban planning goals aimed at smart growth and sustainable development.

In addition to their space efficiency, slender towers fulfill architectural, economic, and environmental objectives. Architecturally, they contribute to iconic city skylines, often becoming symbols of national pride and engineering prowess. Their slim profiles enable greater penetration of natural light and air into surrounding urban spaces, reducing the urban heat island effect and creating visually appealing corridors. Economically, tall slender buildings are attractive investments, as they allow developers to construct more sellable or leasable floor area in high-demand urban cores, where land prices are extraordinarily high. This leads to enhanced land value and improved return on investment, especially in high-end residential and commercial markets. From a planning perspective, vertical development also supports the concept of transit-oriented development (TOD), where tall structures are integrated with public transportation, reducing vehicular dependence and urban congestion.

Furthermore, slender tall buildings address modern lifestyle demands. They offer panoramic views, privacy, natural ventilation, and daylight—qualities increasingly valued by urban dwellers. In cities constrained by historical zoning laws or topographical challenges (e.g., waterfronts or steep slopes), slender towers often become the only permissible and practical vertical solution. As global cities evolve into vertical metropolises, the slender tower typology stands out as a key architectural response to balancing land scarcity, functionality, aesthetics, and environmental impact. Therefore, the necessity of slender tall buildings is not merely driven by land economics but is rooted in a broader pursuit of livable, sustainable, and resilient urban environments.

3. 3 ADVANTAGES OF SLENDER TALL BUILDINGS

Slender tall buildings have emerged as an innovative architectural solution to meet the spatial, aesthetic, and economic demands of rapidly urbanizing cities. One of the most significant advantages of such structures is their efficient land utilization. With limited horizontal space available in major urban centers, slender towers allow vertical expansion on small plots, making them ideal for high-value locations. By minimizing the building footprint, they enable the conservation of ground-level space for other purposes such as green areas, public plazas, or transit infrastructure, which is critical for sustainable urban development.

Another notable advantage is their architectural elegance and visual identity. The slim and vertical proportions of these buildings contribute to iconic skylines and create a sense of vertical dynamism in the built environment. They often serve as landmarks due to their unique form and height, reflecting innovation and technological advancement. Additionally, slender towers provide premium real estate value, particularly for residential use. With a smaller floor plate and fewer units per level, residents enjoy increased privacy, unobstructed panoramic views, better natural lighting, and cross-ventilation, enhancing the overall living experience. This exclusivity significantly boosts market value and attracts high-end buyers or tenants.

From an environmental standpoint, slender buildings offer opportunities for sustainable design integration. Their narrow profiles can be strategically oriented to reduce solar gain, optimize daylight usage, and encourage natural ventilation, thereby minimizing energy consumption. Moreover, by enabling high-density vertical development, these buildings help reduce urban sprawl, promote compact city planning, and support transit-oriented development—an essential goal for climate-resilient cities.

In terms of construction, slender buildings encourage modular and prefabricated systems, which can improve construction efficiency and reduce on-site disruption. Structurally, although they require specialized systems to handle lateral loads, innovations like tuned mass dampers, outrigger systems, and high-performance materials make slender towers both feasible and safe. In many locations, zoning regulations or heritage conservation guidelines restrict horizontal development, making slender towers the only viable solution for maximizing usable space without violating planning norms.

Overall, slender tall buildings not only address the spatial limitations of dense urban environments but also introduce new possibilities in architectural design, real estate strategy, and environmental sustainability. Their rising popularity reflects a global shift toward vertical urbanism, combining efficiency, elegance, and modern living standards in a single structural form.

### 3.4 DISADVANTAGES OF SLENDER TALL BUILDINGS

While slender tall buildings offer many architectural and urban planning advantages, they also pose significant challenges and disadvantages that must be addressed during the design, construction, and operational phases. The most critical concern is their structural vulnerability due to high aspect ratios, which make these buildings highly susceptible to lateral forces, especially from wind and seismic activity. As slenderness increases, the natural lateral stiffness of the building decreases, making it prone to large deflections, sway, and vibrations. Without specialized damping systems or stiffness-enhancing elements, this movement can compromise both structural safety and occupant comfort.

Another major disadvantage is the increased complexity of structural design and construction. Slender buildings require advanced analysis and high-performance materials to ensure stability and functionality. Structural systems such as core-outrigger frameworks, mega-columns, and tuned mass dampers are necessary but add to both the cost and time of construction. Foundations also become more complex, as the concentrated vertical loads on a small footprint can lead to significant settlement or demand deeper and more expensive pile foundations, especially in weak soils.

Occupant discomfort is another notable drawback. In super-slender towers, wind-induced accelerations can cause perceptible swaying, leading to motion sickness or unease, particularly on upper floors. Although not structurally harmful, these effects significantly affect serviceability criteria and require mitigation through vibration control systems. In residential towers, smaller floor plates result in reduced usable floor area per level, making interior layouts more challenging and potentially less efficient.

Economically, while the premium views and exclusivity of slender buildings appeal to high-end buyers, the cost of construction per square meter is generally much higher due to structural reinforcements, sophisticated materials, and technical systems. This may limit their viability in lower-income or cost-sensitive markets. Additionally, maintenance and operational challenges arise from vertical transportation, façade cleaning, and emergency egress systems, especially in cases where elevators need to serve limited floors per core or where redundancy is required for fire safety compliance.

From a planning perspective, extremely tall and slender buildings may face regulatory limitations due to concerns over skyline aesthetics, shadow impact, and environmental effects such as wind tunnels at the pedestrian level. These issues often require extensive negotiation with local authorities and may delay project approval.

In summary, while slender tall buildings offer elegance and urban efficiency, their engineering complexity, cost implications, and performance challenges must be carefully balanced against their benefits to ensure safe, livable, and sustainable development.

### 3.5 EFFECT OF SLENDERNESS UNDER WIND LOADS

The impact of wind loads becomes increasingly critical as buildings become taller and slenderer. In slender tall buildings, typically defined by aspect ratios greater than 6:1, wind-induced forces and responses dominate the design criteria—often more than gravity or seismic loads. The slenderness of a building reduces its lateral stiffness and increases its height, making it more sensitive to dynamic wind effects such as along-wind forces, across-wind excitation (vortex shedding), and torsional motion. These aerodynamic phenomena can result in significant structural displacements, serviceability issues, and discomfort to occupants.

Wind acting on a tall slender structure is not just a static pressure force but also causes dynamic oscillations. Along-wind effects, caused by pressure differentials in the direction of wind flow, result in swaying of the building in the direction of the wind.

However, more critical are the across-wind effects, caused by vortex shedding—a phenomenon where alternating low-pressure vortices are formed on either side of the building, causing it to oscillate perpendicular to the wind direction. The frequency of vortex shedding can synchronize with the natural frequency of the building, leading to resonance, which amplifies lateral vibrations and poses serious structural risks.

As the slenderness ratio increases, the natural frequency of the building decreases, often approaching the range of excitation frequencies from wind gusts. This makes highly slender buildings more prone to resonant amplification and occupant discomfort, especially in the upper floors. To address this, engineers employ aerodynamic modifications such as tapering, setbacks, corner softening, and openings to disrupt vortex formation. In addition, tuned mass dampers (TMDs) or tuned liquid column dampers (TLCDs) are installed to absorb and counteract motion.

Another consequence of increased slenderness is the amplification of lateral accelerations, which can affect human perception. Building codes (such as IS 875 Part 3 or ASCE 7) set limits on permissible acceleration levels to ensure occupant comfort. In many slender high-rise residential buildings, wind-induced motion becomes the governing factor in serviceability design, even more so than strength or stability.

In summary, as buildings grow taller and thinner, wind loads become a dominant design concern. Structural engineers must carefully evaluate aerodynamic response, implement motion control systems, and adopt design modifications to ensure structural integrity, occupant comfort, and long-term performance

### 3.6 EFFECT OF SLENDERNESS UNDER SEISMIC LOADS

Slender tall buildings, typically defined by aspect ratios greater than 3:1, exhibit unique dynamic characteristics under seismic loading conditions. As per IS 1893 (Part 1): 2016 – Criteria for Earthquake Resistant Design of Structures, and IS 16700:2017 – Criteria for Structural Safety of Tall Concrete Buildings, the design of tall slender buildings must account for complex behaviors such as increased natural period, higher mode effects, and amplified inter-storey drifts that are not as prominent in low- or medium-rise structures.

One of the primary seismic implications of increased slenderness is the elongation of the fundamental time period of the structure. As a building becomes taller and more flexible, its natural period increases, often entering a range where the spectral acceleration (as per the response spectrum) may be significant. IS 1893 provides empirical formulas to estimate the natural period ($T = 0.09h/\sqrt{d}$ for moment-resisting frames), where ‘h’ is the height and ‘d’ is base dimension. In slender buildings, where ‘d’ is small, the calculated T increases, potentially aligning with the dominant periods of ground motion and thus amplifying seismic forces.

Furthermore, IS 16700:2017, which specifically addresses tall buildings (typically above 50 meters), emphasizes the need to account for P-Δ effects, lateral-torsional coupling, and higher mode contributions. Slender structures often have low lateral stiffness, which increases inter-storey drift under seismic excitation. This can result in non-structural damage (cracks in partitions, glass breakage) or even structural instability if drift exceeds code-specified limits. IS 1893 mandates drift control limits to 0.004 times the storey height under design-level earthquakes to ensure life safety and damage control.

Seismic mass participation in slender buildings is also more complex due to higher mode effects, especially in buildings exceeding 100 meters or with aspect ratios above 6:1. In such cases, modal response spectrum analysis or time history analysis is mandatory per IS 16700. The code also stipulates ductility provisions, strong-column weak-beam behavior, and capacity design principles to ensure adequate energy dissipation in critical sections. Slenderness increases the demand for well-distributed stiffness, which may be achieved using shear walls, core systems, or outrigger mechanisms. In addition, the torsional irregularity and vertical irregularity often found in slender towers (due to setbacks or tapering) must be checked as per IS 1893, which defines criteria for plan and vertical irregularities and recommends special detailing provisions for seismic zones III and above.

| Seismic Zone | Moment Frame | Structural Wall (well-distributed) | Structural Wall + Moment Frame | Structural Wall + Perimeter Frame | Structural Wall + Framed Tube |
|---|---|---|---|---|---|
| Zone V | N/A | 8 | 8 | 9 | 9 |
| Zone IV | N/A | 8 | 8 | 9 | 9 |
| Zone III | 4 | 8 | 8 | 9 | 10 |
| Zone II | 5 | 9 | 9 | 10 | 10 |

IS 16700:2023 – Table 2: Maximum Allowed Slenderness Ratio (Ht / Bt)

## IV CASE STUDY

### 4.1 GENRAL

This chapter deals with the methodology and numerical studies adopted for carrying out the dissertation work. The following chapter presents the geometrical properties and analysis parameters of the three building models (G+20), (G+30) and (G+40). By using ETABS 2021 software, which helps to analyze and design the models, the analysis method used for this study is the wind dynamic analysis. In the present context of study, a Structure is taken into consideration and the analysis is done as per the Indian standards. This building does not represent a particular real structure that has been built or proposed. However, the dimensions, general layout and other characteristics have been selected to be representative of a building for which the use of outriggers would be a plausible solution.

### 4.2: MODEL INFORMATION

Model 1: First building is modelled with lateral load resisting structural system M1 with Aspect ratio as 9

- M1 with Aspect ratio as 9 for G+40 model
- M1 with Aspect ratio as 9 for G+30 model
- M1 with Aspect ratio as 9 for G+20 model

Model 2: second building is modelled with lateral load resisting structural system M2 - Aspect ratio as 7

- M2 with Aspect ratio as 7 for G+40 model
- M2 with Aspect ratio as 7 for G+30 model
- M2 with Aspect ratio as 7 for G+20 model

Model 3: Third building is modelled with lateral load resisting structural system M3 with Aspect ratio as 4

- M3 with Aspect ratio as 4 for G+40 model
- M3 with Aspect ratio as 4 for G+30 model
- M3 with Aspect ratio as 4 for G+20 model

Model 4: Fourth building is modelled with lateral load resisting structural system M4 - Aspect ratio as 2.25

- M4 with Aspect ratio as 2.25 for G+40 model
- M4with Aspect ratio as 2.25 for G+30 model
- M4 with Aspect ratio as 2.25 for G+20 model

Model 5: First building is modelled with regular structure. The lateral load resisting structural system is adopted by studying IS 1893:2016 and labelled as regular model (M5) with slenderness ratio as 1.0 (Base Model)

40 STORY BUILDING DIMENSIONS AS PER SLENDER RATIOS

| Aspect Ratio | Height (m) | Width (m) (Least Dimension) | Length (m) (1.5× Width) |
|---|---|---|---|
| 2.25 | 120 | 53.33 | 80.00 |
| 4 | 120 | 30.00 | 45.00 |
| 7 | 120 | 17.14 | 25.71 |
| 9 | 120 | 13.33 | 20.00 |

30 STORY BUILDING DIMENSIONS AS PER SLENDER RATIOS

| Aspect Ratio | Height (m) | Width (m) (Least Dimension) | Length (m) (1.5× Width) |
|---|---|---|---|
| 2.25 | 90 | 40.00 | 60.00 |
| 4 | 90 | 22.50 | 33.75 |
| 7 | 90 | 12.86 | 19.29 |
| 9 | 90 | 10.00 | 15.00 |

20 STORY BUILDING DIMENSIONS AS PER SLENDER RATIOS

| Aspect Ratio | Height (m) | Width (m) (Least Dimension) | Length (m) (1.5× Width) |
|---|---|---|---|
| 2.25 | 60 | 26.67 | 40.00 |
| 4 | 60 | 15.00 | 22.50 |
| 7 | 60 | 8.57 | 12.86 |
| 9 | 60 | 6.67 | 10.00 |

4.3: PRELIMINARY DATA FOR 20 STORIES

| S. No | Variable | Data |
|---|---|---|
| 1 | Type of structure | Moment Resisting Frame |
| 2 | Number of Stories | 20 |
| 3 | Floor height | 3m |
| 4 | Live Load | 3.0 KN/m$^2$ |
| 5 | SDL load<br>Wall load | 2 KN/m$^2$<br>10 KN/m |
| 6 | Materials | Concrete (M30) and Reinforced with HYSD bars (Fe550) |
| 7 | Size of Columns | ISMB 600 ENCASED WITH 900X900 MM COLUMN (40 story) |
| 8 | Size of Beams | ISMB 600 in longitudinal direction<br>ISMB 600 in transverse direction |
| 9 | Depth of deck slab | 150mm thick |
| 10 | Specific weight of RCC | 25 KN/M$^3$ |
| 11 | Basic wind speed | 44 m/s |
| 12 | Importance Factor | 1.5 |
| 13 | Terrain category | 3 |
| 14 | Type of soil | Medium |

Table 4.1 Preliminary data for 20 story model

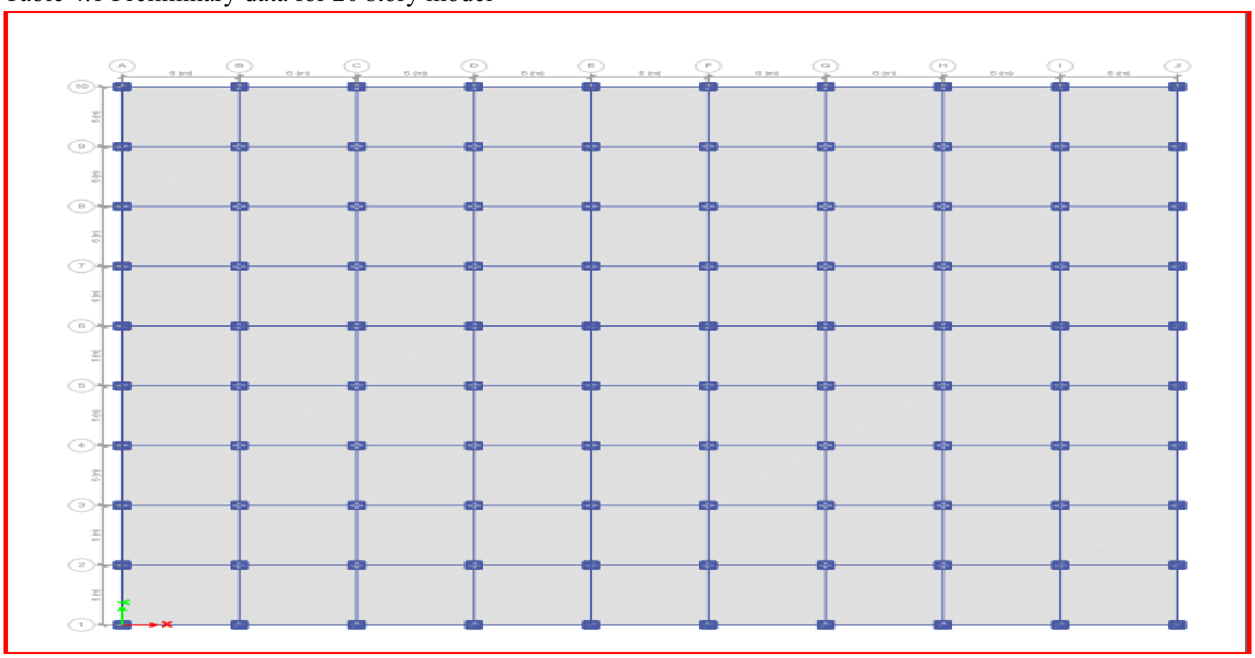

Figure 4.1: Model--plan view of 40 stories with aspect ratio 1.0

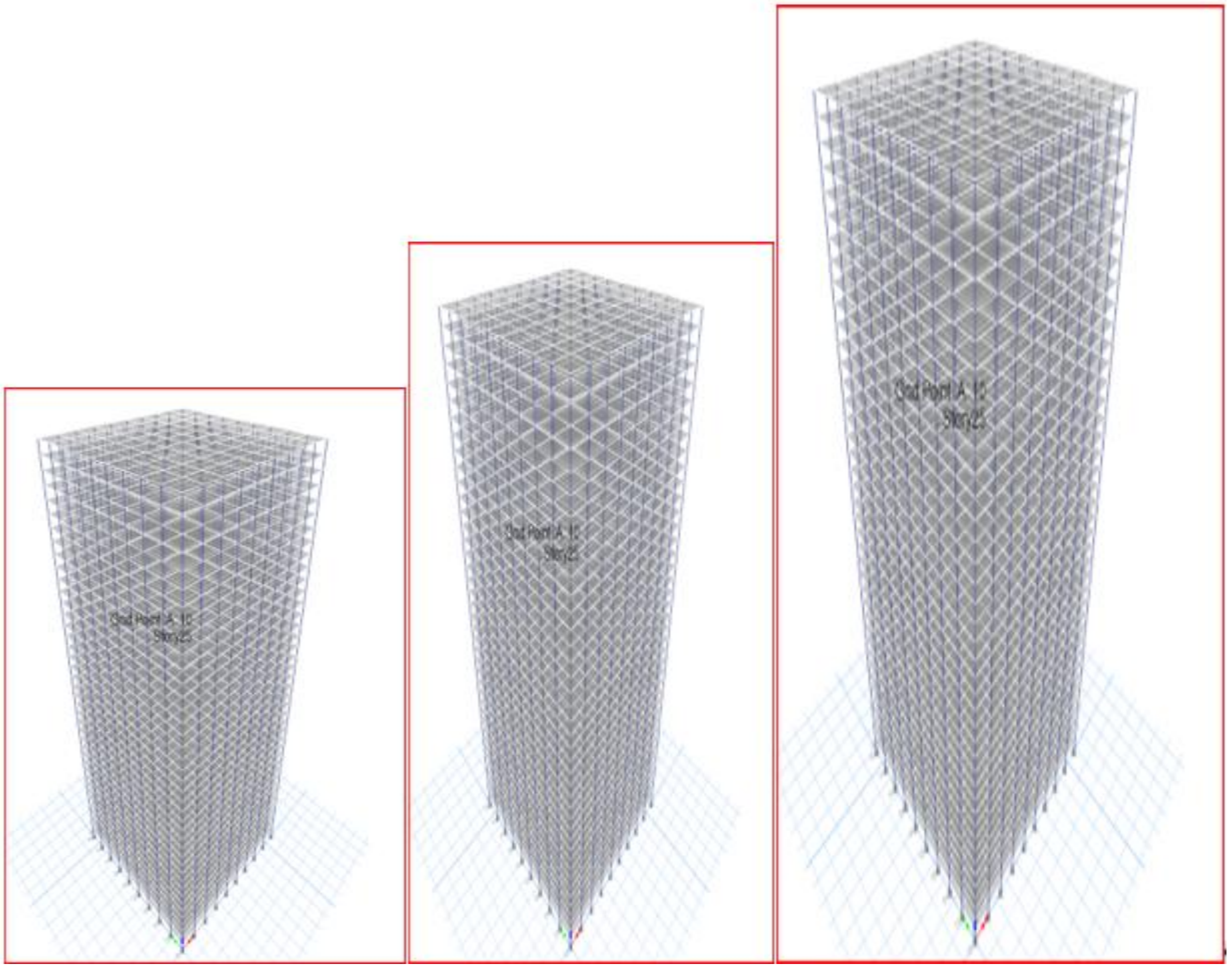

Figure 4.2: Isometric Views of 40, 30 and 20 stories with aspect ratio 1.0

PRELIMINARY DATA FOR 30 STORIES

| S. No | Variable | Data |
|---|---|---|
| 1 | Type of structure | Moment Resisting Frame |
| 2 | Number of Stories | 30 |
| 3 | Floor height | 3m |
| 4 | Live Load | 3.0 $KN/m^2$ |
| 5 | SDL load<br>Wall load | 2 $KN/m^2$<br>10 KN/m |
| 6 | Materials | Concrete (M30) and Reinforced with HYSD bars (Fe550) |
| 7 | Size of Columns | ISMB 600 ENCASED WITH 1200X1200 MM COLUMN (65 story) |
| 8 | Size of Beams | ISMB 600 in longitudinal direction<br>ISMB 600 in transverse direction |
| 9 | Depth of deck slab | 150mm thick |
| 10 | Specific weight of RCC | 25 $KN/M^3$ |
| 11 | Basic wind speed | 44 m/s |
| 12 | Importance Factor | 1.5 |

| | | |
|---|---|---|
| 13 | Terrain category | 3 |
| 14 | Type of soil | Medium |

Table 4.2 Preliminary data for 30 story model.

Figure 4.3: Model view of building with aspect ratio 2.25

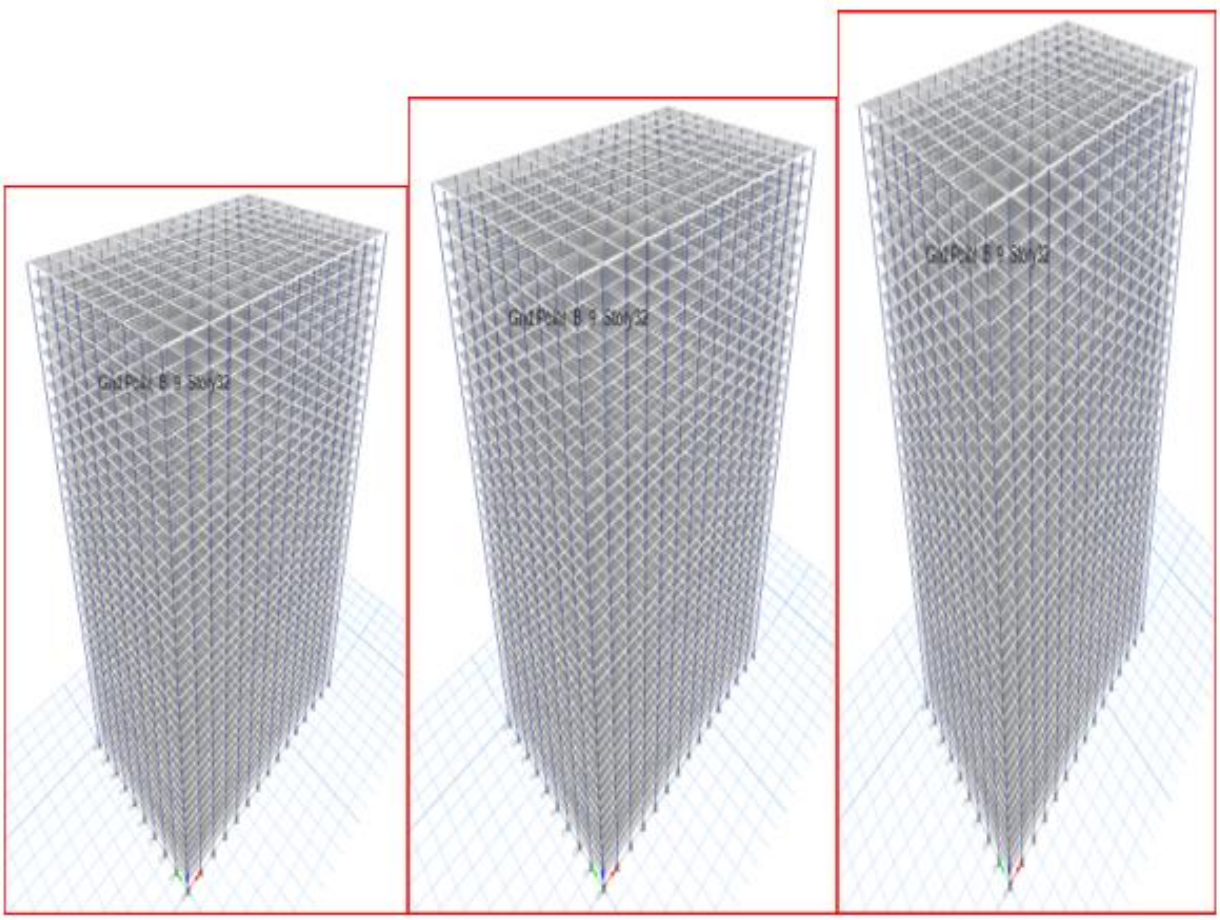

Figure 4.4: Isometric Views of 40, 30 and 20 stories with aspect ratio 2.25

PRELIMINARY DATA FOR 40 STORY MODEL

| S. No | Variable | Data |
|---|---|---|
| 1 | Type of structure | Moment Resisting Frame |
| 2 | Number of Stories | 40 |
| 3 | Floor height | 3m |
| 4 | Live Load | 3.0 $KN/m^2$ |
| 5 | SDL load<br>Wall load | 2 $KN/m^2$<br>10 KN/m |
| 6 | Materials | Concrete (M50) and Reinforced with HYSD bars (Fe550) |
| 7 | Size of Columns | ISMB 600 ENCASED WITH 1500X1500 MM COLUMN (90 story) |
| 8 | Size of Beams | ISMB 600 in longitudinal direction<br>ISMB 600 in transverse direction |
| 9 | Depth of deck slab | 150mm thick |
| 10 | Specific weight of RCC | 25 $KN/M^3$ |
| 11 | Basic wind speed | 44 m/s |
| 12 | Importance Factor | 1.5 |
| 13 | Terrain category | 3 |
| 14 | Type of soil | Medium |

Table 4.3 Preliminary data for 40 story model

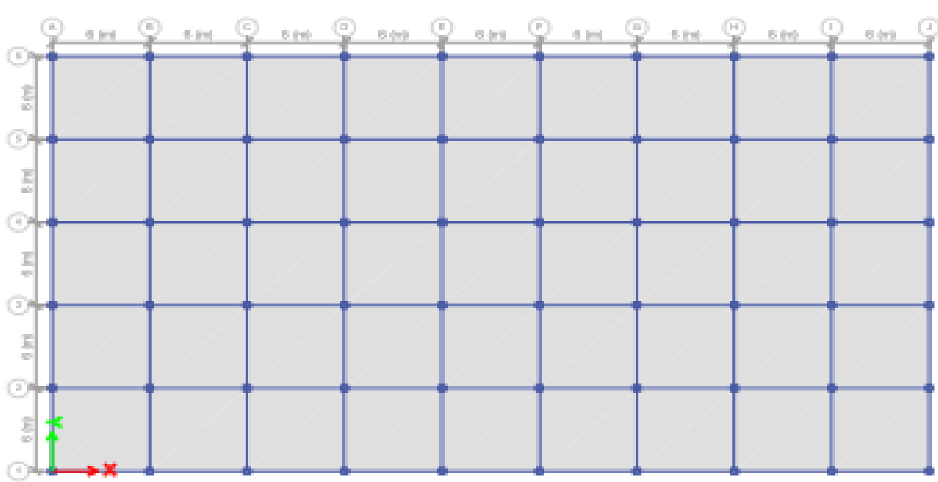

Figure 4.5: Model view of building with aspect ratio 4

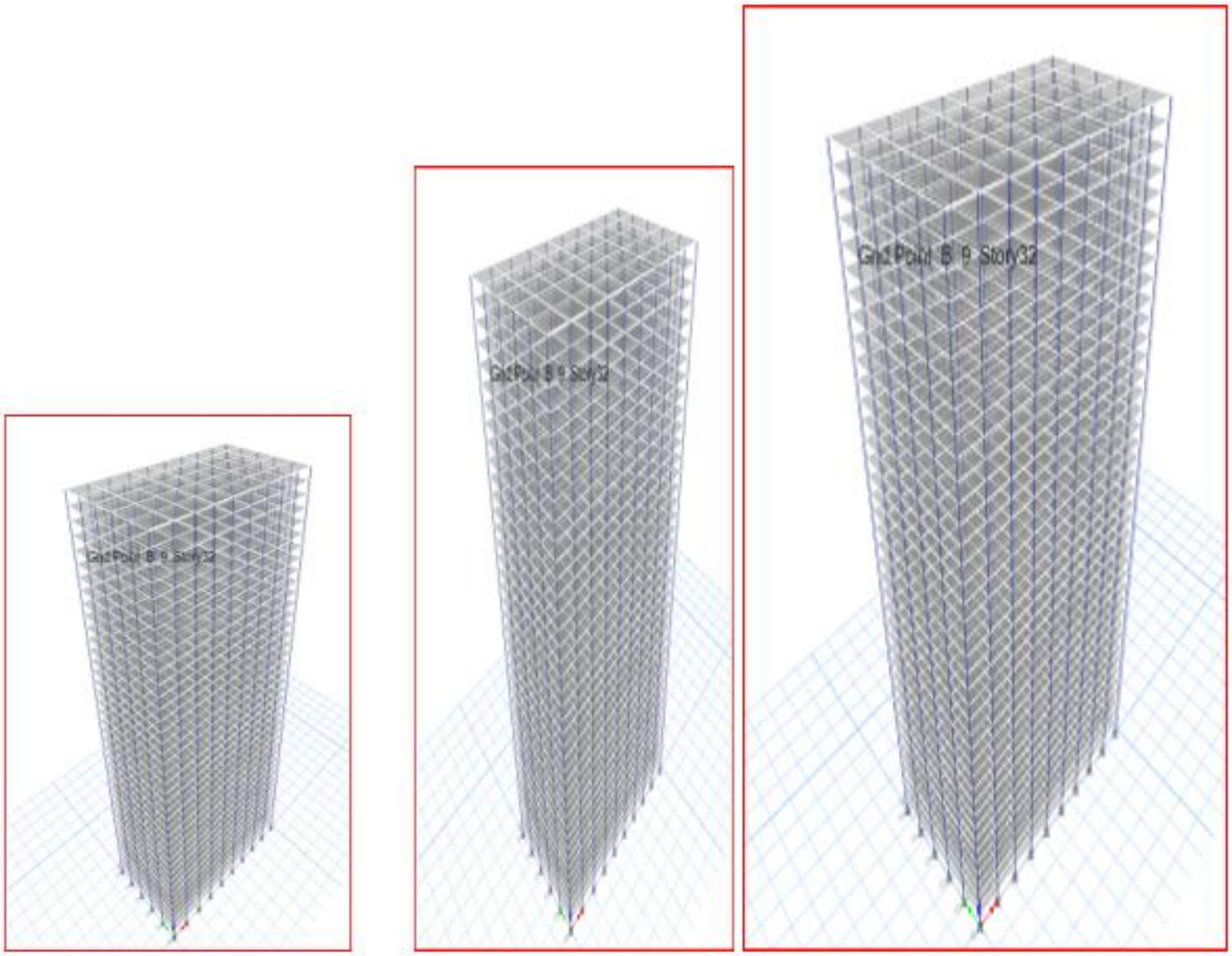

Figure 4.6: Isometric Views of 40, 30 and 20 stories with aspect ratio 4

MODEL 4: BUILDING WITH ASPECT RATIO 7

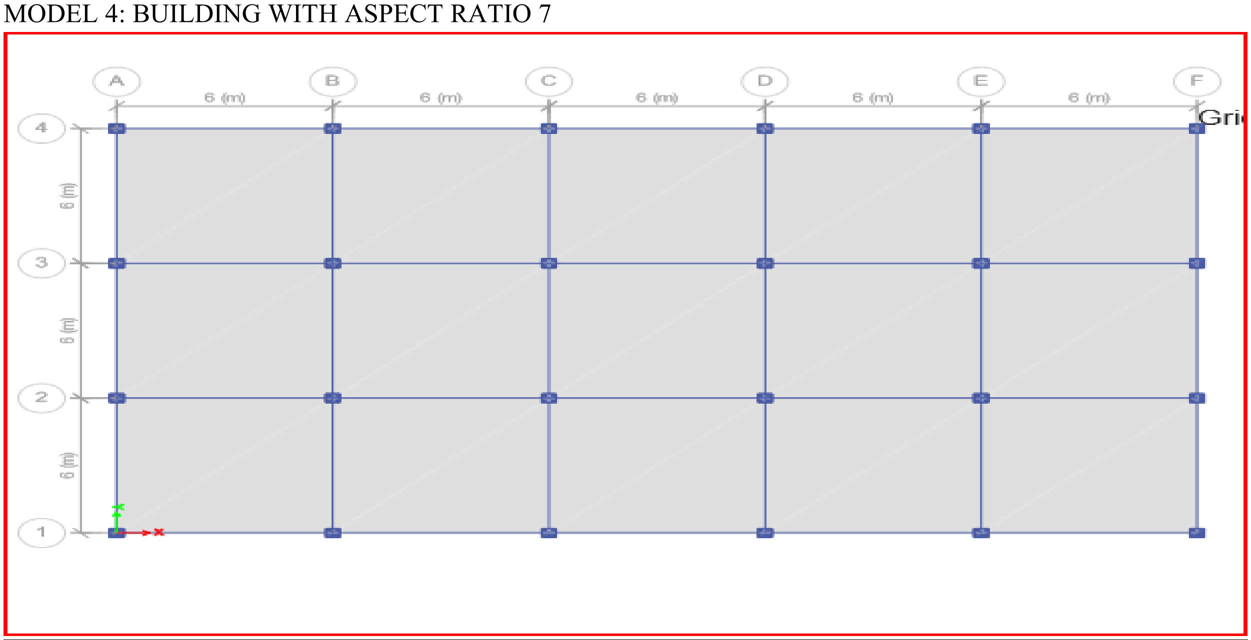


Figure 4.7: Model—plan view of building with aspect ratio 7

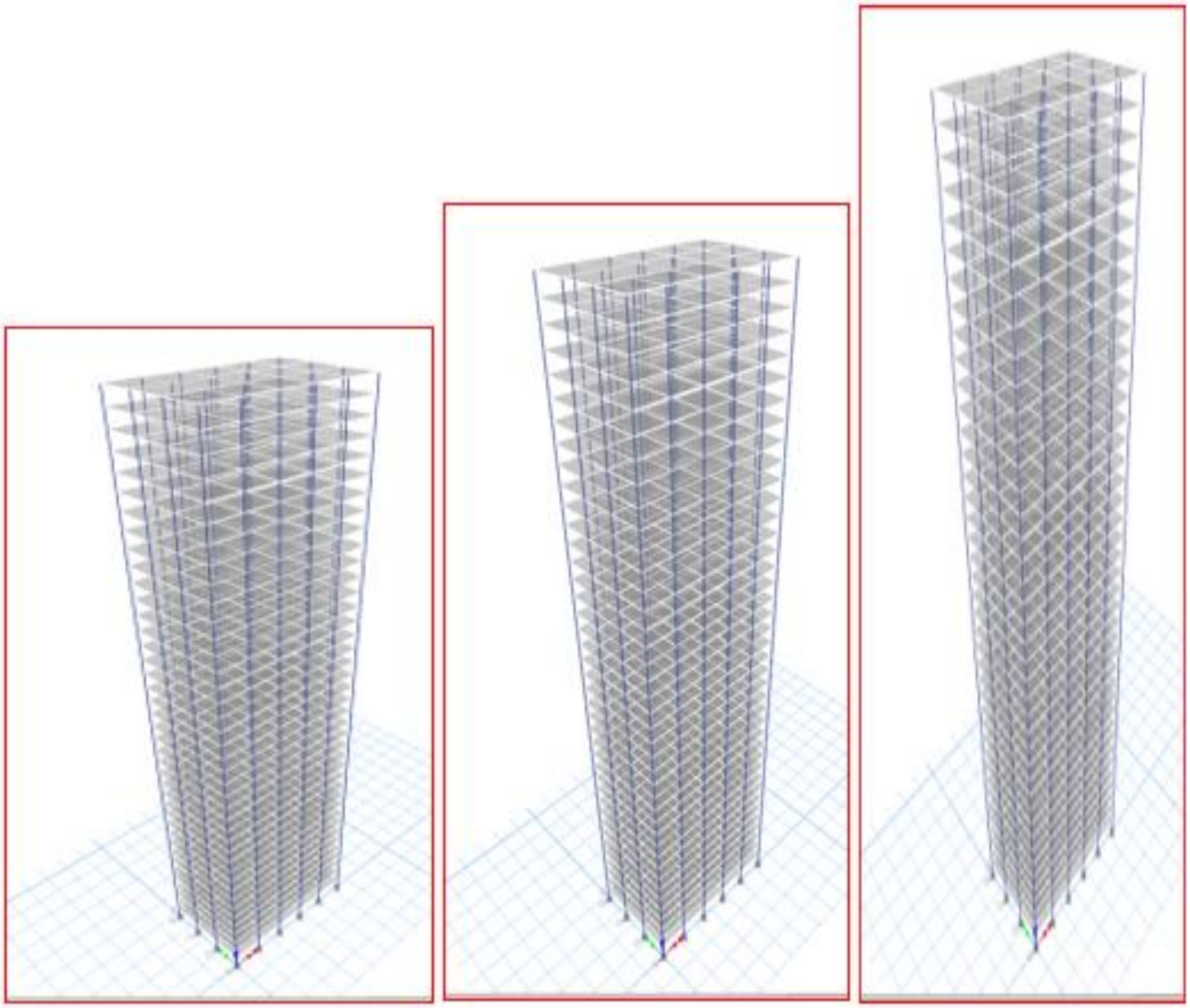

Figure 4.8: Isometric Views of 40, 30 and 20 stories with aspect ratio 7

Model 5: BUILDING WITH ASPECT RATIO 9

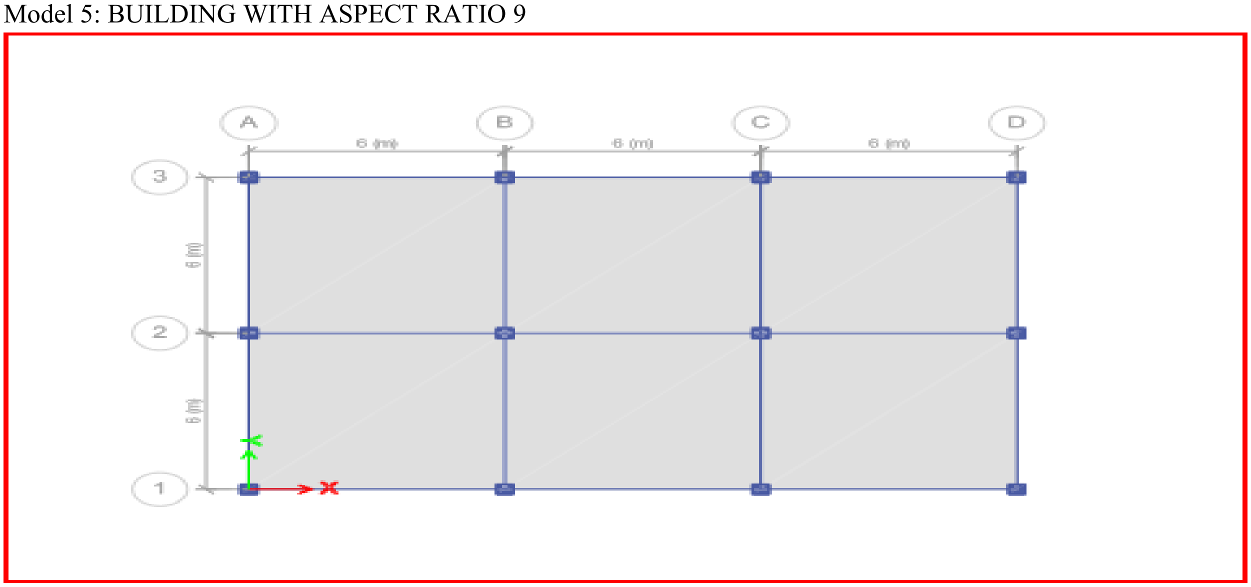


Figure 4.9: Model plan view of building with aspect ratio 9

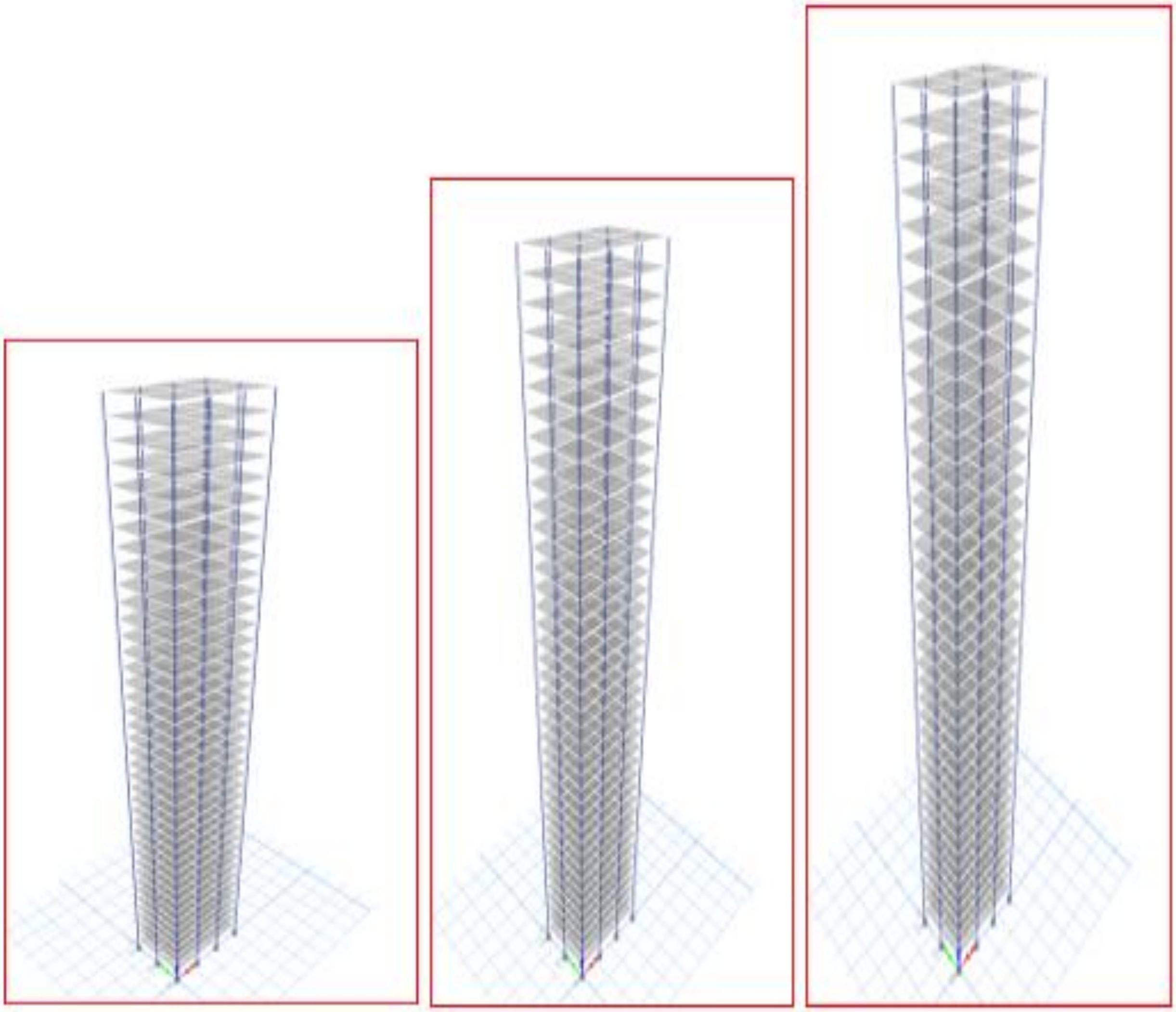

Figure 4.10: Isometric Views of 40, 30 and 20 stories with aspect ratio 9

## 5 RESULTS AND DISCUSSION

### 5.1 General

The Dynamic wind analysis method was employed to gain insight into the overall behavior of the structure and identify any issues within the model. A thorough examination of displacements and time periods was conducted, leading to necessary adjustments in the structure to ensure a satisfactory contribution of mass in the fundamental modes. The Mass source was defined, accounting for a 0.5 reduction for live loads. Eigenvector analysis was then utilized to determine the frequencies and mode shapes of the structure.

In calculating the seismic mass, the weight of the structure participating during excitation was considered, comprising the full dead load and a portion of the live load. This comprehensive approach ensures an accurate representation of the dynamic forces acting on the structure during seismic events. To achieve a meaningful analysis, the number of modes selected was such that at least 90% of mass participation was attained. This meticulous process enhances the reliability of the structural analysis, providing valuable insights into its response to seismic forces and guiding necessary adjustments for optimal performance and safety.

- Model M1 - With Aspect ratio as 9
- Model M2 - Aspect ratio as 7
- Model M3 - Aspect ratio as 4
- Model M4 - Aspect ratio as 2.25
- Model M5 - Aspect ratio as 1 (Base Model)

### 5.2: RESULTS FOR 40 STORY MODEL:

5.2.1 Displacement results

| STORY DISPLACEMENT FOR 40 STORY MODEL | | | | | | | | | | |
|---|---|---|---|---|---|---|---|---|---|---|
| | Model M1 | | Model M2 | | Model M3 | | Model M4 | | Model M5 | |
| Story | X-Dir | Y-Dir | X-Dir | Y-Dir | X-Dir | Y-Dir | X-Dir | Y-Dir | X-Dir | Y-Dir |
| | mm | mm | mm | mm | mm | mm | mm | mm | mm | mm |
| Base | 0 | 0 | 0 | 0 | 0 | 0 | 0 | 0 | 0 | 0 |
| Story1 | 1.699 | 1.708 | 1.649 | 1.653 | 1.459 | 1.462 | 1.373 | 1.375 | 1.123 | 1.125 |
| Story2 | 4.708 | 4.723 | 4.478 | 4.483 | 3.94 | 3.945 | 3.643 | 3.647 | 2.93 | 2.933 |
| Story3 | 8.29 | 8.307 | 7.828 | 7.834 | 6.857 | 6.863 | 6.31 | 6.315 | 5.001 | 5.005 |
| Story4 | 12.318 | 12.337 | 11.603 | 11.61 | 10.126 | 10.131 | 9.311 | 9.316 | 7.283 | 7.287 |
| Story5 | 16.745 | 16.766 | 15.763 | 15.771 | 13.709 | 13.714 | 12.614 | 12.621 | 9.751 | 9.756 |
| Story6 | 21.538 | 21.561 | 20.278 | 20.289 | 17.579 | 17.584 | 16.195 | 16.203 | 12.383 | 12.389 |
| Story7 | 26.667 | 26.692 | 25.121 | 25.134 | 21.712 | 21.718 | 20.031 | 20.04 | 15.16 | 15.167 |
| Story8 | 32.107 | 32.134 | 30.268 | 30.283 | 26.086 | 26.094 | 24.1 | 24.111 | 18.065 | 18.073 |
| Story9 | 37.832 | 37.861 | 35.694 | 35.712 | 30.681 | 30.69 | 28.384 | 28.396 | 21.082 | 21.091 |
| Story10 | 43.82 | 43.85 | 41.378 | 41.398 | 35.478 | 35.488 | 32.863 | 32.876 | 24.195 | 24.205 |
| Story11 | 50.047 | 50.08 | 47.298 | 47.322 | 40.458 | 40.468 | 37.521 | 37.535 | 27.391 | 27.401 |
| Story12 | 56.494 | 56.528 | 53.436 | 53.462 | 45.603 | 45.615 | 42.339 | 42.355 | 30.655 | 30.666 |
| Story13 | 63.139 | 63.176 | 59.771 | 59.801 | 50.898 | 50.911 | 47.303 | 47.32 | 33.975 | 33.987 |
| Story14 | 69.965 | 70.003 | 66.286 | 66.32 | 56.326 | 56.341 | 52.397 | 52.415 | 37.338 | 37.351 |
| Story15 | 76.952 | 76.992 | 72.964 | 73.001 | 61.874 | 61.889 | 57.606 | 57.625 | 40.733 | 40.746 |
| Story16 | 84.084 | 84.126 | 79.788 | 79.829 | 67.526 | 67.542 | 62.915 | 62.937 | 44.148 | 44.163 |
| Story17 | 91.343 | 91.387 | 86.742 | 86.786 | 73.268 | 73.286 | 68.313 | 68.335 | 47.574 | 47.59 |
| Story18 | 98.713 | 98.759 | 93.81 | 93.858 | 79.089 | 79.107 | 73.785 | 73.809 | 51 | 51.017 |
| Story19 | 106.179 | 106.227 | 100.979 | 101.031 | 84.975 | 84.995 | 79.319 | 79.345 | 54.418 | 54.435 |
| Story20 | 113.728 | 113.777 | 108.234 | 108.291 | 90.916 | 90.936 | 84.904 | 84.932 | 57.817 | 57.835 |
| Story21 | 121.344 | 121.395 | 115.563 | 115.624 | 96.9 | 96.921 | 90.53 | 90.559 | 61.19 | 61.209 |
| Story22 | 129.015 | 129.068 | 122.953 | 123.018 | 102.916 | 102.939 | 96.185 | 96.215 | 64.53 | 64.55 |
| Story23 | 136.728 | 136.783 | 130.391 | 130.462 | 108.956 | 108.979 | 101.859 | 101.891 | 67.829 | 67.849 |
| Story24 | 144.471 | 144.528 | 137.868 | 137.943 | 115.01 | 115.034 | 107.543 | 107.577 | 71.079 | 71.101 |
| Story25 | 152.233 | 152.293 | 145.371 | 145.451 | 121.068 | 121.093 | 113.229 | 113.265 | 74.276 | 74.298 |
| Story26 | 160.004 | 160.066 | 152.891 | 152.977 | 127.123 | 127.15 | 118.908 | 118.945 | 77.413 | 77.436 |
| Story27 | 167.773 | 167.836 | 160.418 | 160.509 | 133.168 | 133.195 | 124.571 | 124.61 | 80.484 | 80.508 |
| Story28 | 175.531 | 175.596 | 167.944 | 168.04 | 139.195 | 139.223 | 130.213 | 130.254 | 83.485 | 83.51 |
| Story29 | 183.268 | 183.336 | 175.459 | 175.561 | 145.197 | 145.226 | 135.825 | 135.868 | 86.411 | 86.437 |
| Story30 | 190.978 | 191.047 | 182.955 | 183.064 | 151.168 | 151.198 | 141.402 | 141.447 | 89.258 | 89.285 |
| Story31 | 198.651 | 198.721 | 190.427 | 190.541 | 157.103 | 157.134 | 146.938 | 146.985 | 92.023 | 92.051 |
| Story32 | 206.28 | 206.353 | 197.866 | 197.986 | 162.997 | 163.028 | 152.428 | 152.476 | 94.702 | 94.731 |
| Story33 | 213.86 | 213.934 | 205.266 | 205.393 | 168.845 | 168.877 | 157.867 | 157.917 | 97.293 | 97.323 |
| Story34 | 221.384 | 221.46 | 212.622 | 212.756 | 174.643 | 174.675 | 163.25 | 163.302 | 99.793 | 99.825 |
| Story35 | 228.847 | 228.925 | 219.929 | 220.069 | 180.387 | 180.42 | 168.575 | 168.629 | 102.2 | 102.236 |
| Story36 | 236.244 | 236.324 | 227.182 | 227.329 | 186.075 | 186.109 | 173.837 | 173.893 | 104.517 | 104.555 |

| | | | | | | | | | | |
|---|---|---|---|---|---|---|---|---|---|---|
| Story37 | 243.572 | 243.653 | 234.377 | 234.532 | 191.703 | 191.739 | 179.036 | 179.094 | 106.739 | 106.778 |
| Story38 | 250.826 | 250.91 | 241.512 | 241.674 | 197.271 | 197.307 | 184.169 | 184.232 | 108.867 | 108.907 |
| Story39 | 258.005 | 258.09 | 248.583 | 248.752 | 202.777 | 202.813 | 189.233 | 189.301 | 110.902 | 110.941 |
| Story40 | 265.106 | 265.192 | 255.588 | 255.765 | 208.219 | 208.256 | 194.228 | 194.298 | 112.844 | 112.883 |

Table 5.1: Story Displacement for 40 story model with different slender ratio

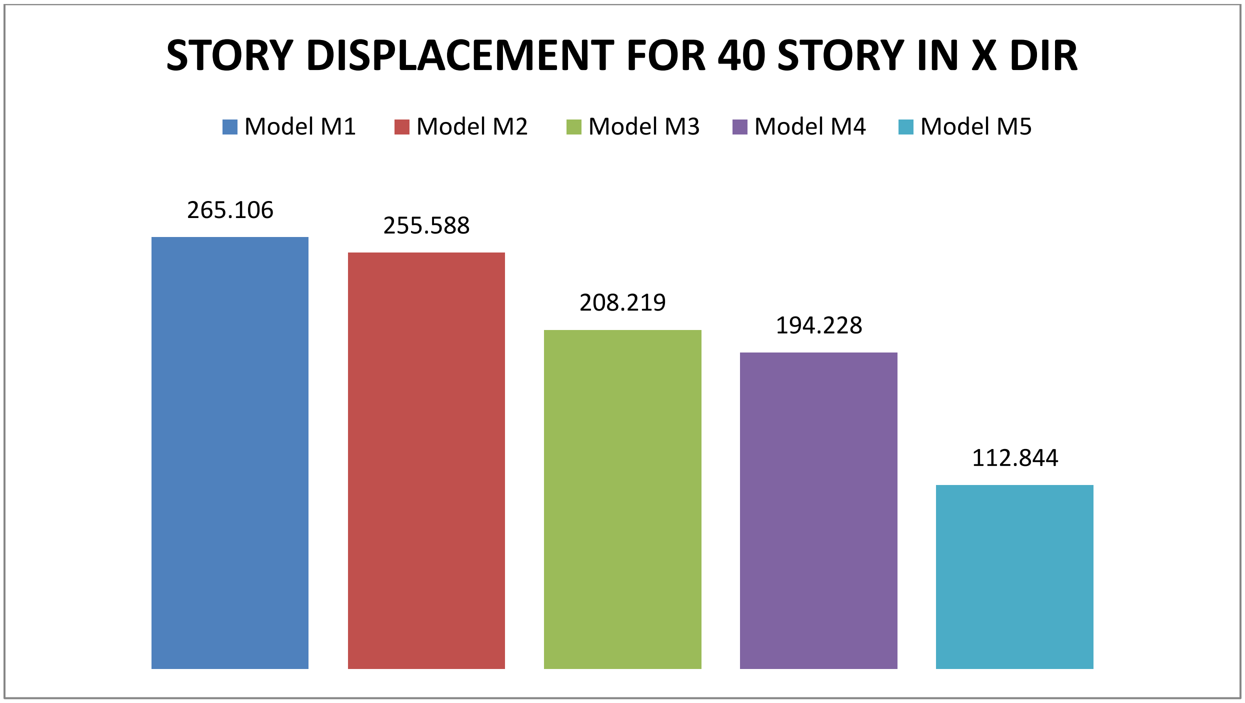


Figure 5.1: Story Displacement in x- dir for 40 stories Model

As per the observation from the above figure 5.1 it is found that the displacement of the building Increases when slenderness of structure is more. It is found that the displacement is reduced by 5.05% 12.43 % and 5.14 % when compared with normal model.

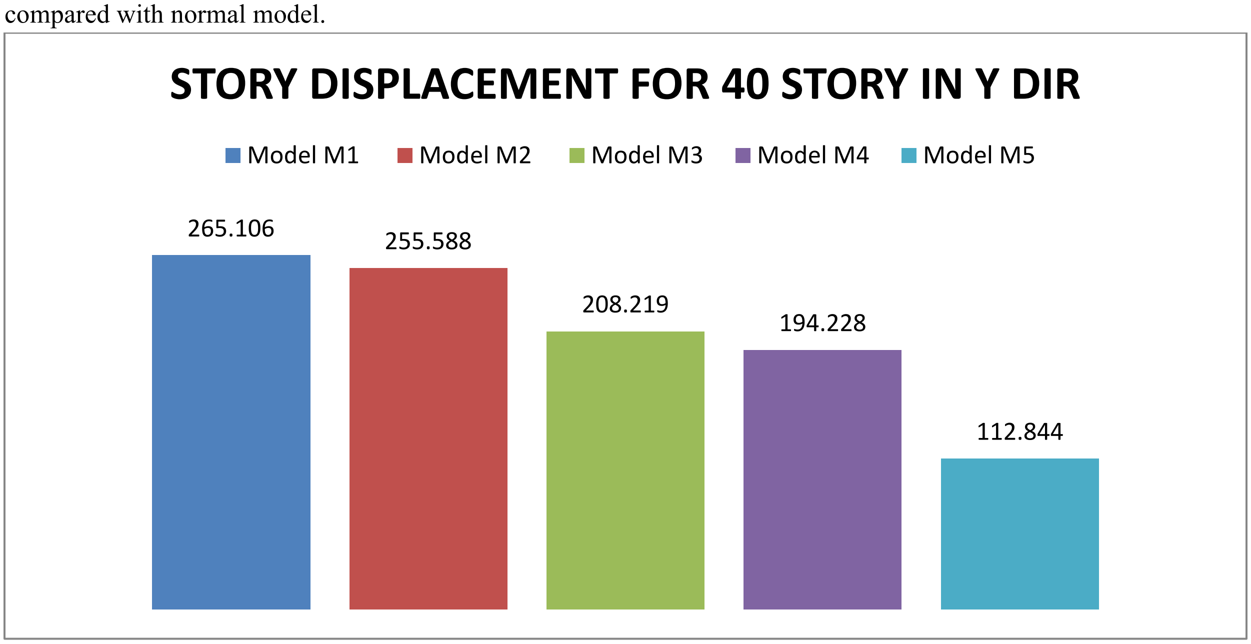


Figure 5.2: Story Displacement in x- dir for 40 stories Model

5.2.2 Story drift results

| STORY DRIFT FOR 40 STORY MODEL | | | | | | | | | | |
|---|---|---|---|---|---|---|---|---|---|---|
| | Model M1 | | Model M2 | | Model M3 | | Model M4 | | Model M5 | |
| Story | X-Dir | Y-Dir | X-Dir | Y-Dir | X-Dir | Y-Dir | X-Dir | Y-Dir | X-Dir | Y-Dir |
| | mm | mm | mm | mm | mm | mm | mm | mm | mm | mm |
| Base | 0 | 0 | 0 | 0 | 0 | 0 | 0 | 0 | 0 | 0 |
| Story1 | 0.000566 | 0.000569 | 0.00055 | 0.000551 | 0.000486 | 0.000487 | 0.000458 | 0.000458 | 0.000374 | 0.000375 |
| Story2 | 0.001003 | 0.001005 | 0.000943 | 0.000943 | 0.000827 | 0.000828 | 0.000757 | 0.000757 | 0.000602 | 0.000603 |
| Story3 | 0.001194 | 0.001195 | 0.001117 | 0.001117 | 0.000972 | 0.000973 | 0.000889 | 0.000889 | 0.00069 | 0.000691 |
| Story4 | 0.001343 | 0.001343 | 0.001258 | 0.001259 | 0.00109 | 0.001089 | 0.001 | 0.001 | 0.000761 | 0.000761 |
| Story5 | 0.001476 | 0.001476 | 0.001387 | 0.001387 | 0.001194 | 0.001194 | 0.001101 | 0.001101 | 0.000823 | 0.000823 |
| Story6 | 0.001598 | 0.001598 | 0.001505 | 0.001506 | 0.00129 | 0.00129 | 0.001194 | 0.001194 | 0.000877 | 0.000878 |
| Story7 | 0.00171 | 0.00171 | 0.001614 | 0.001615 | 0.001378 | 0.001378 | 0.001279 | 0.001279 | 0.000926 | 0.000926 |
| Story8 | 0.001813 | 0.001814 | 0.001715 | 0.001716 | 0.001458 | 0.001458 | 0.001357 | 0.001357 | 0.000968 | 0.000969 |
| Story9 | 0.001908 | 0.001909 | 0.001809 | 0.00181 | 0.001532 | 0.001532 | 0.001428 | 0.001428 | 0.001006 | 0.001006 |
| Story10 | 0.001996 | 0.001996 | 0.001895 | 0.001896 | 0.001599 | 0.001599 | 0.001493 | 0.001494 | 0.001038 | 0.001038 |
| Story11 | 0.002076 | 0.002076 | 0.001974 | 0.001974 | 0.00166 | 0.00166 | 0.001552 | 0.001553 | 0.001065 | 0.001065 |
| Story12 | 0.002149 | 0.002149 | 0.002046 | 0.002047 | 0.001715 | 0.001716 | 0.001606 | 0.001607 | 0.001088 | 0.001088 |
| Story13 | 0.002215 | 0.002216 | 0.002112 | 0.002113 | 0.001765 | 0.001765 | 0.001655 | 0.001655 | 0.001107 | 0.001107 |
| Story14 | 0.002275 | 0.002276 | 0.002172 | 0.002173 | 0.00181 | 0.00181 | 0.001698 | 0.001698 | 0.001121 | 0.001121 |
| Story15 | 0.002329 | 0.00233 | 0.002226 | 0.002227 | 0.001849 | 0.001849 | 0.001736 | 0.001737 | 0.001132 | 0.001132 |
| Story16 | 0.002377 | 0.002378 | 0.002275 | 0.002276 | 0.001884 | 0.001884 | 0.00177 | 0.00177 | 0.001139 | 0.001139 |
| Story17 | 0.00242 | 0.00242 | 0.002318 | 0.002319 | 0.001914 | 0.001915 | 0.001799 | 0.0018 | 0.001142 | 0.001142 |
| Story18 | 0.002457 | 0.002457 | 0.002356 | 0.002357 | 0.00194 | 0.001941 | 0.001824 | 0.001824 | 0.001142 | 0.001142 |
| Story19 | 0.002489 | 0.002489 | 0.00239 | 0.002391 | 0.001962 | 0.001962 | 0.001845 | 0.001845 | 0.001139 | 0.001139 |
| Story20 | 0.002516 | 0.002517 | 0.002418 | 0.00242 | 0.00198 | 0.001981 | 0.001862 | 0.001862 | 0.001133 | 0.001133 |
| Story21 | 0.002539 | 0.002539 | 0.002443 | 0.002444 | 0.001995 | 0.001995 | 0.001875 | 0.001876 | 0.001124 | 0.001125 |
| Story22 | 0.002557 | 0.002558 | 0.002463 | 0.002465 | 0.002006 | 0.002006 | 0.001885 | 0.001885 | 0.001113 | 0.001113 |
| Story23 | 0.002571 | 0.002572 | 0.00248 | 0.002481 | 0.002013 | 0.002014 | 0.001891 | 0.001892 | 0.0011 | 0.0011 |

| | | | | | | | | | | |
|---|---|---|---|---|---|---|---|---|---|---|
| Story24 | 0.002581 | 0.002582 | 0.002492 | 0.002494 | 0.002018 | 0.002018 | 0.001895 | 0.001895 | 0.001084 | 0.001084 |
| Story25 | 0.002587 | 0.002588 | 0.002501 | 0.002503 | 0.00202 | 0.00202 | 0.001895 | 0.001896 | 0.001066 | 0.001066 |
| Story26 | 0.00259 | 0.002591 | 0.002507 | 0.002508 | 0.002019 | 0.002019 | 0.001893 | 0.001893 | 0.001046 | 0.001046 |
| Story27 | 0.00259 | 0.00259 | 0.002509 | 0.002511 | 0.002015 | 0.002015 | 0.001888 | 0.001888 | 0.001024 | 0.001024 |
| Story28 | 0.002586 | 0.002587 | 0.002508 | 0.00251 | 0.002009 | 0.002009 | 0.00188 | 0.001881 | 0.001 | 0.001001 |
| Story29 | 0.002579 | 0.00258 | 0.002505 | 0.002507 | 0.002001 | 0.002001 | 0.001871 | 0.001871 | 0.000975 | 0.000976 |
| Story30 | 0.00257 | 0.00257 | 0.002499 | 0.002501 | 0.001991 | 0.001991 | 0.001859 | 0.00186 | 0.000949 | 0.000949 |
| Story31 | 0.002558 | 0.002558 | 0.00249 | 0.002492 | 0.001978 | 0.001979 | 0.001845 | 0.001846 | 0.000922 | 0.000922 |
| Story32 | 0.002543 | 0.002544 | 0.00248 | 0.002482 | 0.001965 | 0.001965 | 0.00183 | 0.001831 | 0.000893 | 0.000893 |
| Story33 | 0.002527 | 0.002527 | 0.002467 | 0.002469 | 0.001949 | 0.00195 | 0.001813 | 0.001814 | 0.000864 | 0.000864 |
| Story34 | 0.002508 | 0.002509 | 0.002452 | 0.002454 | 0.001933 | 0.001933 | 0.001794 | 0.001795 | 0.000833 | 0.000834 |
| Story35 | 0.002488 | 0.002488 | 0.002436 | 0.002438 | 0.001915 | 0.001915 | 0.001775 | 0.001776 | 0.000803 | 0.000804 |
| Story36 | 0.002466 | 0.002466 | 0.002418 | 0.00242 | 0.001896 | 0.001896 | 0.001754 | 0.001755 | 0.000772 | 0.000773 |
| Story37 | 0.002443 | 0.002443 | 0.002399 | 0.002401 | 0.001876 | 0.001877 | 0.001733 | 0.001734 | 0.000741 | 0.000741 |
| Story38 | 0.002418 | 0.002419 | 0.002378 | 0.002381 | 0.001856 | 0.001856 | 0.001711 | 0.001713 | 0.00071 | 0.00071 |
| Story39 | 0.002393 | 0.002393 | 0.002357 | 0.00236 | 0.001835 | 0.001835 | 0.001688 | 0.00169 | 0.000678 | 0.000678 |
| Story40 | 0.002367 | 0.002367 | 0.002335 | 0.002338 | 0.001814 | 0.001814 | 0.001665 | 0.001666 | 0.000647 | 0.000647 |

Table 5.2: Story Drift for 40 story model with different slender ratio

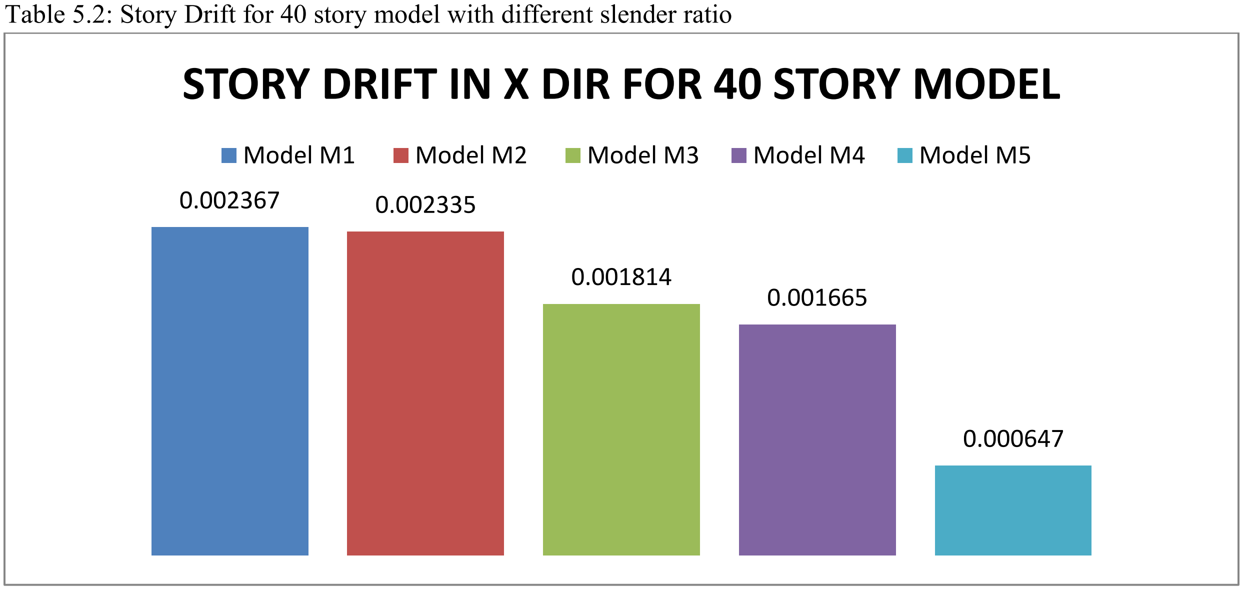


Figure 5.3: Story Drift in x- dir for 40 story Model

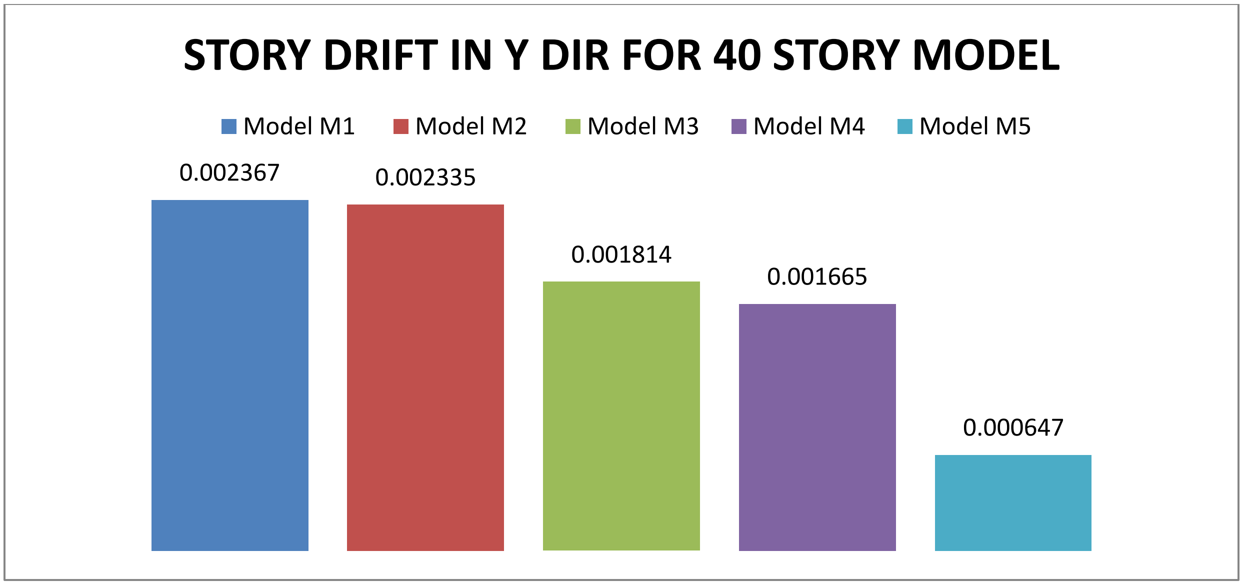


Figure 5.4: Story Drift in y- dir for 40 stories Model

5.2.3 Story stiffness results

| STORY STIFFNESS FOR 40 STORY MODEL | | | | | | | | | | |
|---|---|---|---|---|---|---|---|---|---|---|
| | Model M1 | | Model M2 | | Model M3 | | Model M4 | | Model M5 | |
| Story | X-Dir | Y-Dir | X-Dir | Y-Dir | X-Dir | Y-Dir | X-Dir | Y-Dir | X-Dir | Y-Dir |
| | KN/M | KN/M | KN/M | KN/M | KN/M | KN/M | KN/M | KN/M | KN/M | KN/M |
| Base | 0 | 0 | 0 | 0 | 0 | 0 | 0 | 0 | 0 | 0 |
| Story 1 | 70308356.3 | 70944823.9 | 67989214 | 67822334 | 70274445.5 | 70215706 | 67550413.5 | 67328389 | 73117231.6 | 73344241 |
| Story 2 | 40307603.1 | 40222754.6 | 39108501 | 39049485 | 40757253.1 | 40718358 | 40095478.5 | 40068816 | 44797630.8 | 44766839 |
| Story 3 | 33420048 | 33394527.8 | 32548036 | 32517893 | 34131760.9 | 34118270 | 33546370.2 | 33532674 | 38334159.4 | 38318114 |
| Story 4 | 29320567 | 29306270.9 | 28450033 | 28434916 | 30001755.6 | 29982604 | 29301888.5 | 29291340 | 34114484.4 | 34101948 |
| Story 5 | 26299952.8 | 26289216.7 | 25414506 | 25402031 | 26909536.6 | 26892173 | 26128232.1 | 26119487 | 30905646.1 | 30895141 |
| Story 6 | 23918267.6 | 23909326.8 | 23023271 | 23012223 | 24450713 | 24443029 | 23623353.5 | 23615844 | 28334361.2 | 28325267 |
| Story 7 | 21979410.2 | 21971693 | 21080626 | 21070572 | 22449861.9 | 22443723 | 21587052.1 | 21580466 | 26219659.6 | 26211636 |
| Story 8 | 20364008.6 | 20357208 | 19464994 | 19455705 | 20779425.7 | 20774203 | 19892901.6 | 19887027 | 24444328.5 | 24437138 |
| Story 9 | 18994039.8 | 18987954.6 | 18096889 | 18088206 | 19360191.4 | 19355622 | 18458174.7 | 18452862 | 22930777.5 | 22924248 |
| Story 10 | 17813430.6 | 17807921.5 | 16919330 | 16911139 | 18134948.7 | 18130899 | 17223271.3 | 17218412 | 21621484.5 | 21615492 |
| Story 11 | 16782243.3 | 16777209.2 | 15891856 | 15884072 | 17062983 | 17059356 | 16145899.5 | 16141413 | 20475171.5 | 20469620 |

| | | | | | | | | | | |
|---|---|---|---|---|---|---|---|---|---|---|
| Story 12 | 15872656.7 | 15868018.9 | 14986349 | 14978904 | 16116104.1 | 16112826 | 15196865.6 | 15192690 | 19463664.8 | 19458480 |
| Story 13 | 15062358.9 | 15058056.7 | 14180317 | 14173158 | 15271513.2 | 15268528 | 14352648.1 | 14348734 | 18563518.1 | 18558641 |
| Story 14 | 14333732.1 | 14329718.5 | 13456043 | 13449128 | 14511149.7 | 14508414 | 13594671.6 | 13590980 | 17755913.1 | 17751295 |
| Story 15 | 13672913.7 | 13669151.8 | 12799620 | 12792914 | 13820790.9 | 13818271 | 12908351.4 | 12904853 | 17025928 | 17021532 |
| Story 16 | 13068785.5 | 13065245.7 | 12199924 | 12193400 | 13189020.7 | 13186689 | 12282020.3 | 12278689 | 16361483.8 | 16357277 |
| Story 17 | 12512273 | 12508931.7 | 11647909 | 11641543 | 12606514.4 | 12604348 | 11706186.9 | 11703003 | 15752605 | 15748562 |
| Story 18 | 11996647.2 | 11993484.2 | 11136881 | 11130655 | 12066425.7 | 12064407 | 11173899.9 | 11170846 | 15192170.3 | 15188269 |
| Story 19 | 11516851.3 | 11513848.9 | 10661817 | 10655714 | 11563658.7 | 11561771 | 10679988.9 | 10677050 | 14675086.6 | 14671306 |
| Story 20 | 11067681 | 11064824.5 | 10217567 | 10211572 | 11092862.1 | 11091092 | 10219050.3 | 10216214 | 14195545.3 | 14191868 |
| Story 21 | 10644657.2 | 10641934.5 | 9799714 | 9793816 | 10649429 | 10647766 | 9786442.38 | 9783699 | 13748499.3 | 13744911 |
| Story 22 | 10243934 | 10241335 | 9404480 | 9398669 | 10229407 | 10227842 | 9378195.15 | 9375536 | 13329573.2 | 13326061 |
| Story 23 | 9862168.66 | 9859684.92 | 9028596 | 9022865 | 9829365.91 | 9827891 | 8990874.91 | 8988292 | 12934913.9 | 12931469 |
| Story 24 | 9496424.96 | 9494049.34 | 8669209 | 8663551 | 9446299.43 | 9444908 | 8621483.68 | 8618971 | 12561080.9 | 12557700 |
| Story 25 | 9144098.16 | 9141824.71 | 8323805 | 8318215 | 9077548.48 | 9076234 | 8267380.01 | 8264933 | 12204958.2 | 12201943 |
| Story 26 | 8802854.65 | 8800678.41 | 7990146 | 7984622 | 8720740.02 | 8719499 | 7926215.88 | 7923830 | 11863678.9 | 11860687 |
| Story 27 | 8470583.35 | 8468500.21 | 7666229 | 7660769 | 8373737.86 | 8372565 | 7595885.97 | 7593557 | 11534559.6 | 11531259 |
| Story 28 | 8145356.18 | 8143362.83 | 7350240 | 7344843 | 8034602.87 | 8033495 | 7274486.65 | 7272213 | 11215018.3 | 11211709 |
| Story 29 | 7825395.81 | 7823489.59 | 7040527 | 7035194 | 7701560.73 | 7700515 | 6960282.63 | 6958062 | 10902285.1 | 10899001 |
| Story 30 | 7509049.12 | 7507228 | 6735570 | 6730305 | 7372975.8 | 7371990 | 6651679.92 | 6649511 | 10594667.6 | 10591354 |
| Story 31 | 7194765.4 | 7193027.9 | 6433965 | 6428771 | 7047329.85 | 7046402 | 6347203.76 | 6345086 | 10289657.6 | 10286260 |
| Story 32 | 6881078.17 | 6879423.34 | 6134403 | 6129286 | 6723204.76 | 6722333 | 6045480.71 | 6043414 | 9984040.72 | 9980545 |
| Story 33 | 6566587.83 | 6565015.27 | 5835653 | 5830621 | 6399266.61 | 6398449 | 5745222.73 | 5743207 | 9675754.59 | 9671798 |
| Story 34 | 6250007.01 | 6248516.78 | 5536609 | 5531670 | 6074314.5 | 6073550 | 5445273.56 | 5443308 | 9365297.25 | 9357065 |
| Story 35 | 5930835.21 | 5929427.26 | 5236897 | 5232063 | 5747974.62 | 5747263 | 5145258.7 | 5143344 | 9048051.82 | 9031382 |

| | | | | | | | | | | |
|---|---|---|---|---|---|---|---|---|---|---|
| Story 36 | 5608377.98 | 5607052.35 | 4935973 | 4931254 | 5419680.52 | 5419020 | 4844618 | 4842739 | 8711912.85 | 8700347 |
| Story 37 | 5281510.2 | 5280267.34 | 4632909 | 4628320 | 5088438.34 | 5087828 | 4542388.05 | 4540433 | 8361598.49 | 8360059 |
| Story 38 | 4949158.93 | 4947999.65 | 4326839 | 4322395 | 4753326.67 | 4752766 | 4237680.43 | 4234225 | 7999962.62 | 7999356 |
| Story 39 | 4610302.15 | 4609227.54 | 4016953 | 4012673 | 4413496.54 | 4412985 | 3929698.73 | 3926550 | 7617599.29 | 7617415 |
| Story 40 | 4263969.99 | 4262981.33 | 3702502 | 3698404 | 4068173.44 | 4067711 | 3617686.36 | 3616219 | 7209489.14 | 7209581 |

Table 5.3: Story stiffness for 40 story model with different slender ratio

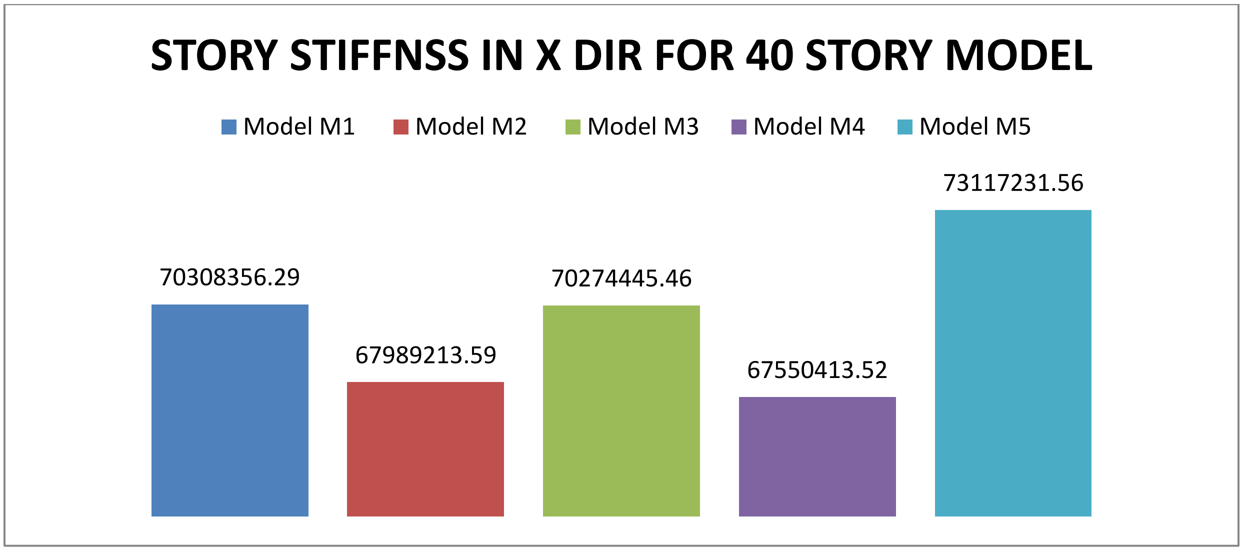


Figure 5.5: Story stiffness in x- dir for 40 stories Model

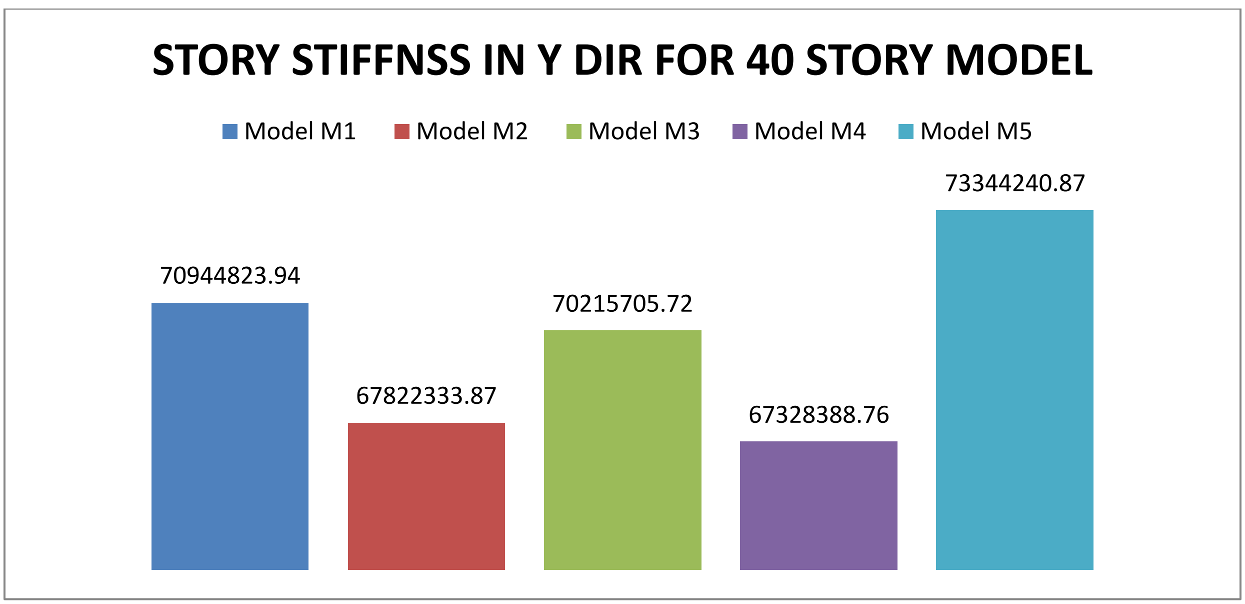


Figure 5.6: Story stiffness in y- dir for 40 stories Model

5.2.4 Time period results

| TIME PERIOD FOR 40 STORY MODEL | | | | | |
|---|---|---|---|---|---|
| MODES | MODEL M1 | MODEL M2 | MODEL M3 | MODEL M4 | MODEL M5 |
| 1 | 3.373 | 2.529 | 2.749 | 2.1 | 1.637 |
| 2 | 3.373 | 2.528 | 2.748 | 2.099 | 1.636 |
| 3 | 2.256 | 1.502 | 1.579 | 1.088 | 0.94 |
| 4 | 0.863 | 0.648 | 0.754 | 0.571 | 0.516 |
| 5 | 0.863 | 0.648 | 0.754 | 0.57 | 0.516 |
| 6 | 0.751 | 0.521 | 0.576 | 0.41 | 0.366 |
| 7 | 0.449 | 0.313 | 0.364 | 0.273 | 0.257 |
| 8 | 0.414 | 0.309 | 0.364 | 0.273 | 0.257 |
| 9 | 0.414 | 0.309 | 0.347 | 0.248 | 0.223 |
| 10 | 0.319 | 0.223 | 0.248 | 0.177 | 0.168 |
| 11 | 0.269 | 0.2 | 0.236 | 0.177 | 0.168 |
| 12 | 0.269 | 0.2 | 0.236 | 0.177 | 0.159 |

Table 5.4: Time period for 40 story model with different slender ratio

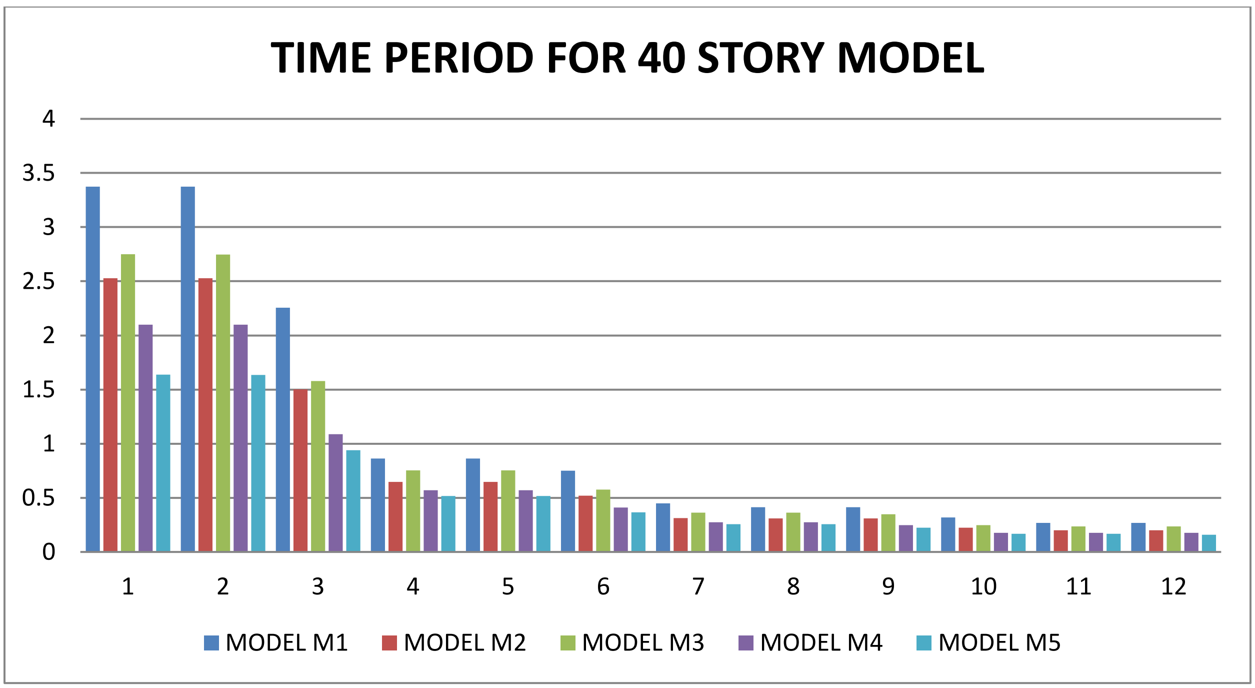


Figure 5.7: Time period for 40 stories Model

5.2.5 Base shear results

| BASE SHEAR FOR 40 STORY MODEL | | | | | |
|---|---|---|---|---|---|
| | MODEL M1 | MODEL M2 | MODEL M3 | MODEL M4 | MODEL M5 |
| X DIR | 131864.651 | 102100.5394 | 102681.9417 | 92290.587 | 82389.2322 |
| Y DIR | 131864.651 | 102100.5394 | 102681.9417 | 92290.587 | 82389.2322 |

Table 5.5: Base shear for 40 story model with different slender ratio

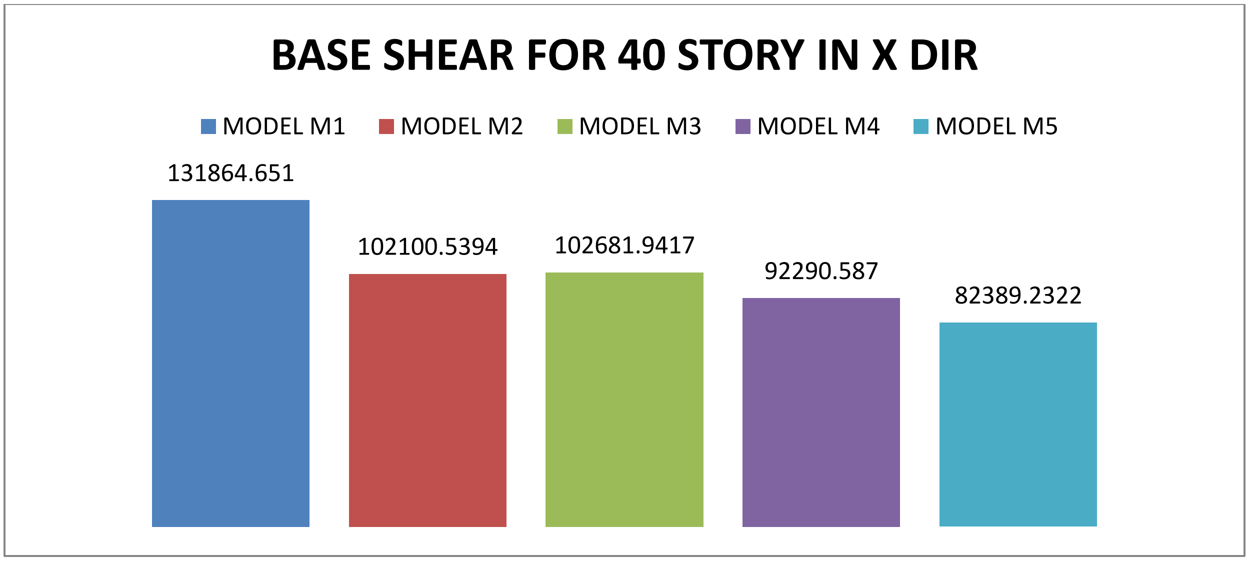


Figure 5.8: Base shear in x dir for 40 stories Model

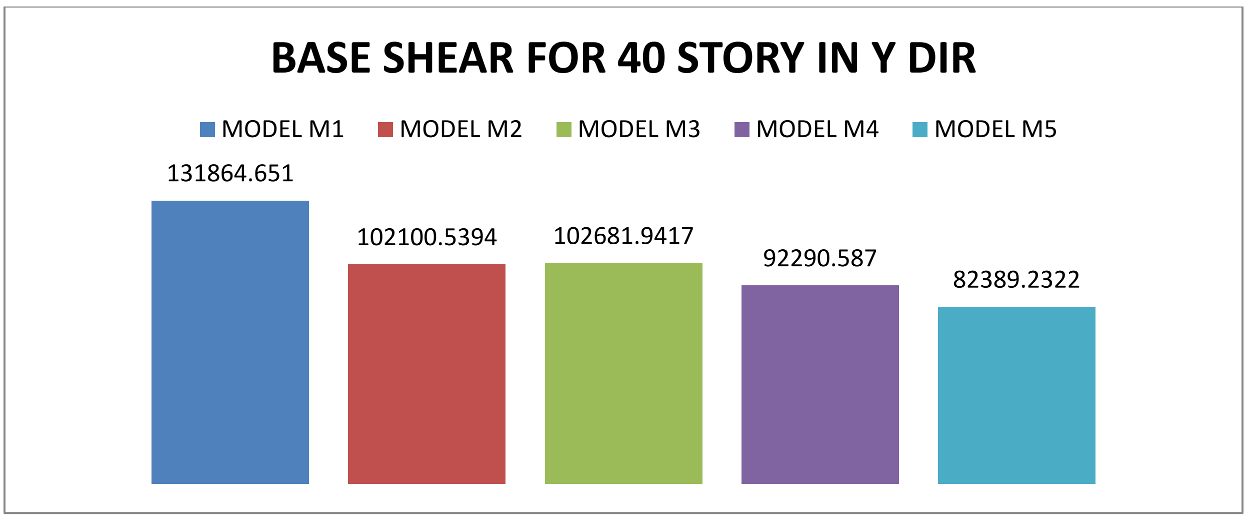


Figure 5.9: Base shear in y dir for 40 stories Model

5.3 RESULTS FOR 30 STORY MODEL

5.3.1 Displacement results for 30 story model:

| STORY DISPLACEMENT FOR 30 STORY MODEL | | | | | | | | | | |
|---|---|---|---|---|---|---|---|---|---|---|
| | Model M1 | | Model M2 | | Model M3 | | Model M4 | | Model M5 | |
| Story | X-Dir | Y-Dir | X-Dir | Y-Dir | X-Dir | Y-Dir | X-Dir | Y-Dir | X-Dir | Y-Dir |
| | mm | mm | mm | mm | mm | mm | mm | mm | mm | mm |
| Base | 0 | 0 | 0 | 0 | 0 | 0 | 0 | 0 | 0 | 0 |
| Story1 | 2.109 | 2.118 | 2.038 | 2.048 | 1.905 | 1.914 | 1.795 | 1.793 | 1.371 | 1.373 |
| Story2 | 5.352 | 5.366 | 5.168 | 5.182 | 4.829 | 4.847 | 4.481 | 4.472 | 3.336 | 3.341 |
| Story3 | 8.999 | 9.015 | 8.684 | 8.7 | 8.109 | 8.128 | 7.504 | 7.485 | 5.534 | 5.54 |
| Story4 | 12.989 | 13.006 | 12.527 | 12.544 | 11.689 | 11.709 | 10.796 | 10.765 | 7.902 | 7.909 |
| Story5 | 17.299 | 17.317 | 16.675 | 16.694 | 15.551 | 15.572 | 14.33 | 14.285 | 10.438 | 10.445 |
| Story6 | 21.915 | 21.935 | 21.117 | 21.138 | 19.684 | 19.706 | 18.103 | 18.043 | 13.103 | 13.112 |

| | | | | | | | | | | |
|---|---|---|---|---|---|---|---|---|---|---|
| Story7 | 26.827 | 26.849 | 25.841 | 25.863 | 24.079 | 24.102 | 22.102 | 22.026 | 15.907 | 15.916 |
| Story8 | 32.025 | 32.048 | 30.837 | 30.861 | 28.726 | 28.75 | 26.32 | 26.225 | 18.846 | 18.855 |
| Story9 | 37.5 | 37.524 | 36.097 | 36.123 | 33.617 | 33.642 | 30.749 | 30.634 | 21.913 | 21.923 |
| Story10 | 43.241 | 43.267 | 41.611 | 41.639 | 38.744 | 38.77 | 35.38 | 35.244 | 25.102 | 25.113 |
| Story11 | 49.242 | 49.269 | 47.372 | 47.401 | 44.099 | 44.127 | 40.207 | 40.048 | 28.407 | 28.419 |
| Story12 | 55.493 | 55.521 | 53.371 | 53.402 | 49.676 | 49.705 | 45.222 | 45.04 | 31.823 | 31.836 |
| Story13 | 61.987 | 62.016 | 59.602 | 59.635 | 55.467 | 55.497 | 50.42 | 50.212 | 35.345 | 35.359 |
| Story14 | 68.716 | 68.747 | 66.056 | 66.091 | 61.465 | 61.496 | 55.794 | 55.559 | 38.968 | 38.982 |
| Story15 | 75.674 | 75.706 | 72.728 | 72.765 | 67.665 | 67.697 | 61.338 | 61.075 | 42.688 | 42.703 |
| Story16 | 82.853 | 82.886 | 79.609 | 79.648 | 74.06 | 74.093 | 67.046 | 66.753 | 46.499 | 46.515 |
| Story17 | 90.245 | 90.281 | 86.694 | 86.735 | 80.643 | 80.677 | 72.913 | 72.588 | 50.398 | 50.414 |
| Story18 | 97.846 | 97.882 | 93.976 | 94.019 | 87.409 | 87.445 | 78.938 | 78.575 | 54.38 | 54.397 |
| Story19 | 105.647 | 105.685 | 101.448 | 101.493 | 94.353 | 94.389 | 85.123 | 84.725 | 58.442 | 58.459 |
| Story20 | 113.643 | 113.682 | 109.105 | 109.155 | 101.468 | 101.505 | 91.415 | 90.983 | 62.578 | 62.596 |
| Story21 | 121.827 | 121.868 | 116.941 | 116.995 | 108.749 | 108.787 | 97.837 | 97.376 | 66.785 | 66.804 |
| Story22 | 130.194 | 130.236 | 124.949 | 125.006 | 116.19 | 116.229 | 104.402 | 103.903 | 71.06 | 71.079 |
| Story23 | 138.736 | 138.78 | 133.124 | 133.183 | 123.787 | 123.827 | 111.094 | 110.556 | 75.398 | 75.418 |
| Story24 | 147.45 | 147.494 | 141.461 | 141.522 | 131.533 | 131.575 | 117.907 | 117.33 | 79.796 | 79.817 |
| Story25 | 156.327 | 156.373 | 149.952 | 150.016 | 139.425 | 139.467 | 124.838 | 124.22 | 84.25 | 84.271 |
| Story26 | 165.364 | 165.411 | 158.594 | 158.66 | 147.456 | 147.499 | 131.881 | 131.221 | 88.757 | 88.778 |
| Story27 | 174.553 | 174.602 | 167.381 | 167.449 | 155.623 | 155.667 | 139.032 | 138.329 | 93.312 | 93.334 |
| Story28 | 183.891 | 183.941 | 176.307 | 176.378 | 163.919 | 163.964 | 146.287 | 145.539 | 97.913 | 97.936 |
| Story29 | 193.37 | 193.422 | 185.368 | 185.441 | 172.341 | 172.386 | 153.641 | 152.848 | 102.556 | 102.58 |
| Story30 | 202.987 | 203.04 | 194.557 | 194.633 | 180.883 | 180.929 | 161.089 | 160.25 | 107.238 | 107.262 |

Table 5.6: Story displacement for 30 story model with different slender ratio

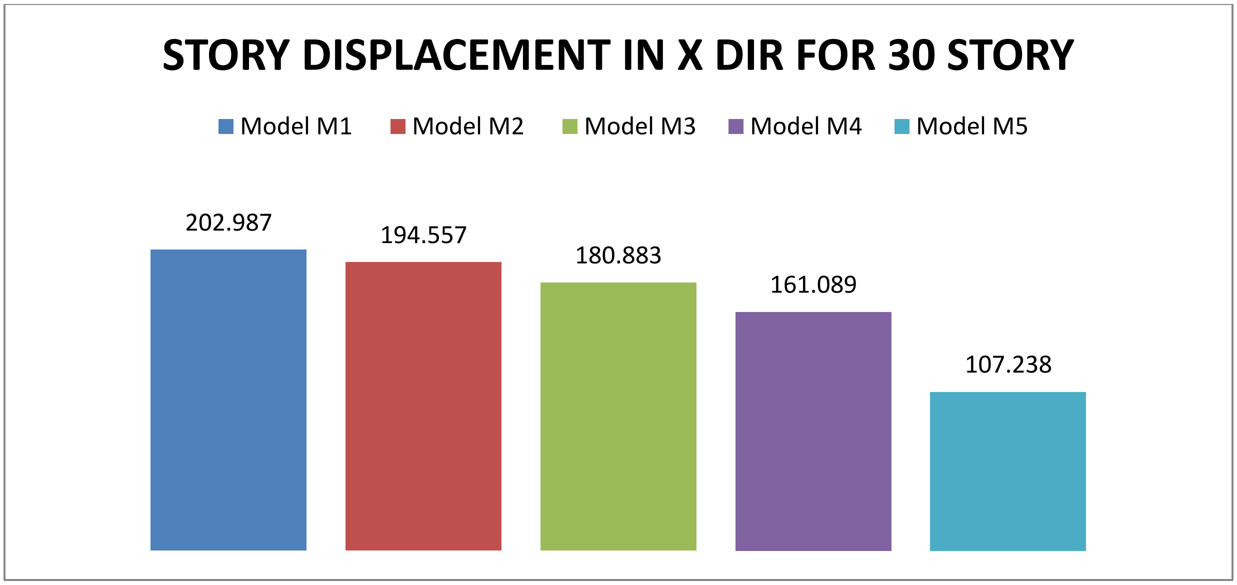


Figure 5.10: Story displacement in x -dir for 30 story model with different slender ratio

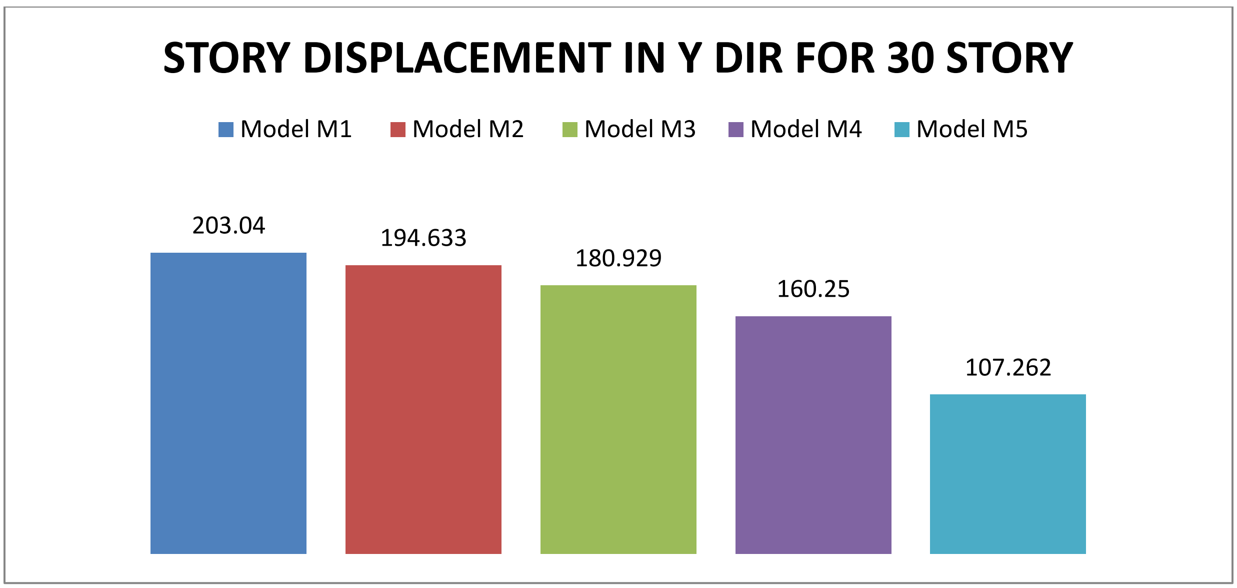


Figure 5.11: Story displacement in y -dir for 30 story model with different slender ratio

5.3.2 Drift results for 30 story model:

| STORY DRIFT FOR 30 STORY MODEL | | | | | | | | | | |
|---|---|---|---|---|---|---|---|---|---|---|
| | Model M1 | | Model M2 | | Model M3 | | Model M4 | | Model M5 | |
| Story | X-Dir | Y-Dir | X-Dir | Y-Dir | X-Dir | Y-Dir | X-Dir | Y-Dir | X-Dir | Y-Dir |
| | mm | mm | mm | mm | mm | mm | mm | mm | mm | mm |
| Base | 0 | 0 | 0 | 0 | 0 | 0 | 0 | 0 | 0 | 0 |
| Story1 | 0.000703 | 0.000706 | 0.000679 | 0.000683 | 0.000635 | 0.000638 | 0.000598 | 0.000598 | 0.000457 | 0.000458 |
| Story2 | 0.001081 | 0.001083 | 0.001043 | 0.001045 | 0.000975 | 0.000977 | 0.000945 | 0.000943 | 0.000698 | 0.000699 |

| | | | | | | | | | | |
|---|---|---|---|---|---|---|---|---|---|---|
| Story3 | 0.001216 | 0.001216 | 0.001172 | 0.001173 | 0.001093 | 0.001094 | 0.001037 | 0.001034 | 0.000787 | 0.000787 |
| Story4 | 0.00133 | 0.00133 | 0.001281 | 0.001282 | 0.001193 | 0.001194 | 0.001099 | 0.001095 | 0.000815 | 0.000815 |
| Story5 | 0.001436 | 0.001437 | 0.001383 | 0.001383 | 0.001287 | 0.001288 | 0.001179 | 0.001174 | 0.000846 | 0.000847 |
| Story6 | 0.001539 | 0.001539 | 0.001481 | 0.001481 | 0.001378 | 0.001378 | 0.001258 | 0.001252 | 0.00089 | 0.00089 |
| Story7 | 0.001637 | 0.001638 | 0.001575 | 0.001575 | 0.001465 | 0.001465 | 0.001333 | 0.001328 | 0.000936 | 0.000936 |
| Story8 | 0.001733 | 0.001733 | 0.001665 | 0.001666 | 0.001549 | 0.001549 | 0.001406 | 0.0014 | 0.00098 | 0.000981 |
| Story9 | 0.001825 | 0.001825 | 0.001753 | 0.001754 | 0.00163 | 0.001631 | 0.001476 | 0.00147 | 0.001023 | 0.001023 |
| Story10 | 0.001914 | 0.001914 | 0.001838 | 0.001839 | 0.001709 | 0.001709 | 0.001544 | 0.001537 | 0.001063 | 0.001063 |
| Story11 | 0.002 | 0.002001 | 0.00192 | 0.001921 | 0.001785 | 0.001786 | 0.001609 | 0.001601 | 0.001102 | 0.001102 |
| Story12 | 0.002084 | 0.002084 | 0.002 | 0.002 | 0.001859 | 0.001859 | 0.001672 | 0.001664 | 0.001139 | 0.001139 |
| Story13 | 0.002165 | 0.002165 | 0.002077 | 0.002077 | 0.00193 | 0.001931 | 0.001733 | 0.001724 | 0.001174 | 0.001174 |
| Story14 | 0.002243 | 0.002244 | 0.002151 | 0.002152 | 0.002 | 0.002 | 0.001791 | 0.001782 | 0.001208 | 0.001208 |
| Story15 | 0.002319 | 0.00232 | 0.002224 | 0.002224 | 0.002067 | 0.002067 | 0.001848 | 0.001839 | 0.00124 | 0.00124 |
| Story16 | 0.002393 | 0.002393 | 0.002294 | 0.002294 | 0.002132 | 0.002132 | 0.001903 | 0.001893 | 0.001271 | 0.001271 |
| Story17 | 0.002464 | 0.002465 | 0.002362 | 0.002362 | 0.002195 | 0.002195 | 0.001956 | 0.001945 | 0.0013 | 0.0013 |
| Story18 | 0.002533 | 0.002534 | 0.002427 | 0.002428 | 0.002255 | 0.002256 | 0.002009 | 0.001998 | 0.001328 | 0.001328 |
| Story19 | 0.0026 | 0.002601 | 0.002491 | 0.002492 | 0.002314 | 0.002315 | 0.002062 | 0.00205 | 0.001354 | 0.001354 |
| Story20 | 0.002665 | 0.002666 | 0.002552 | 0.002554 | 0.002372 | 0.002372 | 0.002102 | 0.002091 | 0.001379 | 0.001379 |
| Story21 | 0.002728 | 0.002729 | 0.002612 | 0.002613 | 0.002427 | 0.002427 | 0.002145 | 0.002133 | 0.001403 | 0.001403 |
| Story22 | 0.002789 | 0.002789 | 0.002669 | 0.00267 | 0.00248 | 0.002481 | 0.002188 | 0.002176 | 0.001425 | 0.001425 |
| Story23 | 0.002848 | 0.002848 | 0.002725 | 0.002726 | 0.002532 | 0.002533 | 0.002231 | 0.002218 | 0.001446 | 0.001446 |
| Story24 | 0.002904 | 0.002905 | 0.002779 | 0.002779 | 0.002582 | 0.002583 | 0.002271 | 0.002258 | 0.001466 | 0.001466 |
| Story25 | 0.002959 | 0.00296 | 0.002831 | 0.002831 | 0.002631 | 0.002631 | 0.00231 | 0.002297 | 0.001485 | 0.001485 |
| Story26 | 0.003012 | 0.003013 | 0.002881 | 0.002881 | 0.002677 | 0.002677 | 0.002348 | 0.002334 | 0.001502 | 0.001502 |

| | | | | | | | | | | |
|---|---|---|---|---|---|---|---|---|---|---|
| Story27 | 0.003063 | 0.003064 | 0.002929 | 0.00293 | 0.002722 | 0.002722 | 0.002384 | 0.002369 | 0.001519 | 0.001519 |
| Story28 | 0.003112 | 0.003113 | 0.002975 | 0.002976 | 0.002765 | 0.002766 | 0.002418 | 0.002404 | 0.001534 | 0.001534 |
| Story29 | 0.00316 | 0.00316 | 0.00302 | 0.003021 | 0.002807 | 0.002807 | 0.002451 | 0.002436 | 0.001548 | 0.001548 |
| Story30 | 0.003206 | 0.003206 | 0.003063 | 0.003064 | 0.002847 | 0.002848 | 0.002483 | 0.002467 | 0.001561 | 0.001561 |

Table 5.7: Story drift for 30 story model with different slender ratio

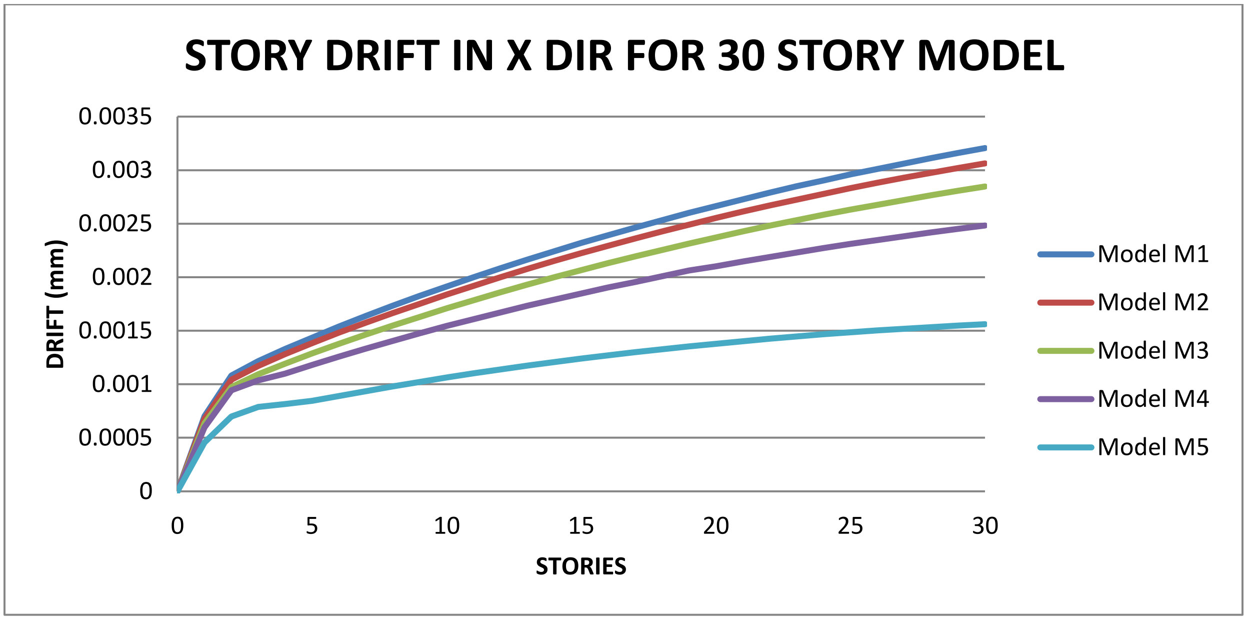


Figure 5.12: Story drift in x -dir for 30 story model with different slender ratio

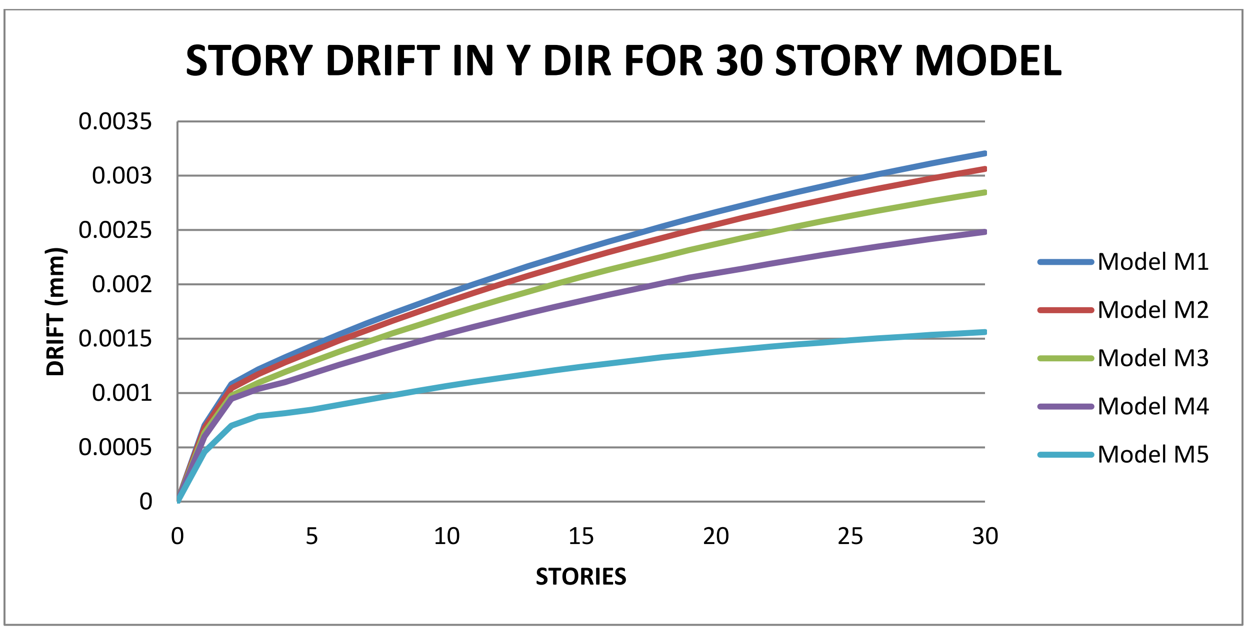


Figure 5.13: Story drift in y -dir for 30 story model with different slender ratio

5.3.3 Story stiffness results for 30 story model:

| STORY STIFFNESS FOR 30 STORY MODEL | | | | | | | | | | |
|---|---|---|---|---|---|---|---|---|---|---|
| | Model M1 | | Model M2 | | Model M3 | | Model M4 | | Model M5 | |
| Story | X-Dir | Y-Dir | X-Dir | Y-Dir | X-Dir | Y-Dir | X-Dir | Y-Dir | X-Dir | Y-Dir |
| | KN/M | KN/M | KN/M | KN/M | KN/M | KN/M | KN/M | KN/M | KN/M | KN/M |
| Base | 0 | 0 | 0 | 0 | 0 | 0 | 0 | 0 | 0 | 0 |
| Story 1 | 212978191 | 212055773 | 213242485 | 212270727 | 213182467 | 212404435 | 214011313 | 213537343 | 245710142 | 244913772 |
| Story 2 | 137695826 | 137491760 | 138093800 | 137872620 | 137955215 | 137749509 | 142022036 | 141952348 | 153990450 | 153834895 |
| Story 3 | 121722932 | 121666459 | 122171341 | 122113865 | 122101849 | 122051693 | 125451421 | 125467972 | 139849832 | 139863420 |
| Story 4 | 110644369 | 110602527 | 111111166 | 111065638 | 111111344 | 111072424 | 114420778 | 114461103 | 130493322 | 130479318 |
| Story 5 | 101812469 | 101778892 | 102285729 | 102247427 | 102266777 | 102235377 | 105707495 | 105764536 | 121838938 | 121797769 |
| Story 6 | 94415912 | 94386983.4 | 94887400.1 | 94853326 | 94846383.86 | 94819491.7 | 98329645.9 | 98396983 | 114344823 | 114308754 |
| Story 7 | 88110677.8 | 88085411.3 | 88575555 | 88544865 | 88516312.17 | 88492985.9 | 91999617.4 | 92074297.1 | 107899042 | 107868781 |
| Story 8 | 82658847.4 | 82636513.2 | 83114055.4 | 83086117 | 83040288.62 | 83019823.8 | 86498879.9 | 86578734.3 | 102263594 | 102236752 |
| Story 9 | 77891489.7 | 77871560.1 | 78335173.4 | 78309521 | 78246113.84 | 78228000.3 | 81667689.6 | 81751160.9 | 97282274.7 | 97258065.9 |
| Story 10 | 73679994.4 | 73662069 | 74110993.4 | 74087267 | 74006372.54 | 73990218.2 | 77382697.3 | 77468619.2 | 92841037 | 92819109.9 |
| Story 11 | 69927079 | 69910846.8 | 70344710.2 | 70322628 | 70224654.39 | 70210152.2 | 73550257.5 | 73637747.2 | 88852276.3 | 88832332.8 |
| Story 12 | 66559789.2 | 66544998 | 66963774 | 66943104 | 66829251.54 | 66816153.5 | 70100345.3 | 70188733.8 | 85249180.7 | 85230948.2 |
| Story 13 | 63518673.1 | 63505120 | 63908952.9 | 63889508 | 63761097.32 | 63749203.4 | 66975266.5 | 67064037.3 | 81975695.3 | 81958947.5 |
| Story 14 | 60755631.6 | 60743152.4 | 61132282.3 | 61113908 | 60972223.24 | 60961371.2 | 64128049.5 | 64216798.6 | 78985894.5 | 78970447.3 |
| Story 15 | 58231687.5 | 58220147.2 | 58594875.2 | 58577442 | 58423740.11 | 58413796.4 | 61520460.7 | 61608868.2 | 76242251.6 | 76227951.6 |
| Story 16 | 55914842.1 | 55904128.7 | 56264797.8 | 56248194 | 56083697.61 | 56074551.2 | 59120896.7 | 59208707.8 | 73713628.1 | 73700346.7 |
| Story 17 | 53778510.1 | 53768530.6 | 54115507.7 | 54099637 | 53925540.37 | 53917098.5 | 56902984.1 | 56989984.9 | 71373799.9 | 71361429.4 |
| Story 18 | 51801503.1 | 51792177.7 | 52125767.8 | 52110342 | 51927874.66 | 51920058.5 | 54847145.8 | 54933185.1 | 69201909.5 | 69190356 |
| Story 19 | 49966690.1 | 49957948.8 | 50278594 | 50263344 | 50073229.29 | 50065970.7 | 52940751.8 | 53025611 | 67181212.2 | 67170392.2 |
| Story 20 | 48258131.6 | 48249915 | 48557553.2 | 48528248 | 48345642.75 | 48338883.7 | 51193179.2 | 51276992.1 | 65295588.5 | 65285430.7 |
| Story 21 | 46662128.6 | 46654385.8 | 46950012.4 | 46922152 | 46731400.3 | 46725090.9 | 49560968.6 | 49643674 | 63531130.8 | 63521573.8 |
| Story 22 | 45166887.5 | 45159574.6 | 45444085.7 | 45430704 | 45218686.42 | 45212783.5 | 47996588.9 | 48077865.4 | 61875798.4 | 61866789 |
| Story 23 | 43762185.6 | 43755264.1 | 44028560 | 44016111 | 43797254.68 | 43791720.5 | 46520375.7 | 46600249.9 | 60319074.1 | 60310565.4 |

| | | | | | | | | | | |
|---|---|---|---|---|---|---|---|---|---|---|
| Story 24 | 42439112 | 42432548.3 | 42694953 | 42683177 | 42458170.24 | 42452971.9 | 45127500.9 | 45205917.5 | 58851721.9 | 58843672.3 |
| Story 25 | 41189859.9 | 41183624.5 | 41435469.8 | 41424165 | 41193602.55 | 41188711.1 | 43810362.9 | 43887284.4 | 57465592.1 | 57457965.1 |
| Story 26 | 40007557.2 | 40001623.9 | 40243236.4 | 40232358 | 39996656.55 | 39992046.5 | 42561875.8 | 42637264.6 | 56153460.5 | 56146223.6 |
| Story 27 | 38886127.4 | 38880473 | 39112157.7 | 39101671 | 38861234.08 | 38856882.8 | 41375898.8 | 41449722.3 | 54908895 | 54902019.2 |
| Story 28 | 37820175.1 | 37814779 | 38036835.1 | 38026709 | 37781919.36 | 37777806.8 | 40246982.7 | 40319210.9 | 53726144.4 | 53719604 |
| Story 29 | 36804890.6 | 36799734.4 | 37012436.7 | 37002644 | 36753883.84 | 36749992 | 39170253.4 | 39240858.6 | 52600046.2 | 52593818 |
| Story 30 | 35835970.3 | 35831037.4 | 36034651.8 | 36025169 | 35772806.51 | 35769119.3 | 38141339 | 38210294.8 | 51525947.8 | 51520011.1 |

Table 5.8: Story stiffness for 30 story model with different slender ratio

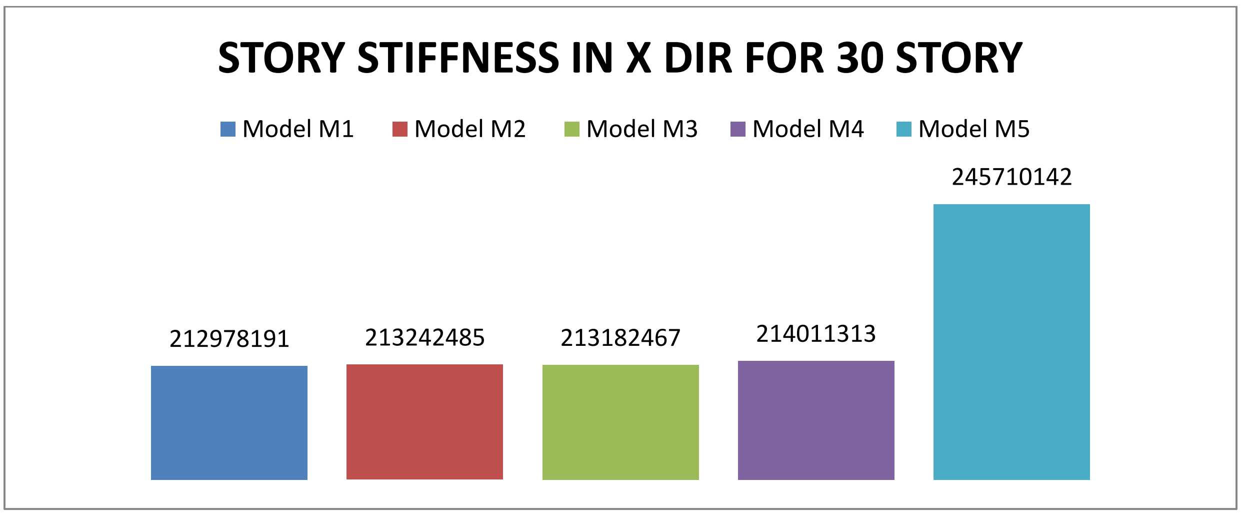


Figure 5.14: Story stiffness in x -dir for 30 story model with different slender ratio

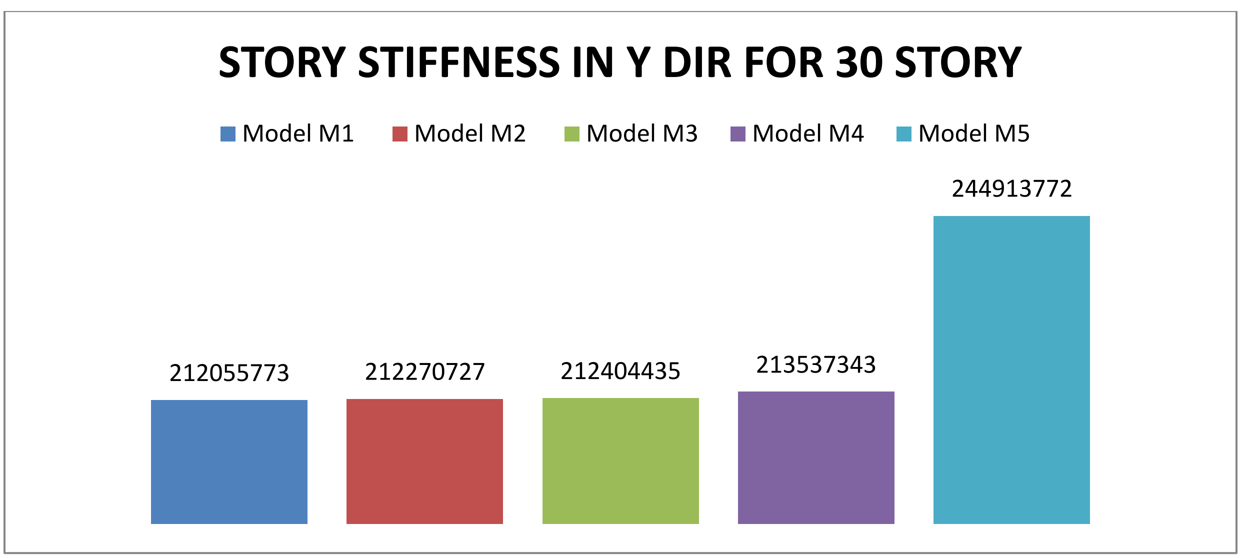


Figure 5.15: Story stiffness in y -dir for 30 story model with different slender ratio

5.3.4 Time period results for 30 story model:

| TIME PERIOD FOR 30 STORY MODEL | | | | | |
|---|---|---|---|---|---|
| MODES | MODEL M1 | MODEL M2 | MODEL M3 | MODEL M4 | MODEL M5 |
| 1 | 2.718 | 2.038 | 2.215 | 1.692 | 1.319 |
| 2 | 2.718 | 2.037 | 2.215 | 1.692 | 1.318 |
| 3 | 1.818 | 1.211 | 1.273 | 0.877 | 0.758 |
| 4 | 0.696 | 0.522 | 0.608 | 0.46 | 0.416 |
| 5 | 0.696 | 0.522 | 0.608 | 0.459 | 0.416 |
| 6 | 0.605 | 0.42 | 0.464 | 0.33 | 0.295 |
| 7 | 0.362 | 0.252 | 0.293 | 0.22 | 0.207 |
| 8 | 0.334 | 0.249 | 0.293 | 0.22 | 0.207 |
| 9 | 0.334 | 0.249 | 0.28 | 0.2 | 0.18 |
| 10 | 0.257 | 0.18 | 0.2 | 0.143 | 0.135 |
| 11 | 0.217 | 0.161 | 0.19 | 0.143 | 0.135 |
| 12 | 0.217 | 0.161 | 0.19 | 0.143 | 0.128 |

Table 5.9: Time period for 30 story model with different slender ratio

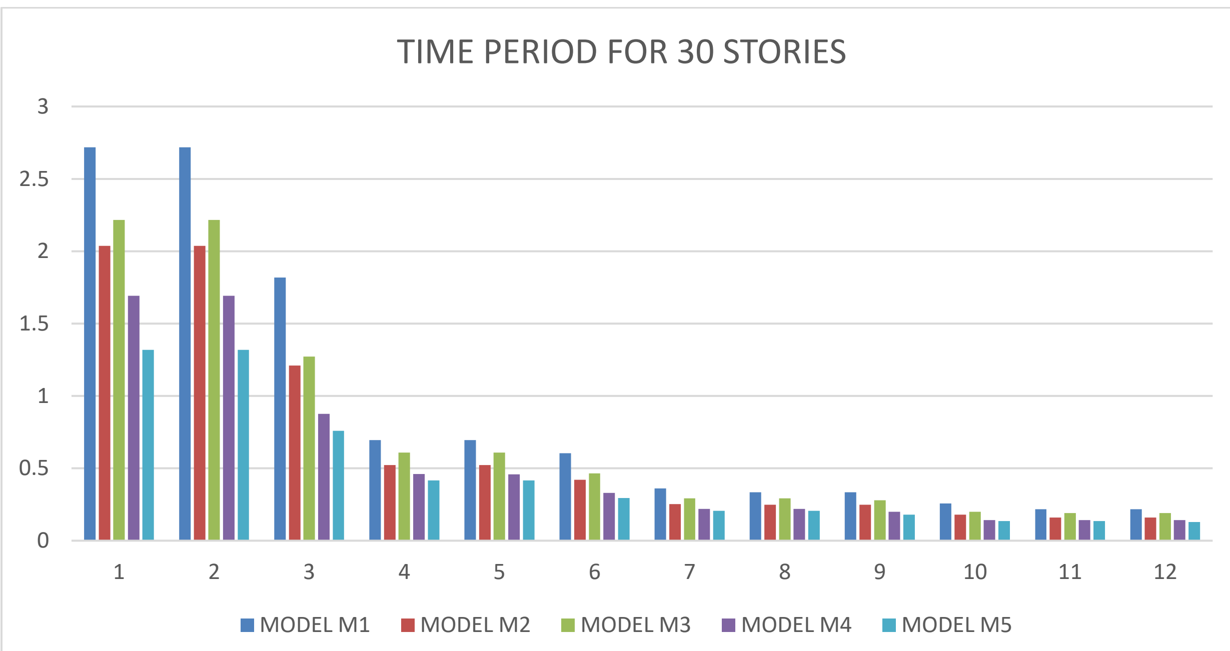


Figure 5.16: Time period for 30 story model with different slender ratio

5.3.5 Base shear results for 30 story model:

| BASE SHEAR FOR 30 story MODEL | | | | | |
|---|---|---|---|---|---|
| | MODEL M1 | MODEL M2 | MODEL M3 | MODEL M4 | MODEL M5 |
| X DIR | 449099.262 | 434664.894 | 405835.549 | 384072.81 | 314369.5075 |
| Y DIR | 449099.262 | 434666.437 | 405835.549 | 382794.01 | 314369.5075 |

Table 5.10: Base shear for 30 story model with different slender ratio

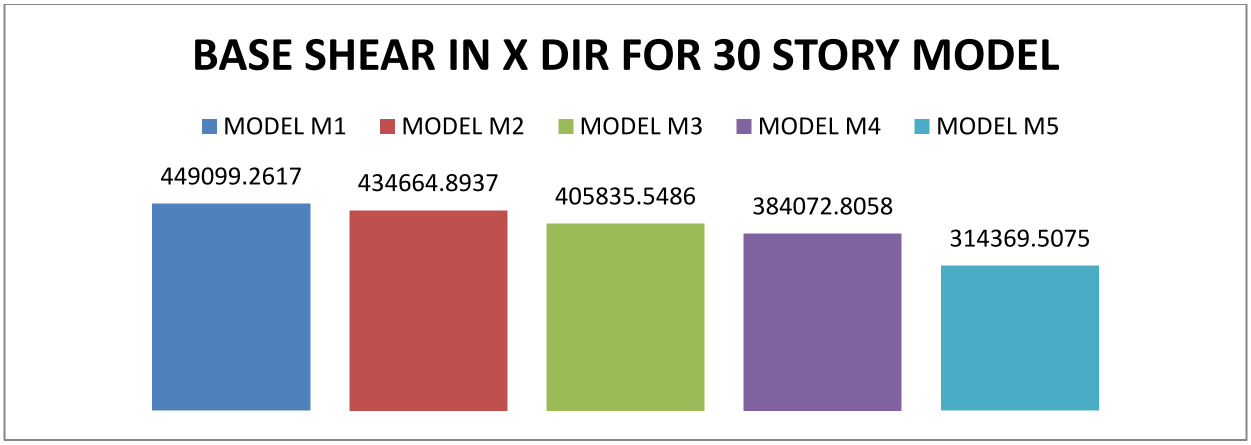


Figure 5.17: Base shear in x-dir for 30 story model with different slender ratio

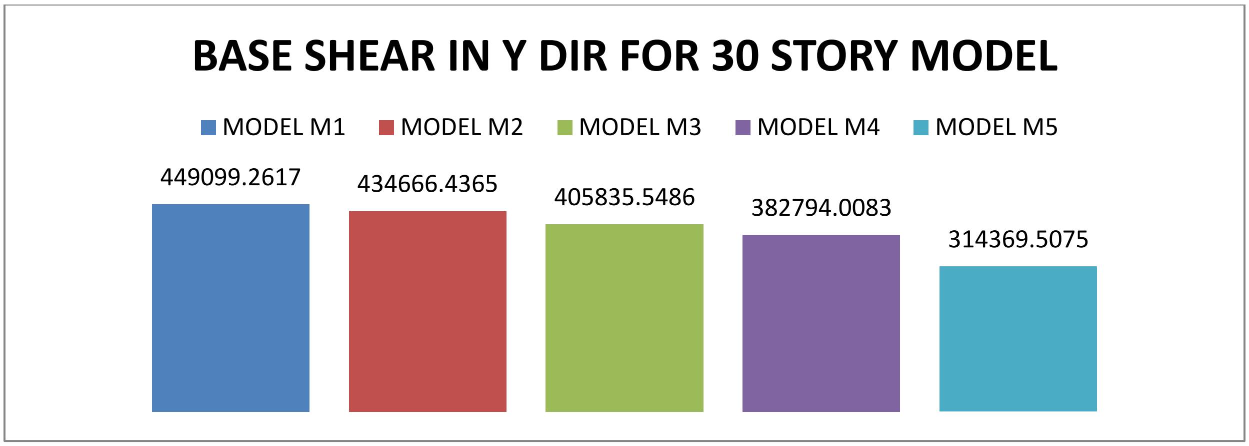


Figure 5.18: Base shear in y-dir for 30 story model with different slender ratio

5.4 RESULTS FOR 20 STORY MODEL:

5.4.1 Story displacement results for 20 story model:

| STORY DISPLACEMENT FOR 20 STORY MODEL | | | | | | | | | | |
|---|---|---|---|---|---|---|---|---|---|---|
| | Model M1 | | Model M2 | | Model M3 | | Model M4 | | Model M5 | |
| Story | X-Dir | Y-Dir | X-Dir | Y-Dir | X-Dir | Y-Dir | X-Dir | Y-Dir | X-Dir | Y-Dir |
| | mm | mm | mm | mm | mm | mm | mm | mm | mm | mm |
| Base | 0 | 0 | 0 | 0 | 0 | 0 | 0 | 0 | 0 | 0 |
| Story1 | 2.109 | 2.118 | 2.038 | 2.048 | 1.905 | 1.914 | 1.795 | 1.793 | 1.371 | 1.373 |
| Story2 | 5.352 | 5.366 | 5.168 | 5.182 | 4.829 | 4.847 | 4.481 | 4.472 | 3.336 | 3.341 |
| Story3 | 8.999 | 9.015 | 8.684 | 8.7 | 8.109 | 8.128 | 7.504 | 7.485 | 5.534 | 5.54 |
| Story4 | 12.989 | 13.006 | 12.527 | 12.544 | 11.689 | 11.709 | 10.796 | 10.765 | 7.902 | 7.909 |
| Story5 | 17.299 | 17.317 | 16.675 | 16.694 | 15.551 | 15.572 | 14.33 | 14.285 | 10.438 | 10.445 |
| Story6 | 21.915 | 21.935 | 21.117 | 21.138 | 19.684 | 19.706 | 18.103 | 18.043 | 13.103 | 13.112 |

| | | | | | | | | | | |
|---|---|---|---|---|---|---|---|---|---|---|
| Story7 | 26.827 | 26.849 | 25.841 | 25.863 | 24.079 | 24.102 | 22.102 | 22.026 | 15.907 | 15.916 |
| Story8 | 32.025 | 32.048 | 30.837 | 30.861 | 28.726 | 28.75 | 26.32 | 26.225 | 18.846 | 18.855 |
| Story9 | 37.5 | 37.524 | 36.097 | 36.123 | 33.617 | 33.642 | 30.749 | 30.634 | 21.913 | 21.923 |
| Story10 | 43.241 | 43.267 | 41.611 | 41.639 | 38.744 | 38.77 | 35.38 | 35.244 | 25.102 | 25.113 |
| Story11 | 49.242 | 49.269 | 47.372 | 47.401 | 44.099 | 44.127 | 40.207 | 40.048 | 28.407 | 28.419 |
| Story12 | 55.493 | 55.521 | 53.371 | 53.402 | 49.676 | 49.705 | 45.222 | 45.04 | 31.823 | 31.836 |
| Story13 | 61.987 | 62.016 | 59.602 | 59.635 | 55.467 | 55.497 | 50.42 | 50.212 | 35.345 | 35.359 |
| Story14 | 68.716 | 68.747 | 66.056 | 66.091 | 61.465 | 61.496 | 55.794 | 55.559 | 38.968 | 38.982 |
| Story15 | 75.674 | 75.706 | 72.728 | 72.765 | 67.665 | 67.697 | 61.338 | 61.075 | 42.688 | 42.703 |
| Story16 | 82.853 | 82.886 | 79.609 | 79.648 | 74.06 | 74.093 | 67.046 | 66.753 | 46.499 | 46.515 |
| Story17 | 90.245 | 90.281 | 86.694 | 86.735 | 80.643 | 80.677 | 72.913 | 72.588 | 50.398 | 50.414 |
| Story18 | 97.846 | 97.882 | 93.976 | 94.019 | 87.409 | 87.445 | 78.938 | 78.575 | 54.38 | 54.397 |
| Story19 | 105.647 | 105.685 | 101.448 | 101.493 | 94.353 | 94.389 | 85.123 | 84.725 | 58.442 | 58.459 |
| Story20 | 113.643 | 113.682 | 109.105 | 109.155 | 101.468 | 101.505 | 91.415 | 90.983 | 62.578 | 62.596 |

Table 5.11: Story displacement for 20 story model with different slender ratio

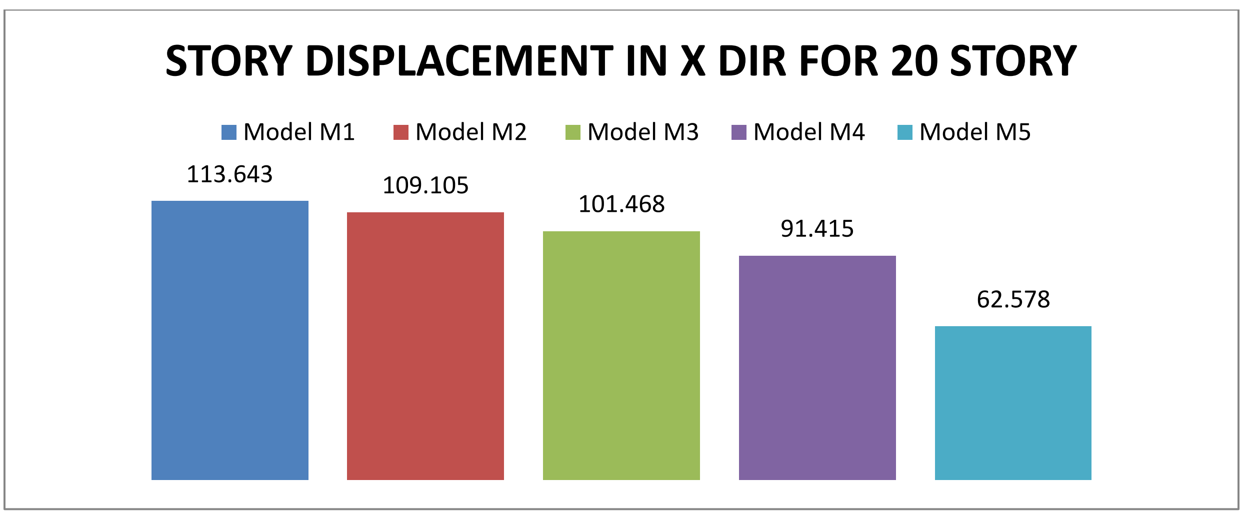


Figure 5.19: Story displacement in x-dir for 20 story model with different slender ratio

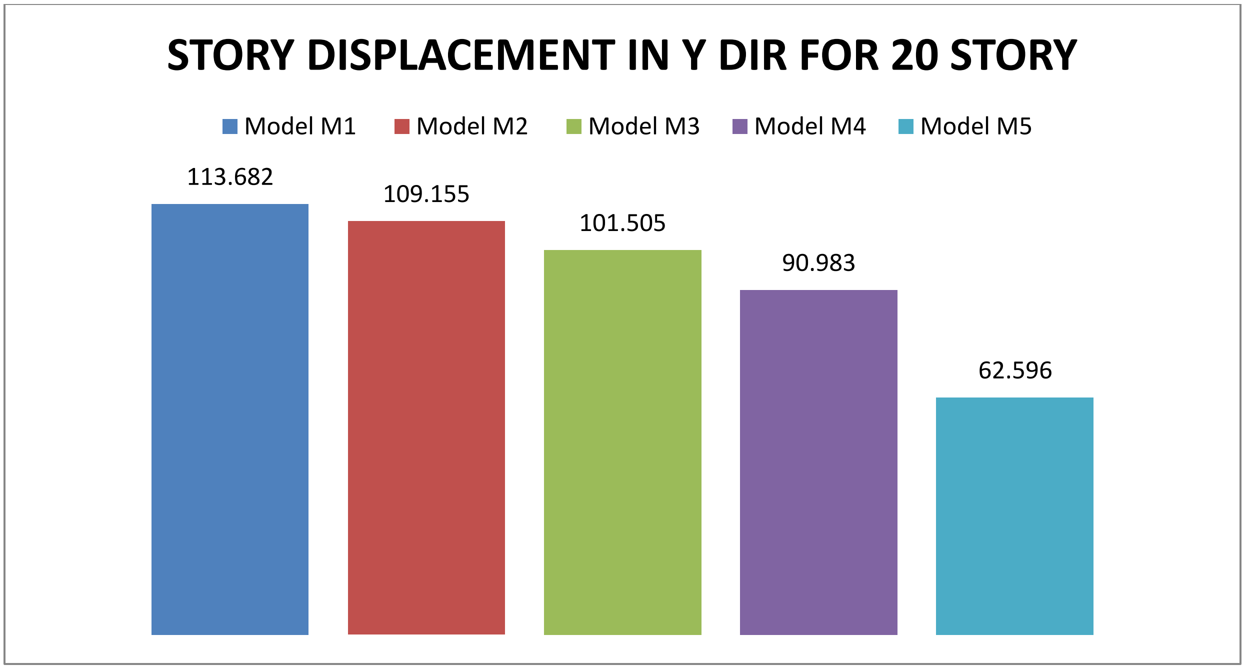


Figure 5.20: Story displacement in y-dir for 20 story model with different slender ratio

5.4.2 Story drift results for 20 story model:

| STORY DRIFT FOR 20 STORY MODEL | | | | | | | | | | |
|---|---|---|---|---|---|---|---|---|---|---|
| | Model M1 | | Model M2 | | Model M3 | | Model M4 | | Model M5 | |
| Story | X-Dir | Y-Dir | X-Dir | Y-Dir | X-Dir | Y-Dir | X-Dir | Y-Dir | X-Dir | Y-Dir |
| | mm | mm | mm | mm | mm | mm | mm | mm | mm | mm |
| Base | 0 | 0 | 0 | 0 | 0 | 0 | 0 | 0 | 0 | 0 |
| Story 1 | 0.000703 | 0.000706 | 0.000679 | 0.000683 | 0.000635 | 0.000638 | 0.000598 | 0.000598 | 0.000457 | 0.000458 |
| Story 2 | 0.001081 | 0.001083 | 0.001043 | 0.001045 | 0.000975 | 0.000977 | 0.000945 | 0.000943 | 0.000698 | 0.000699 |
| Story 3 | 0.001216 | 0.001216 | 0.001172 | 0.001173 | 0.001093 | 0.001094 | 0.001037 | 0.001034 | 0.000787 | 0.000787 |
| Story 4 | 0.00133 | 0.00133 | 0.001281 | 0.001282 | 0.001193 | 0.001194 | 0.001099 | 0.001095 | 0.000815 | 0.000815 |
| Story 5 | 0.001436 | 0.001437 | 0.001383 | 0.001383 | 0.001287 | 0.001288 | 0.001179 | 0.001174 | 0.000846 | 0.000847 |
| Story 6 | 0.001539 | 0.001539 | 0.001481 | 0.001481 | 0.001378 | 0.001378 | 0.001258 | 0.001252 | 0.00089 | 0.00089 |
| Story 7 | 0.001637 | 0.001638 | 0.001575 | 0.001575 | 0.001465 | 0.001465 | 0.001333 | 0.001328 | 0.000936 | 0.000936 |
| Story 8 | 0.001733 | 0.001733 | 0.001665 | 0.001666 | 0.001549 | 0.001549 | 0.001406 | 0.0014 | 0.00098 | 0.000981 |
| Story 9 | 0.001825 | 0.001825 | 0.001753 | 0.001754 | 0.00163 | 0.001631 | 0.001476 | 0.00147 | 0.001023 | 0.001023 |

| | | | | | | | | | | |
|---|---|---|---|---|---|---|---|---|---|---|
| Story 10 | 0.001914 | 0.001914 | 0.001838 | 0.001839 | 0.001709 | 0.001709 | 0.001544 | 0.001537 | 0.001063 | 0.001063 |
| Story 11 | 0.002 | 0.002001 | 0.00192 | 0.001921 | 0.001785 | 0.001786 | 0.001609 | 0.001601 | 0.001102 | 0.001102 |
| Story 12 | 0.002084 | 0.002084 | 0.002 | 0.002 | 0.001859 | 0.001859 | 0.001672 | 0.001664 | 0.001139 | 0.001139 |
| Story 13 | 0.002165 | 0.002165 | 0.002077 | 0.002077 | 0.00193 | 0.001931 | 0.001733 | 0.001724 | 0.001174 | 0.001174 |
| Story 14 | 0.002243 | 0.002244 | 0.002151 | 0.002152 | 0.002 | 0.002 | 0.001791 | 0.001782 | 0.001208 | 0.001208 |
| Story 15 | 0.002319 | 0.00232 | 0.002224 | 0.002224 | 0.002067 | 0.002067 | 0.001848 | 0.001839 | 0.00124 | 0.00124 |
| Story 16 | 0.002393 | 0.002393 | 0.002294 | 0.002294 | 0.002132 | 0.002132 | 0.001903 | 0.001893 | 0.001271 | 0.001271 |
| Story 17 | 0.002464 | 0.002465 | 0.002362 | 0.002362 | 0.002195 | 0.002195 | 0.001956 | 0.001945 | 0.0013 | 0.0013 |
| Story 18 | 0.002533 | 0.002534 | 0.002427 | 0.002428 | 0.002255 | 0.002256 | 0.002009 | 0.001998 | 0.001328 | 0.001328 |
| Story 19 | 0.0026 | 0.002601 | 0.002491 | 0.002492 | 0.002314 | 0.002315 | 0.002062 | 0.00205 | 0.001354 | 0.001354 |
| Story 20 | 0.002665 | 0.002666 | 0.002552 | 0.002554 | 0.002372 | 0.002372 | 0.002102 | 0.002091 | 0.001379 | 0.001379 |

Table 5.12: Story drift for 20 story model with different slender ratio

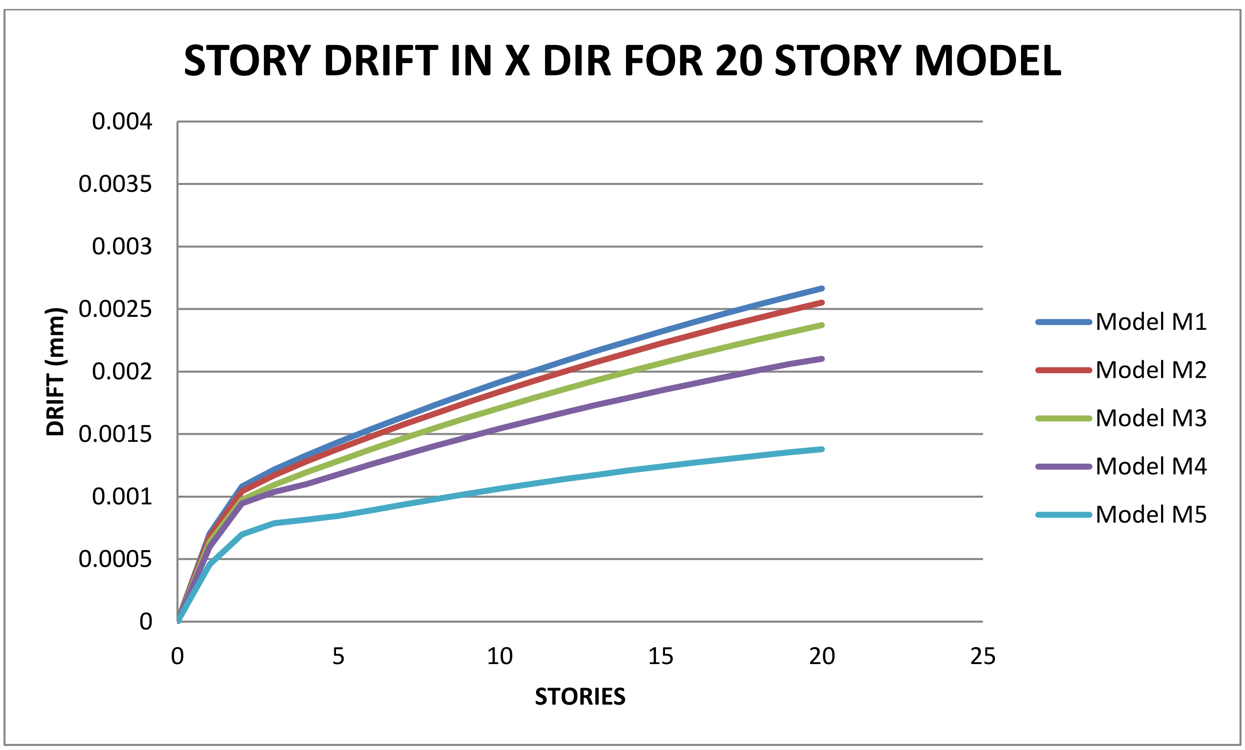


Figure 5.21: Story drift in x-dir for 20 story model with different slender ratio

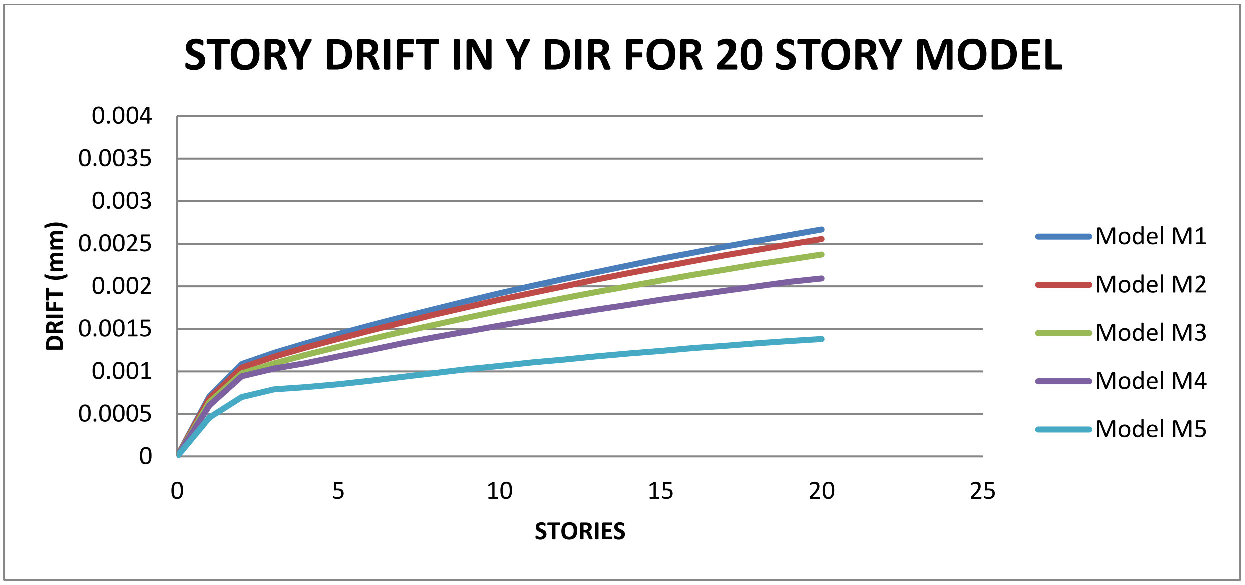


Figure 5.22: Story drift in y-dir for 20 story model with different slender ratio

5.4.3 Story stiffness results for 20 story model

| STORY STIFFNESS FOR 20 STORY MODEL | | | | | | | | | | |
|---|---|---|---|---|---|---|---|---|---|---|
| | Model M1 | | Model M2 | | Model M3 | | Model M4 | | Model M5 | |
| Story | X-Dir | Y-Dir | X-Dir | Y-Dir | X-Dir | Y-Dir | X-Dir | Y-Dir | X-Dir | Y-Dir |
| | KN/M | KN/M | KN/M | KN/M | KN/M | KN/M | KN/M | KN/M | KN/M | KN/M |
| Base | 0 | 0 | 0 | 0 | 0 | 0 | 0 | 0 | 0 | 0 |
| Story 1 | 212978191 | 212055773 | 213242485 | 212270727 | 213182467 | 212404435 | 214011313 | 213537343 | 245710142 | 244913772 |
| Story 2 | 137695826 | 137491760 | 138093800 | 137872620 | 137955215 | 137749509 | 142022036 | 141952348 | 153990450 | 153834895 |
| Story 3 | 121722932 | 121666459 | 122171341 | 122113865 | 122101849 | 122051693 | 125451421 | 125467972 | 139849832 | 139863420 |
| Story 4 | 110644369 | 110602527 | 111111166 | 111065638 | 111111344 | 111072424 | 114420778 | 114461103 | 130493322 | 130479318 |
| Story 5 | 101812469 | 101778892 | 102285729 | 102247427 | 102266777 | 102235377 | 105707495 | 105764536 | 121838938 | 121797769 |
| Story 6 | 94415912 | 94386983.4 | 94887400.1 | 94853326 | 94846383.86 | 94819491.7 | 98329645.9 | 98396983 | 114344823 | 114308754 |
| Story 7 | 88110677.8 | 88085411.3 | 88575555 | 88544865 | 88516312.17 | 88492985.9 | 91999617.4 | 92074297.1 | 107899042 | 107868781 |
| Story 8 | 82658847.4 | 82636513.2 | 83114055.4 | 83086117 | 83040288.62 | 83019823.8 | 86498879.9 | 86578734.3 | 102263594 | 102236752 |
| Story 9 | 77891489.7 | 77871560.1 | 78335173.4 | 78309521 | 78246113.84 | 78228000.3 | 81667689.6 | 81751160.9 | 97282274.7 | 97258065.9 |
| Story 10 | 73679994.4 | 73662069 | 74110993.4 | 74087267 | 74006372.54 | 73990218.2 | 77382697.3 | 77468619.2 | 92841037 | 92819109.9 |
| Story 11 | 69927079 | 69910846.8 | 70344710.2 | 70322628 | 70224654.39 | 70210152.2 | 73550257.5 | 73637747.2 | 88852276.3 | 88832332.8 |
| Story 12 | 66559789.2 | 66544998 | 66963774 | 66943104 | 66829251.54 | 66816153.5 | 70100345.3 | 70188733.8 | 85249180.7 | 85230948.2 |
| Story 13 | 63518673.1 | 63505120 | 63908952.9 | 63889508 | 63761097.32 | 63749203.4 | 66975266.5 | 67064037.3 | 81975695.3 | 81958947.5 |

| | | | | | | | | | | |
|---|---|---|---|---|---|---|---|---|---|---|
| Story 14 | 60755631.6 | 60743152.4 | 61132282.3 | 61113908 | 60972223.24 | 60961371.2 | 64128049.5 | 64216798.6 | 78985894.5 | 78970447.3 |
| Story 15 | 58231687.5 | 58220147.2 | 58594875.2 | 58577442 | 58423740.11 | 58413796.4 | 61520460.7 | 61608868.2 | 76242251.6 | 76227951.6 |
| Story 16 | 55914842.1 | 55904128.7 | 56264797.8 | 56248194 | 56083697.61 | 56074551.2 | 59120896.7 | 59208707.8 | 73713628.1 | 73700346.7 |
| Story 17 | 53778510.1 | 53768530.6 | 54115507.7 | 54099637 | 53925540.37 | 53917098.5 | 56902984.1 | 56989984.9 | 71373799.9 | 71361429.4 |
| Story 18 | 51801503.1 | 51792177.7 | 52125767.8 | 52110342 | 51927874.66 | 51920058.5 | 54847145.8 | 54933185.1 | 69201909.5 | 69190356 |
| Story 19 | 49966690.1 | 49957948.8 | 50278594 | 50263344 | 50073229.29 | 50065970.7 | 52940751.8 | 53025611 | 67181212.2 | 67170392.2 |
| Story 20 | 48258131.6 | 48249915 | 48557553.2 | 48528248 | 48345642.75 | 48338883.7 | 51193179.2 | 51276992.1 | 65295588.5 | 65285430.7 |

Table 5.13: Story stiffness for 20 story model with different slender ratio

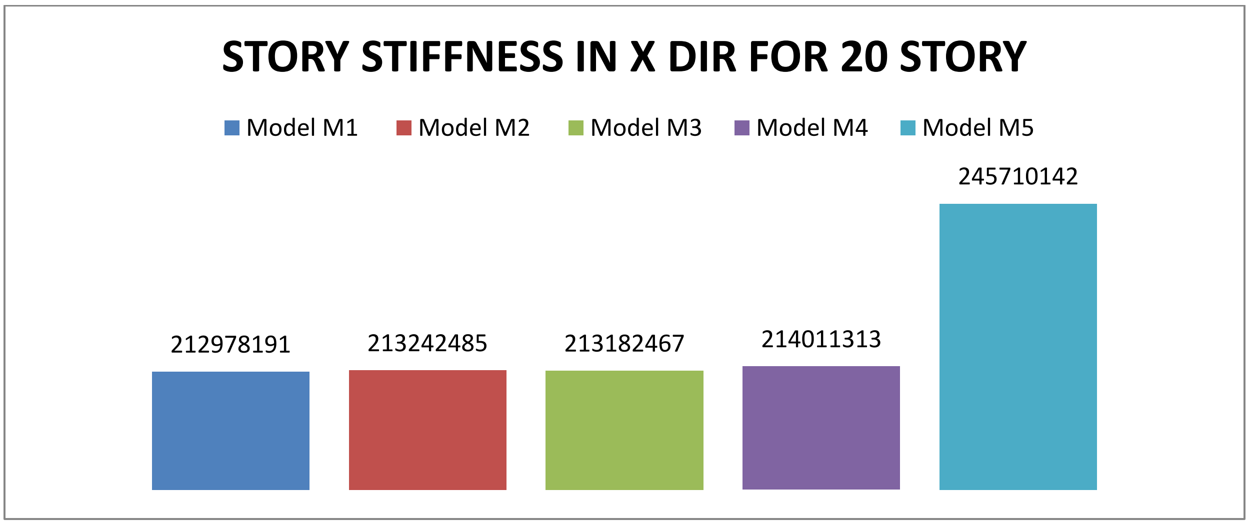


Figure 5.23: Story stiffness in x-dir for 20 story model with different slender ratio

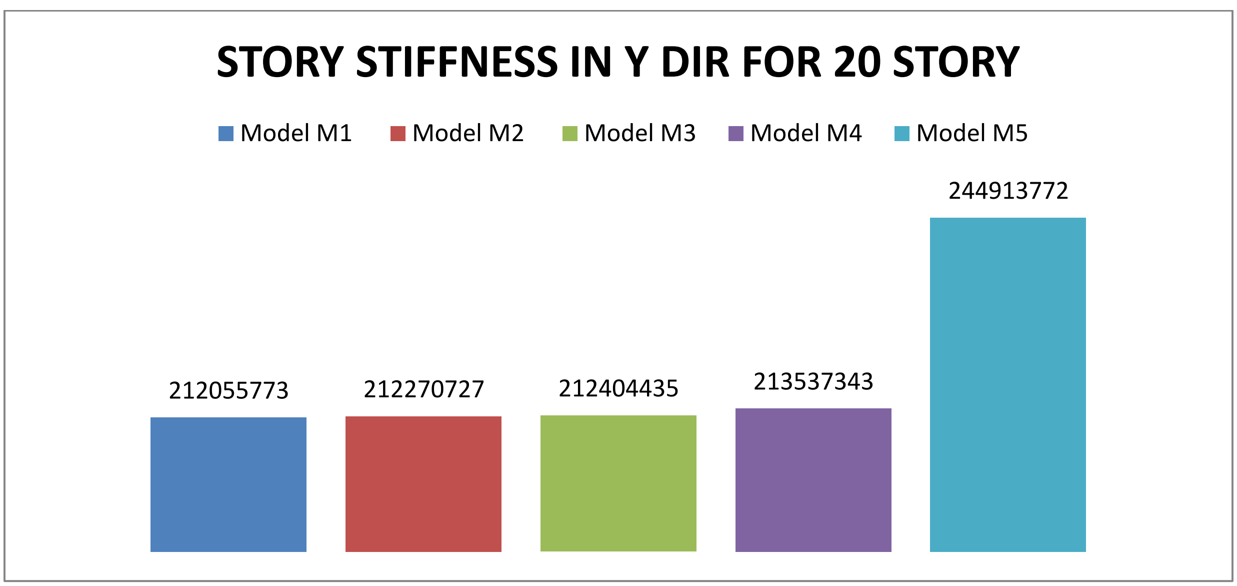


Figure 5.24: Story stiffness in y-dir for 20 story model with different slender ratio

5.4.4 Time period results for 20 story model

| TIME PERIOD FOR 20 STORY MODEL | | | | | |
|---|---|---|---|---|---|
| MODES | MODEL M1 | MODEL M2 | MODEL M3 | MODEL M4 | MODEL M5 |
| Mode | M1 | M2 | M3 | M4 | M5 |
| 1 | 2.006 | 1.504 | 1.635 | 1.249 | 0.973 |
| 2 | 2.006 | 1.503 | 1.634 | 1.248 | 0.973 |
| 3 | 1.341 | 0.893 | 0.939 | 0.647 | 0.559 |
| 4 | 0.513 | 0.385 | 0.448 | 0.34 | 0.307 |
| 5 | 0.513 | 0.385 | 0.448 | 0.339 | 0.307 |
| 6 | 0.447 | 0.31 | 0.342 | 0.244 | 0.218 |
| 7 | 0.267 | 0.186 | 0.216 | 0.162 | 0.153 |
| 8 | 0.246 | 0.184 | 0.216 | 0.162 | 0.153 |
| 9 | 0.246 | 0.184 | 0.206 | 0.147 | 0.133 |
| 10 | 0.19 | 0.133 | 0.147 | 0.105 | 0.1 |
| 11 | 0.16 | 0.119 | 0.14 | 0.105 | 0.1 |

Table 5.14: Time period for 20 story model with different slender ratio

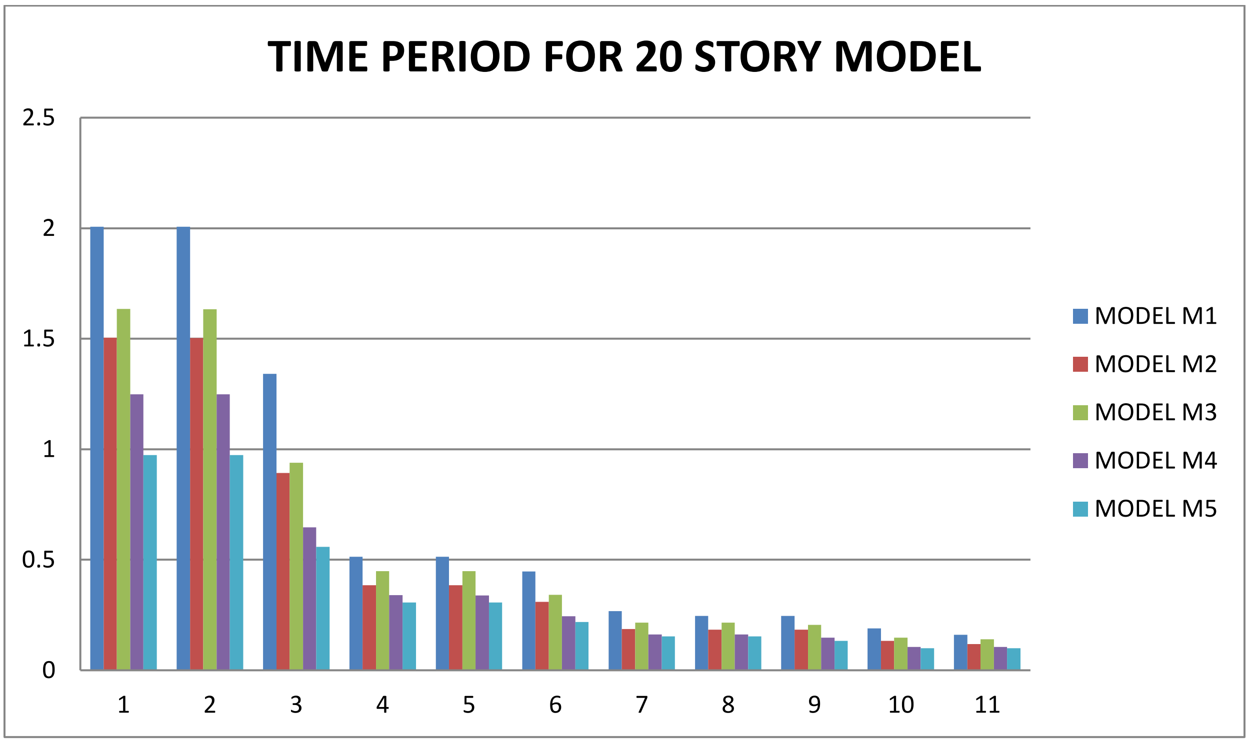


Figure 5.25: Time period for 20 story model with different slender ratio

5.4.5 Base shear results for 20 story model

| **BASE SHEAR FOR 20 story MODEL** | | | | | |
|---|---|---|---|---|---|
| | **MODEL M1** | **MODEL M2** | **MODEL M3** | **MODEL M4** | **MODEL M5** |
| X DIR | 449099.262 | 434664.894 | 405835.549 | 384072.81 | 314369.5075 |
| Y DIR | 449099.262 | 434666.437 | 405835.549 | 382794.01 | 314369.5075 |

Table 5.15: Base shear for 20 story model with different slender ratio

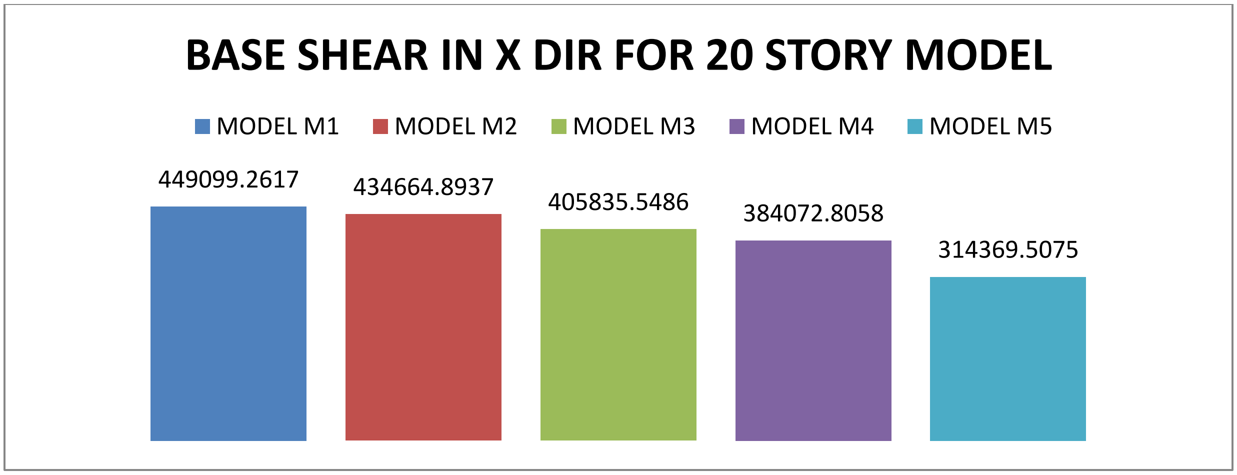


Figure 5.26: Base shear in x dir for 20 story model with different slender ratio

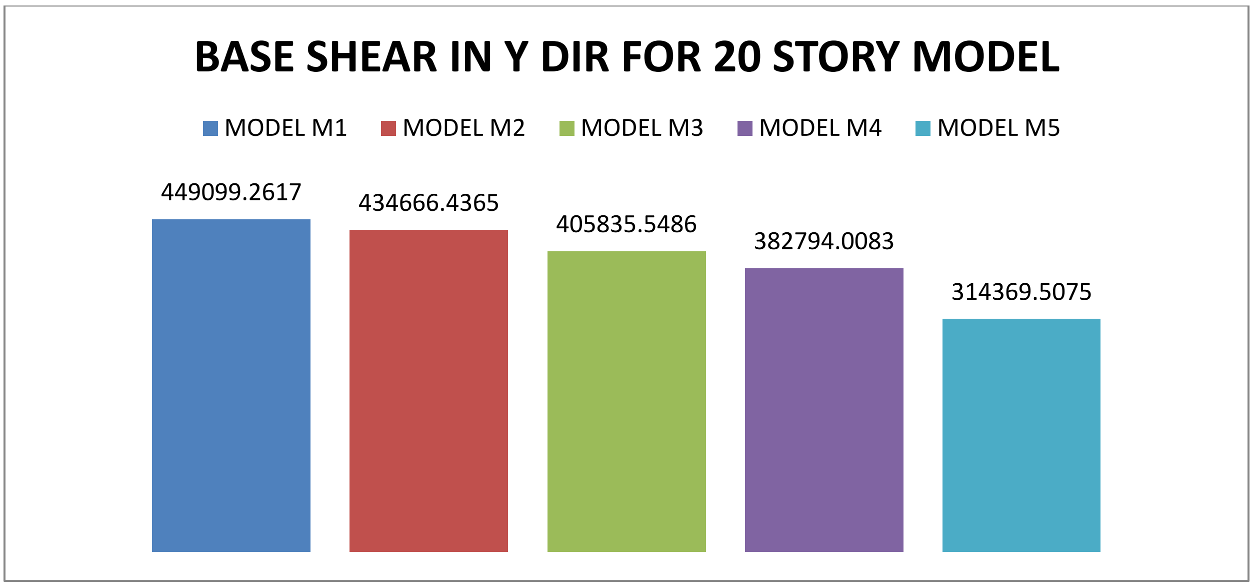


Figure 5.27: Base shear in y dir for 20 story model with different slender ratio

5.5 DISCUSSION ON G+40 RESULTS

DISPLACEMENT

- The maximum displacement observed for Model M1 (Aspect Ratio = 9) is approximately 265 mm in both X and Y directions. As the aspect ratio decreases to 7, 4, 2.25, and finally 1, the displacement values steadily reduce, with Model M5 (Aspect Ratio = 1) showing the minimum displacement of around 113 mm.

DRIFT

- The maximum drift occurs in Model M1 and M2 (Aspect Ratio = 9 and 7) with a value of approximately 0.002367. As the aspect ratio decreases—i.e., the building becomes shorter and stiffer—the drift values reduce significantly. By the time we reach Model M5 (Aspect Ratio = 1), the drift reduces to 0.000647, which is almost a 73% decrease from the tallest model.

STORY STIFFNESS

- M5 (AR = 1) shows the highest story stiffness in both X and Y directions — over 73117231.6 KN/m, indicating a very stiff, squat structure.
- As the aspect ratio increases (becomes more slender) (from 1 → 9), stiffness decreases, particularly visible in models M2 and M4.M1 (AR = 9), being the most slender model, still maintains a relatively high stiffness due to possible reinforcement or design configuration, but it is ~4% lower than M5.

- The fluctuations between models (like M3 having high stiffness again) may be due to differences in core placement, bracing configuration, or mass distribution.

TIME PERIOD

M1 (AR = 9) has the highest time period of 3.373 sec, while M5 (AR = 1) has the lowest time period of 1.637 seas the aspect ratio increases, buildings become taller and more slender, which makes them more flexible, thereby increasing their natural time period. Conversely, buildings with a lower aspect ratio (shorter and stockier) are stiffer, leading to lower time periods.

5.6 DISCUSSION ON G+30 RESULTS

DISPLACEMENT

The story displacement values show a gradual reduction from Model M1 (highest aspect ratio) to Model M5 (lowest aspect ratio):

Model M1 (tallest/slender, AR = 9) shows maximum displacement (~191 mm).

Model M5 (stocky, AR = 1) has minimum displacement (~89 mm).

This implies that as aspect ratio decreases, the lateral stiffness increases, thereby reducing displacement.

DRIFT

Model M1 (AR = 9) exhibits the highest drift (~0.00257), indicating more lateral flexibility.

Model M5 (AR = 1) shows the lowest drift (~0.00095), signifying greater stiffness and resistance to lateral sway.

There is a progressive reduction in story drift as the aspect ratio decreases from tall slender forms to stockier configurations.

STORY STIFFNESS

Model M5 (AR = 1) has the highest stiffness in both X and Y directions, approximately 11–15% greater than the other models. Model M2 (AR = 7) shows the lowest stiffness, highlighting how slender buildings (with higher AR) offer less lateral rigidity. Interestingly, Model M3 (AR = 4) exhibits a slight increase in stiffness compared to M1 and M2, likely due to an optimized geometry or better structural efficiency in that proportion range.

5.7 DISCUSSION ON G+20 RESULTS

DISPLACEMENT

- The maximum displacement observed for Model M1 (Aspect Ratio = 9) is approximately 265 mm in both X and Y directions. As the aspect ratio decreases to 7, 4, 2.25, and finally 1, the displacement values steadily reduce, with Model M5 (Aspect Ratio = 1) showing the minimum displacement of around 113 mm.

DRIFT

- The maximum drift occurs in Model M1 and M2 (Aspect Ratio = 9 and 7) with a value of approximately 0.002367. As the aspect ratio decreases—i.e., the building becomes shorter and stiffer—the drift values reduce significantly. By the time we reach Model M5 (Aspect Ratio = 1), the drift reduces to 0.000647, which is almost a 73% decrease from the tallest model.

STORY STIFFNESS

- M5 (AR = 1) shows the highest story stiffness in both X and Y directions — over 73117231.6 kN/m, indicating a very stiff, squat structure.
- As the aspect ratio increases (becomes more slender) (from 1 → 9), stiffness decreases, particularly visible in models M2 and M4.M1 (AR = 9), being the most slender model, still maintains a relatively high stiffness due to possible reinforcement or design configuration, but it is ~4% lower than M5.
- The fluctuations between models (like M3 having high stiffness again) may be due to differences in core placement, bracing configuration, or mass distribution.

## 6 CONCLUSIONS

### 6.1 SUMMARY

This dissertation investigates the comparison of the high-rise buildings with considering 20, 30 and 40 Storey buildings with a slender ratio of (1, 2.25, 4,7and 9), typical Storey height as 3.5m, the first structural system i.e. composite structure with mega frame system moment resisting frame, in this system the elements or the structural members are designed for gravity and lateral loads. In the second structural system i.e. the Regular 40 story model with different slender ratio it is a system commonly used in high rise building to increase lateral stiffness, and in third structural systems i.e. 30 story model with different slender ratio. The fourth structural system is 20 story models with different slender ratio. Thus, by investing response of the structure like Lateral displacement, Storey drift, Storey stiffness, Time period. The seismic performance is studied using nonlinear dynamic analysis

It was found that, comparing all the different slender ratio structural systems, slender ratio 1.0 story provides more effectiveness then other slender ratio model. In terms of these parameters like lateral displacement, Storey drifts, time period, Storey stiffness and base shear.

6.2 CONCLUSIONS

This trend clearly indicates that higher aspect ratios (taller and slenderer buildings) experience greater lateral displacement, primarily due to their reduced lateral stiffness and higher flexibility. The slender geometry makes the structure more susceptible to lateral loads, especially wind and seismic forces, causing increased sway at the top stories.

In contrast, lower aspect ratio buildings (broader and shorter) are inherently stiffer, which significantly reduces their susceptibility to lateral displacements under dynamic loads. Hence, displacement decreases as the aspect ratio approaches 1, showing enhanced stability.

As aspect ratio decreases, story drift significantly reduces, demonstrating improved control over lateral deformation. This confirms the need for careful aspect ratio selection in high-rise buildings to comply with serviceability and seismic performance requirements.

The time period increases with aspect ratio, confirming that slender structures are more flexible and may be more susceptible to wind and seismic excitations. This highlights the importance of adopting proper lateral load-resisting systems, especially for high-rise structures with high aspect ratios, to control dynamic responses.

Lower aspect ratio (stocky buildings) results in a broader base and shorter height, improving lateral force resistance due to: Better moment arm distribution, shorter column lengths, reducing slenderness effects, more effective load path for lateral and gravity forces. Higher aspect ratio (slender buildings) are more flexible, leading to: Lower stiffness, particularly in lateral directions, Greater susceptibility to drift and sway under seismic/wind loads.

6.3 Limitations

The following are the limitations of the present study

6.4 Future Scope

Further research can be carried out by considering the effect of wind loads on irregular shaped structures and also by considering the impact effects due to the seismic loading on structure. Further research can be carried by using the same system with soil interaction properties.

## 7. ACKNOWLEDGEMENTS

I would like to express my sincere and heartfelt gratitude to my beloved mentor

Mr, Mohammed Imtiyaz Qureshi, Assistant Professor, Department of Civil Engineering, Nawab Shah Alam Khan College of Engineering and Technology, for his guidance. I am thankful for his motivation and active supervision at every stage of the thesis work. It is his immense patience and co-operation that has helped for the successful completion of this work.

I would also like to thank Prof. Syed Farrukh Anwar, Head of the Department of Civil Engineering, Nawab Shah Alam Khan College of Engineering and Technology, his strategic direction and oversight of this research, particularly in the early stages and his ongoing advice throughout the project.

I express my sincere thanks to Prof. K. Shahsikanth Chairman, Board of Studies, Civil Engineering Department, Osmania University, for his valuable support and advice for preparation of this report as per the format and facilitating viva-voce.

I express my sincere thanks to Prof. K.L Radhika, Professor and Head of Civil Engineering, Osmania University,Hyderabad for facilitating the conduct of viva-voce examination.

I am thankful to, Principal Prof. P.Chandra Sekhar, University College of Engineering, Osmania University,Hyderabad for facilitating the conduct of viva-voce examination.

I am thankful to Dr. Mohammed Abdul Sattar, Principal of Nawab Shah Alam Khan College of Engineering and Technology for his constant zeal and supervision. Many thanks also go to the teaching and non-teaching staff in the university and colleges.

REFERENCES


[1] Adrian Smith, Gordon Gill Architecture LLP, (2022). Wuhan Greenland Center, Retrieved from: (http://smithgill.com/work/wuhan_greenland_center/)

[2] Alaghmandan, M., Bahrami, P., and Elnimeiri, M. (2014). The Future Trend of Architectural Form and Structural System in High-Rise Buildings, Architecture Research, 4(3), 55-62, 10.5923/j.arch.20140403.01.

[3] Ali, M., and Al-Kodmany, K. (2012). Tall Buildings and Urban Habitat of the 21st Century: A Global Perspective. Buildings, 2(4), 384–423.

[4] Ali, M.M. and Al-Kodmany, K. (2022). Structural Systems for Tall Buildings, Encyclopedia, 2, 1260-1286. doi.org/10.3390/encyclopedia2030085

[5] Ali, M. M. and Moon, K.S. (2018). Advances in structural systems for tall buildings: Emerging developments for contemporary urban giants. Buildings 8 (104): 1–34.

[6] Beardsley, S., Stochetti, A. and Cerone, M. (2018). The Design of Akhmat Tower, E3S Web of Conferences, HRC 2017, 33, 01022, doi.org/10.1051/e3sconf/20183301022

[7] Binder, G. (ed.) (2015). Tall Buildings of China, Images Publishing, CTBUH, Victoria, Australia.

[8] Cooper, K.R., Nakayama, M., Sasaki, Y., Fediw, A.A., Resende-Ide, S. and Zan, S.J. (1997). Unsteady aerodynamic force measurements on a super-tall building with a tapered cross section Journal of Wind Engineering and Industrial Aerodynamics, 72, 199–212.

[9] CTBUH (2022), Council on Tall Buildings and Urban Habitat; Illinois Institute of Technology, S.R. Crown Hall: 3360 South State Street, Chicago, IL, USA, available at: https://www.ctbuh.org.

[10] Daemei, A. B., Khotbehsara, E. M., Nobarani, E. M. and Bahrami, P. (2019). Study on wind aerodynamic and flow characteristics of triangular-shaped tall buildings and CFD simulation in order to assess drag coefficient. Ain Shams Engineering Journal, 10, 541–548.

[11] Deng, T., Yu, X. and Xin, Z. (2015). Aerodynamic measurements of across-wind loads and responses of tapered super high-rise buildings. Wind and Structures an International Journal, 21, 3, 331–352.

[12] Elshaer, A., Bitsuamlak, G. and El Damatty, A. (2017). Enhancing wind performance of tall buildings using corner aerodynamic optimization, Engineering Structures, 136, 133–148, dx.doi.org/10.1016/j.engstruct.2017.01.019.

[13] Fu, F. (2018). Design and Analysis of Tall and Complex Structures. Oxford and Cambridge.

[14] ButterworthHeinemann, Elsevier.Golasz-Szolomicka, H. and Szolomicki, J. (2019). Architectural and Structural Analysis of Selected Twisted Tall Buildings. IOP Conference Series. Materials Science and Engineering.

[15] Ilgın, H.E. (2021a). A search for a new tall building typology: structural hybrids, LIVENARCH VII Livable Environments and Architecture 7th International Congress OTHER ARCHITECT/URE(S), September 28-30, Trabzon, Turkey, Vol. 1, pp. 95-107.

[16] Ilgın, H.E. (2021b). Space efficiency in contemporary supertall office buildings, Journal of Architectural Engineering, 27(3), 4021024, 10.1061/(ASCE)AE.1943-5568.0000486.

[17] Ilgın, H.E. (2021c). Space efficiency in contemporary supertall residential buildings, Architecture, 1(1), 25-37, 10.3390/architecture1010004.

[18] Ilgın, H.E. (2022). A study on interrelations of structural systems and main planning considerations in contemporary supertall buildings, International Journal of Building Pathology and Adaptation,

[19] Ilgın, H.E., Ay, B.Ö., Gunel, M.H. (2021). A study on main architectural and structural design considerations of contemporary supertall buildings, Architectural Science Review

[20] Ilgın, H.E. and Karjalainen, M. (2022). Tallest Timber Buildings: Main Architectural and Structural Design Considerations.

[21] Ilgın, H.E. and Günel, M.H. (2021). Contemporary trends in supertall building form: aerodynamic design considerations, Livenarch VII Livable Environments and Architecture 7th International Congress Other Architect/Ure(S), September 28-30, Trabzon, Turkey, Vol. 1, pp. 61-81.